Study on Prevention of Acid Mine Drainage at Dumping Site by Using Cover System with Coal Ash and Organic Material in Open-cast Coal Mine, Indonesia

センディ, ドゥイキ

STUDY ON PREVENTION OF ACID MINE DRAINAGE AT DUMPING SITE BY USING COVER SYSTEM WITH COAL ASH AND ORGANIC MATERIAL IN OPEN-CAST COAL MINE, INDONESIA

July 2018

Department of Earth Resources Engineering

Graduate School of Engineering

Kyushu University

SENDY DWIKI

STUDY ON PREVENTION OF ACID MINE DRAINAGE AT DUMPING SITE BY USING COVER SYSTEM WITH COAL ASH AND ORGANIC MATERIAL IN OPEN-CAST COAL MINE, INDONESIA

A DOCTORAL THESIS

Submitted to the Department of Earth Resources Engineering,
Graduate School of Engineering, Kyushu University,
as a partial fulfillment of the requirements of the degree of
Doctor of Engineering

By:

Sendy DWIKI

S.T., Department of Mining Engineering, Institut Teknologi Bandung (ITB), 2013
M.Eng., Department of Earth Resources Engineering, Kyushu University, 2015

Supervised by:
Prof. Dr. Eng. Hideki SHIMADA

Department of Earth Resources Engineering
Graduate School of Engineering
Kyushu University
JAPAN
2018

ABSTRACT

Acid mine drainage (AMD) is a prominent issue in the coal mining area as it can pollute the surrounding area when it flows into the water bodies, brings along toxic constituents that are dangerous to living organisms. AMD is characterized by low pH (usually pH<4.5), high sulfate concentration and elevated heavy metal concentration. Three main factors that generate AMD are the available sulfide mineral, oxygen that acts as the primary oxidizer, and water. Coal-bearing rock contains abundant sulfide minerals that are exposed during the exploitation stage of mining. This introduces the sulfide minerals to the oxidizing environment, meaning that the minerals become chemically unstable because the weathering process is promoted. In the presence of water, acidic water is produced. The acidic water dissolves more metals sourced from not only sulfides but also gangue minerals. Moreover, in acidic condition, microbial activity plays a vital role to accelerate the reaction of AMD generation. The reaction rate with microbial activity is several order magnitudes larger than the reaction rate of the abiotic conditions. Therefore, the study of AMD prevention considering the effect of microbial activity is significant to minimize the negative impact to the environment.

The dry cover method is one of the common methods to prevent AMD generation in mining site for a long term. In this method, the oxidation of sulfide mineral can be reduced with minimizing the oxidation reaction of the potential acid-forming (PAF) rock by encapsulating with the non-acid forming (NAF) rock. However, based on past studies, Indonesia coal mine faces a critical problem where NAF rock is not sufficient in volume and in the capacity of neutralizing. Hence, this study proposes the utilization of coal ash and organic material as the alternative materials of the additional cover layer. Coal ash and organic material are industrial waste, which easy to be found in the coal mine, with potential to neutralize AMD, impede the fluid and also consume oxygen. However, due to those materials status as waste, the application of these materials needs to be further investigated. The dissertation describes and discusses the application of coal ash and organic materials as the cover system for AMD prevention, and consists of six chapters as follows:

Chapter 1 presents about the background of the current situation in Indonesian coal mining, the process of AMD generation within the mine, especially overburden dumping area, and the prevention of AMD. The problem statements and objectives of the studies, as well as an outline of the dissertation, are also introduced in this chapter.

Chapter 2 describes the current condition of Indonesian coal mine that related to AMD by performing a site investigation. One of the Indonesian coal mines is selected to investigate the AMD problem, including the sulfide mineral and geochemical capacities of coal-bearing rocks. It was found out that pyrite in the shape of framboid, a micromorphological structure common in sedimentary rock, dominated coal-bearing rock. This relates to the rapid reactivity of AMD generation reaction in coal mine compared to the ore mine. Furthermore, the dry cover method that is applied in this mine also investigated for its effectiveness to reduce oxygen and water infiltration. In the coal mine, PAF rock outsized in volume and also high capacity in producing acid. Additionally, the dry cover system with only NAF layer was not effective to reduce oxygen and water moisture in this mine based on the results of the direct measurement on-site.

Chapter 3 discusses characterization of coal ash and organic material related to the application in dry cover system. Coal ash is divided into fly ash and bottom ash, due to its distinguished collect location. It is separated due to the particle size, which affect the settlement of particles. The conventional classification systems of coal ash, i.e. ASTM C618 and JISA6201, are usually for the use in concrete; they do not include to assess the neutralizing capacity of coal ash. Therefore, another approach is needed to classify the coal ash in terms of cover layer for AMD prevention. Based on the shape and mineral observation, coal ash can be classified in the temperature of the coal burning process. This affects coal ash composition, which influence the neutralizing capacity of coal ash. The coal ash from the burning process with high temperature more than 700 °C can be classified as Type 1 which has spherical particles and high neutralizing capacity (>100 kg H_2SO_4/ton). On the other hands, the coal ash of Type 2 from the lower coal burning temperature has the particles of irregular shape and the intermediate neutralizing capacity (<50 kg H_2SO_4/ton) with unburned carbon. The different neutralizing capacity of Types 1 and 2 can be explained by the mineral contained in coal

ash, meaning that the acid neutralizing minerals, i.e. the calcite and dolomite, are left as the dominant minerals due to dihydroxylation under the high temperature of coal burning. In addition, bottom ash is not effective to use for AMD prevention because it has the insignificant neutralizing capacity. The organic material which is suitable in Indonesia coal mine under the humid tropical climate is the less inherent moisture content, as shown by plant based empty fruit bunches of palm oil (EFB) compared to well-studied sewage sludge. Moreover, based on the oxygen consumption rate measurement, the plant-based organic material can consume more oxygen in weight basis compared to sewage sludge. The rate can differ into 3.6 folds higher than the sewage sludge.

Chapter 4 discusses the optimization of both materials for utilization in dry cover system. Laboratory-scale simulations to understand the effectiveness of these materials as cover layer are carried out by monitoring the behavior of leachate water. Net acid producing potential (NAPP) ratio of coal ash and PAF rock can be utilized to determine the sufficient amount of coal ash to be used. Based on the results of the experiment to simulate the balance of coal ash and PAF, it is recommended to have NAPP ratio less than 10 kg H_2SO_4/ton in order to make sure the acidic water can be completely improved by the addition of coal ash. Additionally, coal ash of Type 2 which has low acid neutralizing capacity can be used if the waste rock is classified as PAF low capacity: NAPP ratio is less than 10 kg H_2SO_4/ton and NAG pH is below 4.5. Thickness ratio is also an important factor to be considered. It was reported that the hydraulic conductivity was reduced due to the sedimentation of Ca and Mg in PAF rock when the coal ash was placed on PAF. From the results of the experiment to discuss the effective thickness of coal ash, the reduction of hydraulic conductivity can be expected when the thickness of cover layer is more than 0.25 times for the coal ash of Type 1 and 0.5 times for the coal ash of Type 2, respectively. For organic material, it can be expected to enhance the oxygen consumption in the layer. However, it was indicated that the reduction of the thickness had to be taken into consideration for long-term AMD prevention since the EFB was decomposed by the microorganisms activity. Based on the result of a simulation on dry cover method combined with coal ash and organic material, leachate water shows an improvement in pH value and the reduction of metal

concentrations without negative impacts, meaning that the cover layer is effective for AMD prevention. Therefore, the utilization of these cover layer is promising to apply in the overburden dumping area.

Chapter 5 describes the effect of iron-oxidizing bacteria existence and the inhibition due to the application of a dry cover layer. The same leaching test as described in the Chapter 4 is utilized to understand the behavior of leachate water and metal dissolution that related to the iron-oxidizing bacteria. It is found out that AMD reaction is enhanced due to the existence of the iron-oxidizing bacteria in the PAF rock. Moreover, the effect of the iron-oxidizing bacteria on AMD reaction cannot be ignored by the conventional dry cover system. However, utilization of coal ash and organic material could inhibit the iron-oxidizing bacteria activity in the dry cover system. Additionally, the useful life of the cover system can be extended by increasing the thickness of the cover layer. Therefore, the materials are recommended to be used in a dry cover system as it could comprehensively reduce AMD generation, both biotic and abiotic conditions.

Chapter 6 summarizes the conclusions of each chapter, including the recommendations.

TABLE OF CONTENTS

ABSTRACT ii

TABLE OF CONTENTS vi

LIST OF FIGURES xi

LIST OF TABLES xiv

CHAPTER 1 1

Introduction 1

1.1 Background 1

1.2 Literature review 6

1.2.1 AMD generation process 6

1.2.2 Rock characterization of its geochemical properties 8

1.2.3 Prevention and treatment method 10

1.2.4 Dry cover system in overburden dumping area 12

1.3 Problem statement and objectives 13

1.4 Dissertation outline 14

CHAPTER 2 18

AMD issue in Indonesian coal mine and its current prevention countermeasure 18

2.1 Background 18

2.2 AMD in Indonesian coal mine 20

2.3 Site description: PT. Bukit Asam 21

2.3.1 Location and geological conditions 21

2.3.2 Field investigation of current AMD problems 22

2.4 Long-term potential of AMD generation 24

2.4.1 Sulfide mineral existence in the coal bearing rock 24

2.4.2 Geochemical characterization of rock on the Bukit Asam 27
2.4.3 Kinetic test study for predicting net acid producing potential reaction..... 30
2.5 Practice of AMD management: prevention method 32
2.5.1 Evaluation of dry cover strategies in overburden dumping to minimize oxygen ingress and water infiltration 32
2.5.2 Materials and methods 35
2.5.2.1 Materials 36
2.5.2.2 Methods 36
2.5.3 Results and discussions 37
2.6 Conclusions 41
CHAPTER 3 46
Fundamental study of coal ash and organic material composition and individual role to prevent AMD generation 46
3.1 Introduction 46
3.2 Fundamental studies of coal ash from coal-fired power plant..... 47
3.2.1 Materials and experimental method 47
3.2.1.1 Materials 47
3.2.1.2 Experimental methods 48
3.2.2 The characterization of coal ash 49
3.2.2.1 Physical properties..... 49
3.2.2.2 Particle size distribution 50
3.2.2.3 Shape and morphology by direct observation of micro-structure 51
3.2.2.4 Mineralogical characterization 54
3.2.3 The neutralization capacity of coal ash 58
3.3 Fundamental studies of organic material..... 61

3.3.1 Materials and experimental method 62
3.3.1.1 Materials 62
3.3.1.2 Experimental methods 62
3.3.2 The characterization of organic material 62
3.3.3 Oxygen consumption of organic material 66
3.5 Conclusions 68
CHAPTER 4 73
Study on the use of fly ash and organic material as a barrier cover on dry cover strategy73
4.1 Introduction 73
4.2 Addition of fly ash to PAF samples by using net acid generation (NAG) test..... 74
4.2.1 Materials and methods 74
4.2.2 Results 76
4.3 Fly ash usage due to its neutralizing capacity classification based on the net acid generation in blending variation 77
4.3.1 Materials and experimental method 78
4.3.1.1 Materials 78
4.3.1.2 Experimental methods 79
4.3.2 Result and discussion 80
4.4 Mixing and layering scenario of fly ash with high neutralizing capacity 82
4.4.1 Materials and experimental method 83
4.4.1.1 Materials 83
4.4.1.2 Experimental methods 83
4.4.2 Result and discussion 83
4.5 Fly ash usage due to its neutralizing capacity classification based on thickness variation 84

4.5.1 Materials and experimental method 84
4.5.1.1 Materials 84
4.5.1.2 Experimental methods 85
4.5.2 Result and discussion 86
4.6 Organic material as oxygen consuming barrier on dry cover strategies 89
4.7 Simulation of fly ash (coal ash) and empty fruit bunches (EFB) of fruit palm oil as cover layer by Free Draining Column Leach test 92
4.7.1 Materials and methods 92
4.7.1.1 Materials 92
4.7.1.2 Methods 97
4.7.2 Results and discussions 99
4.8 Conclusions 112
CHAPTER 5 117
Effect of fly ash and organic material as a cover layer of iron-oxidizing bacteria 117
5.1 Introduction 117
5.2 Iron-oxidizing bacteria growth from coal-bearing rock in mining 118
5.2.1 Materials and Methods 118
5.2.1.1 Materials 118
5.2.1.2 Methods 119
5.2.2 Result and discussions 122
5.3 Small and large column leaching test 127
5.3.1 Materials and methods 127
5.3.2 Results and Discussions 128
5.4 Conclusions 136
CHAPTER 6 138

Conclusions 138

6.1 Conclusions 138

ACKNOWLEDGEMENT 140

LIST OF FIGURES

Fig. 1.1 Number of new mine openings in different country categories (Soderholm & Svahn, 2015) 1

Fig. 1.2 Generalized conceptual model of sources, pathways and receiving environment (Ferguson, Borden, Verburg, & Bezuidenhout, 2009) 3

Fig. 1.3 Dry cover configuration (Natural Resources Canada, 2004) 4

Fig. 1.4 Stages in the AMD generation process (Broughton & Robertson, 1992) 7

Fig. 1.5 Anoxic limestone design (INAP, 2012) 11

Fig. 1.6 Example of waste rock encapsulation strategy (INAP, 2012) 12

Fig. 1.7 Variations of cover layer design (Hogan & Tremblay, 2010) 13

Fig. 2.1 Thermal coal exports (EIA, 2017) 18

Fig. 2.2 Map showing the generalized location of coal-bearing sequences in Indonesia (after Belkin et al., 2009) 19

Fig. 2.3 Bukit Asam mine location 21

Fig. 2.4 Regional stratigraphy of Bukit Asam 22

Fig. 2.5 Occurrence of AMD in the field 23

Fig. 2.6 Pyrite euhedral 25

Fig. 2.7 Pyrite framboidal 25

Fig. 2.8 Comparison of progressive oxidation with two pyrite morphologies: A. euhedral pyrite; B. framboidal pyrite (C.G. Weisener and P.A. Weber, 2010) 26

Fig. 2.9 Geochemical characterization of Bukit Asam coal-bearing rock 28

Fig. 2.10 Result of paste pH vs NAG pH 29

Fig. 2.11 Kinetic test results 31

Fig. 2.13 Current dry cover strategies practice on Bukit Asam 35

Fig. 2.14 Installation of oxygen and soil moisture sensor in PAF and NAF layer 36

Fig. 2.15 Bangko Barat dumping site; NAF and PAF layer; point measurement of investigation 37

Fig. 2.16 Geochemical characterizations of rocks in sampling point..... 38

Fig. 2.17 Water moisture and oxygen measurement result of NAF and PAF layer..... 40

Fig. 3.1 Transmitted-light microscopy result of coal ash..... 50

Fig. 3.2 Particle size distribution of coal ash..... 51

Fig. 3.3 SEM-EDX result of coal ash (top, left to right, 1000x: FA KYU, FA ADR and FA AI – middle, left to right, 1000x: FA KPC, FA ICA and FA BA – bottom, left to right, 40x: BA BA and BA ICA)..... 53

Fig. 3.4 Sequential extraction of coal ash..... 56

Fig. 3.5 Geochemical characterization of coal ash..... 60

Fig. 3.6 Paste pH vs NAG pH result of coal ash..... 61

Fig. 3.7 Inherent moisture content of organic material..... 63

Fig. 3.8 SEM EDX result of AI-OM..... 65

Fig. 3.9 SEM EDX result of SW-OM..... 65

Fig. 3.10 Oxygen reduction of organic material..... 67

Fig. 4.1 Fly ash addition to PAF high capacity..... 76

Fig. 4.2 Fly ash addition to PAF low capacity..... 77

Fig. 4.3 Comparison result of AD bottom ash and fly ash..... 81

Fig. 4.4 Comparison result of BA bottom ash and fly ash columns..... 82

Fig. 4.5 The pH measurement result for control column (upper figure) and blending and layering scenario (lower figure)..... 84

Fig. 4.6 Dimension of column and configuration of material within the column..... 86

Fig. 4.7 Hydraulic conductivity result of the columns..... 87

Fig. 4.8 pH measurement of simulation columns..... 88

Fig. 4.9 Thickness reduction of EFB in the field..... 92

Fig. 4.10 SEM image of Fly Ash 1000x (a), PAF Mix 2000x (b), NAF Mix 2000x (c), and EFB 1000x (d) 96

Fig. 4.11 Particle size distribution of material before the leaching test 97

Fig. 4.12 Leaching column configuration 99

Fig. 4.13 pH and EC leachate water measurement result 100

Fig. 4.14 Major cation-anion measurement result of each column 104

Fig. 4.15 Major cations and anions in the leachate water of column 106

Fig. 4.16 Portion of average concentration of major cations 107

Fig. 4.17 Dissolved organic carbon measurement 110

Fig. 4.18 SEM image of PAF layer 111

Fig. 5.1. Illustration of the grid in the hemocytometer 122

Fig. 5.2 The flask condition before shaking was started 123

Fig. 5.3 Sample solution condition after 30 days shaking 124

Fig. 5.4 Initial condition of plastic bottle in the mine 125

Fig. 5.5 Isolation growth of iron-oxidizing bacteria in the mine site 126

Fig. 5.6 Scenario of column leaching test with bacteria inoculation 127

Fig. 5.7 Scenario of large column leaching test 128

Fig. 5.8 Graphic of pH and EC result measurement 130

Fig. 5.9 Eh (oxidation-reduction potential) measurement 131

Fig. 5.10 Metal concentration with (a) and without (b) initial measurement 133

Fig. 5.11 Metal concentration with (a) and without (b) initial measurement (*cont.*) 134

Fig. 5.12 Result of the large column leaching test 135

LIST OF TABLES

Table 2.1 Indonesia details of coal production and usage 18

Table 2.2 Distribution of coal basin based on the geochemical properties 20

Table 2.3 Mined coal quality in Bukit Asam 22

Table 2.4 Summary of sampling point measurement 24

Table 2.5 Measurement results of several sampling points in surrounding overburden dumping area 35

Table 3.1 Coal ash samples 48

Table 3.2 Specific gravity of coal ash 50

Table 3.3 XRF result of coal ash 54

Table 3.4 Fly ash classification by ASTM C-618 55

Table 3.5 XRD result of coal ash 57

Table 3.6 Dehydration and dehydroxylation of some clays, oxides and salts as a function of temperature in ^{o}C 58

Table 3.7 Organic matter measurement result of organic material 64

Table 3.8 XRF measurement result of organic material 64

Table 3.9 Box dimension 67

Table 4.1 Classification of dry cover material based on its function 73

Table 4.2 XRF result of PAF rocks 75

Table 4.3 Geochemical characterization of PAF rocks 75

Table 4.4 Geochemical characterization of Type 1 78

Table 4.5 Geochemical characterization of Type 2 78

Table 4.6 Weight ratio of AD simulation column 79

Table 4.7 Weight ratio of fly ash and PAF rocks in the layering scenario 83

Table 4.8 Geochemical characterization of AI-FA, BA-FA and PAF 85
Table 4.9 Details of thickness within a column..... 85
Table 4.10 Property of several biomass of palm oil 90
Table 4.11 Decomposition water for oil palm biomass types 90
Table 4.12 Release of measured parameter by decomposition of EFB..... 91
Table 4.13 Geochemical characterization of samples 93
Table 4.14 Static test results of material for column test 94
Table 4.15 Organic matter measurement of EFB 94
Table 4.16 Result of XRF analysis for elemental composition..... 95
Table 4.17 Weight distribution of material in the column 98
Table 4.18 Statistic of leachate water measurement result..... 101
Table 4.19 Statistic data of major cation-anion measurement..... 102
Table 4.20 Statistic of metal concentration measurement result 108
Table 4.21 Surface element measurement of PAF and fly ash material..... 112
Table 5.1 PAF rock geochemical characterization..... 118
Table 5.2 XRF result of rock sample..... 119
Table 5.3 Static test result of rock sample in the field 119
Table 5.4 Physical changes and the bacteria presence observation..... 124
Table 5.5 Weight distribution for each layer in the column..... 128

CHAPTER 1

Introduction

1.1 Background

Mining industry gives a significant contribution to the country's income and consequently, it has an important role in developing economies of the region where mining takes place. As the economic growth increases, the energy demand within a country will also increase. This demand is mostly supplied by fossil energy, derived from unrenewable resources such as petroleum, natural gas or thermal coal. In order to meet the demand and develop economic state, extraction of the fossil energy is essential to be conducted. Every year an increasing number of new coal mine opening has been observed and as a result, the number of mine keeps expanding, as shown in Fig.1.1 (Söderholm & Svahn, 2015). Based on the data from 2000 until 2013, increasing number of new mines opening are generally increased, especially in the high-income countries. Despite the income level within a country (low-income and lower middle-income, upper middle-income and high income), the mining industry is still able to develop and therefore takes a major part in the economic wealth growth.

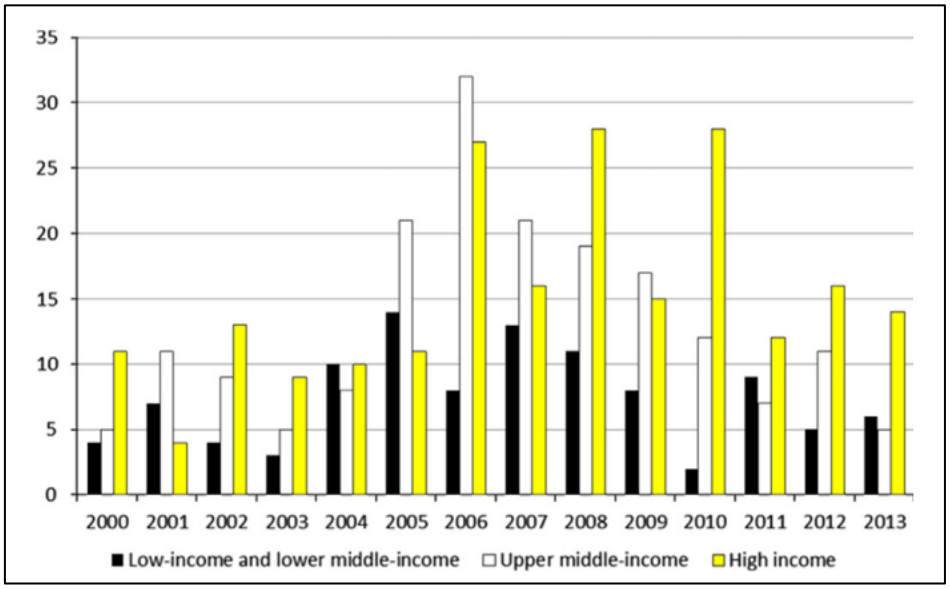

Fig. 1.1 Number of new mine openings in different country categories (Soderholm & Svahn, 2015)

Coal mining is one of the major parts of mining that provide worldwide energy. A lot of countries depend on thermal coal for generating the electricity that will be used

for industrial scale until household purposes. The United States have been using thermal coal as their primary source of electricity generation from 52% of the total fuel consumption in 2000 to 39% in 2013 (U.S. Energy Information Administration, 2015). It is decreased to 34% in 2040, accounts for primary fuel compare to natural gas (31% in 2040 and 27% in 2013) and nuclear (16% in 2040 and 19% in 2013). A similar trend is also shown by other countries. China and India, as current leading countries with the most rapid economic growth in the world, have increased their demand for natural gas and coal (Betz, Partridge, Farren, & Lobao, 2015) in order to fulfill their energy demands. As the result, development of new coal mines is inevitable in the world.

As the number of new coal mine openings is increased, negative impact that happens as the effect of coal extraction also arise. These negative impacts could be happened as indirect problems, such as global warming that is caused by the increasing carbon dioxide concentration in the atmosphere (released by the burning coal) or social problems in the region of mining location. On the other hand, negative impacts as direct problems can also take place. For example, the environmental degradation because of the removal of coal at the mine site or issue due to mining activity, i.e. flying rock, dust issue or AMD (AMD).

Among those problems, AMD is the prominent issue that should be controlled and well-treated. Mining, especially coal mining, is associated with AMD problems that occur on-site nevertheless the effect might be broadly affected the surrounding environment. AMD can cause long-term impairment to waterways and biodiversity as the effluents contain toxic substances that have serious impact to human health and ecology (Akcil & Koldas, 2006). Once occurring, AMD might last for years or even decades without human intervention; strictly depend on the availability of its sources.

Source of AMD on mining site could originate from various locations, e.g. tailings, waste rock stockpiles, etc., as provided in Fig 1.2. Numerous pathways of this acidic water are available, as runoff water, infiltration through mine waste or soil, groundwater and then pollute the received environment. In the nature, AMD is generated from a sulfide mineral that exposed to the atmosphere and leached by the water. Even though the sulfide mineral is a stable form, oxygen in the air has the capability to directly

oxidize sulfide mineral. Thus rightly after sulfide mineral exposure, metal cation and sulfate anion are produced by the oxidation reaction, together with the release of acidity in the water. It has consequences in lowering the water pH, increasing sulfate and dissolving other metal contents in the mineral (also might be from gangue minerals) that enclose to the sulfide mineral oxidation reaction and leachate water pathway. In the AMD reaction, numerous numbers of factors control the rate of sulfide oxidation, classified as chemical factors, physical factors and biological factors (Ferguson et al., 2009). Both of factors are dependent on each other, because one factor can affect the others during AMD generation process. Hence, it is important to study AMD in comprehensive point of view in order to have better control and treatment performed in the field site.

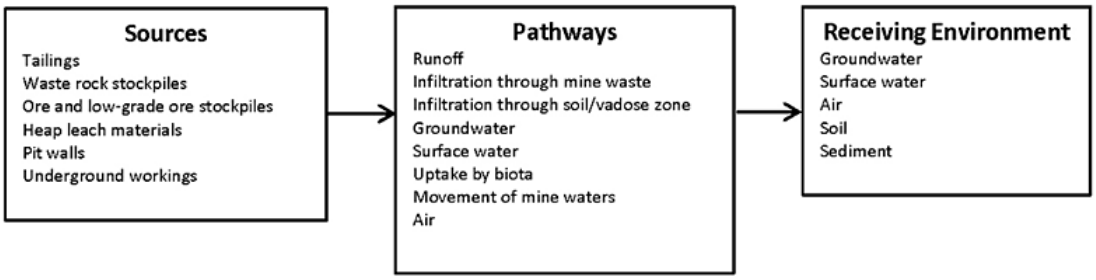

Fig. 1.2 Generalized conceptual model of sources, pathways and receiving environment (Ferguson, Borden, Verburg, & Bezuidenhout, 2009)

Prevention is always better than conducting treatment after AMD occurs. Before occuring, more options to treat acidic water are available compared to the after AMD formation stage. It also means prior to the generation, economical factor can be considered since mining company can choose an AMD management that suit them the best based on a lot of considerations. Therefore, AMD prevention is needed to minimize environmental pollution and avoid costly mitigation.

AMD prevention consists of several methods. Generally, a purpose of the prevention is the minimization of AMD factors. This includes oxygen supply, water infiltration and leaching, sulfide mineral availability and bacteria (related to biogeochemical process). Moreover, in the prevention method, maximizing the availability of acid neutralizing minerals or increasing the infiltrated water pH could be an option. So far, the best practice methods in mining site are special handling, segregation, encapsulation, dry and water cover (Lottermoser, 2010) while dry cover is

considered as the most effective method to minimize penetration of air and water. Dry cover is also an inexpensive method to be constructed, as the cover layer usually depends on the material availability on the mining site. Example of a dry cover configuration can be seen in the Fig 1.3. The common practice in dry cover is segregating non-acid forming rock material and potentially acid forming material, then placed the potentially acid forming below the non-acid forming. Subsequently, the material layer with acid forming potential is located underneath the non-acid forming rock layer. Non-acid forming layer thus cut off the oxygen supply and water infiltration.

Dry cover construction is moderately simple to be conducted. The numerous mining sites already applied this method in their field while several researches were conducted to study about the efficiency and long-term impact of dry cover to AMD (J. Kusuma, 2012; Natural Resources Canada, 2004; Soares et al., 2010). The problem with dry cover is the availability of material as the cover layer on the mining site, which is site specific, varies from site to site. The common problem that happens, especially in Indonesia, is the shortage amount of non-acid forming rock which limits the efficiency of cover layer to minimize the oxygen ingress and water percolation. Indeed, more than a few studies of geochemical characteristic in Indonesia showed great potential in generating AMD along with abundance in the total amount (J. Kusuma, 2012). Hence, the study of material that can be used as cover layer is vital to be performed.

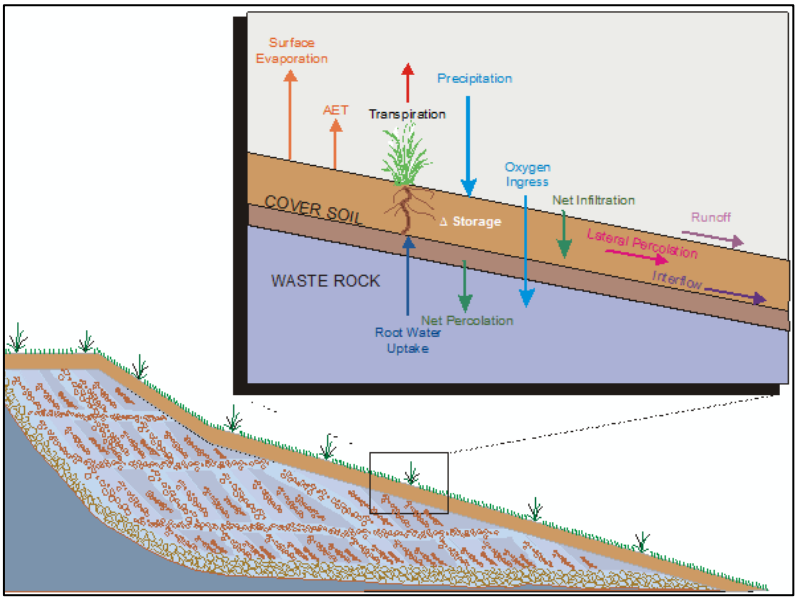

Fig. 1.3 Dry cover configuration (Natural Resources Canada, 2004)

Fly ash and organic material combination are considered as new material strategies which need further investigation in order to be utilized as the AMD countermeasure in overburden coal mine site. Fly ash, as the residue from unburned thermal coal, is the waste that produced from coal-steam power plant. This power plant is usually located near the coal mining site in order to reduce transportation cost between power plant and coal stockpile. Even though considered as waste, fly ash has several characteristics that beneficial in improving AMD quality (Yeheyis, Shang, & Yanful, 2008). Unfortunately, the utilization of fly ash is limited because of its classification as hazardous waste and should be managed well. In order to reduce the volume of fly ash utilization, the cover layer combination with other material is proposed and need further study.

Coal fly ash has been used for several purposes, by mixing with various material. Mixing of fly ash with mine tailings to control sulfides oxidation has been conducted, since the coal fly-ash, due to its alkaline nature, could increase the leachate water pH and stabilize the heavy metal concentration (Yeheyis, Shang, & Yanful, 2009). The study found out that a certain percentage of fly ash mixing with mine tailings may steadily increase the pH of effluent of water for 80 weeks consecutively, in the laboratory column test. Study of fly ash, red mud and bauxite ore mixing to immobilize the dissolved metals in the contaminated soil was also carried out (Ciccu et al., 2003). By adding the fly ash and red mud, leachate water from the contaminated soil drastically reduced, which indicate the capacity of fly ash also to stabilize the metals in the soil. The fly ash also could form a coating by Fe-precipitation on the sulfide mineral surface, in this case is pyrite, which prevent the oxidizing agent to have interaction with sulfide minerals (Pérez-López, Nieto, & de Almodóvar, 2007).

The organic material is chosen because of its ability to consume the oxygen during degradation process and the content of organic matter which can improve soil quality for vegetation. Application of organic materials has also been studied to be the control of AMD. Peppas, Komnitsas, & Halikia, 2000 discussed about the effectiveness of organic material to suppress oxidation of the reactive sulfides. The organic layer has high alkalinity, cation exchange and low permeability, which also can act as an oxygen barrier for reducing the oxidizing agent. Moreover, the organic matter also can precipitate the metal become the metal sulfides and oxyhydroxide.

The combination of fly ash and organic material is therefore expected to improve the AMD water quality and minimize the oxygen ingress and water percolation, even though non-acid forming material as dry cover layer is limited on the mining site. Moreover, by applying fly ash and organic material as cover material, it is expected to not only cut off the oxygen ingress and water percolation, but also reducing microorganism growth that could accelerate the AMD generation rate under acidic condition.

1.2 Literature review

1.2.1 AMD generation process

Sulfide minerals are common minor constituents of the Earth's crust (Lottermoser, 2010). Coal seams may contain abundant sulfide minerals that can be exposed during its exploitation stage. This will introduce the sulfide mineral to the oxidizing environment with oxygen as the oxidizer, therefore makes the sulfides will chemically unstable. Then it results in the weathering process.

Pyrite mineral is represented as a main source of acidity in the AMD process, because of the abundance and high reactivity compare to other minerals which produce acidity, H^+. The following reaction is a pyrite weathering that produces sulfate and also release soluble ferrous iron (Fe^{2+}) and acidity.

$$2FeS_{2(s)} + 7O_{2(aq)} + 2H_2O \rightarrow 2Fe^{2+} + 4SO_4^{2-} + 4H^+ \qquad \textit{Equation 1.1}$$

If sufficient dissolved oxygen is present, the dissolve ferrous iron will be oxidized to ferric iron and consuming the acidity.

$$2Fe^{2+} + 0.5O_2 + 2H^+ \rightarrow 2Fe^{3+} + H_2O \qquad \textit{Equation 1.2}$$

The AMD process can occur abiotically or biotically, with or without microorganisms presence. In acidic condition (below pH 4), oxygen's role in oxidizing ferrous iron to ferric iron is going under a slow rate that this process can be ignored (Stumm & Morgan, 1981). Microbial activity plays a vital role to accelerate the reaction above (i.e. *Acidithiobacillus ferooxidants*) in acid condition, oxidizing the ferric iron to ferrous iron to obtain metabolic energy, therefore the rapid formation of ferric iron could be achieved. This could happen by many orders of magnitudes faster than the

abiotic rate (Nordstrom & Southam, 1997). Microorganisms act as catalysts that do not change the reaction products while the contribution in accelerating the reaction cannot be ignored.

Ferric iron can react further and precipitate as iron oxyhydroxide to form ochre, then produce a greater net production of acid. Ferric iron can also react with remaining pyrite to produce acidity and also ferrous iron, in the rapid oxidation reaction than oxygen.

$2Fe^{3+} + 6H_2O \rightarrow 2Fe(OH)_{3(s)} + 6H^+$ *Equation 1.3*

$14Fe^{3+} + FeS_{2(s)} + 8H_2O \rightarrow 2SO_4^{2-} + 15Fe^{2+} + 16H^+$ *Equation 1.4*

Neutralizing minerals could buffer the reaction of acid generation, depend on the amount of alkalinity that could be produced. The carbonates generally produce higher neutralization than the rest of minerals, therefore the carbonate mineral occurrence can relatively improve the AMD water quality. The reaction of acid consumption from carbonates and silicates follow the reaction 1.5 and 1.6 below.

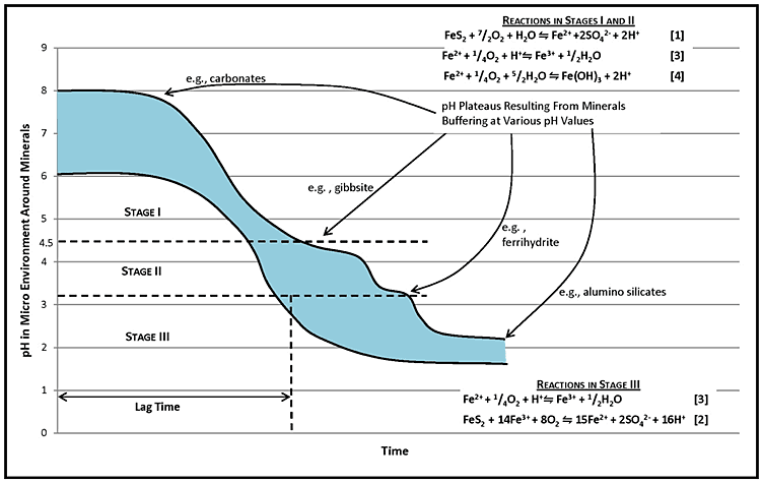

Fig. 1.4 Stages in the AMD generation process (Broughton & Robertson, 1992)

$CaCO_3 + H^+ \rightarrow Ca^{2+} + H_2O + CO_2$ *Equation 1.5*

$MeAlSiO_4(s) + H^+_{(aq)} + 3H_2O \rightarrow Me^{x+}_{(aq)} + Al^{3+}_{(aq)} + H_4SiO_{4(aq)} + 3)H^-_{(aq)}$ *Equation 1.6*

Note: (Me = Ca, Na, K, Mg, Mn or Fe)

However, when the sulfide mineral oxidation product is higher than the capability of acid consumption of available mineral, the lag time likely to establish (Fig. 1.4). This happens as consequences of the neutralizing process that initially happens thus increase the pH to near neutral, which follow by the rapid formation of AMD when the neutralizing is depleted, hence producing the acidic water. Therefore, even in the area

which seems to have no indication of producing AMD, the risk of acid generation possibly still occurs in the future. It is important to evaluate the risk of AMD by characterizing the acid forming and acid neutralizing nature of all rock types within mine site.

1.2.2 Rock characterization of its geochemical properties

Prediction of AMD potential is carried out by investigating the characteristic of rock geochemistry in capability to produce and consume acidity. This can be characterized by two methods: static and kinetic tests. In the mining site, it generally uses static test to characterize because this test not time-dependent. The common static test methods are the acid base accounting (ABA) based on Sobek et al. 1978, and net acid generation (NAG) test from (Miller, Robertson, & Donahue, 1997). The ABA method consists of paste pH and EC, total sulfur (TS) test and acid neutralizing capacity (ANC) test. Further explanation of this test is explained as follows:

Paste pH and EC

pH and EC are measured to the paste of the sample with a ratio of rock and distilled water is 1 : 2. Rock sample is pulverized beforehand in order to obtain a fine mixture of paste. In that way, the sulfide mineral is well oxidized after letting the paste reacts over night (12 to 16 hours). The determination of pH and EC is directly measured to the paste mixture of distilled water and powder sample, which indicate the inherent acidity and salinity of the rock within the initial exposition to the air.

Acid base accounting (ABA) method

In Indonesia, the most common total sulfur determination is based on the total sulfur determination by using LECO elemental analyzer (furnace) which the procedure follows Indonesian Standard, determination of total sulfur by ISO 334-1992, standard test method for forms of sulfur in coal by ASTM 2492 or total sulfur with X-ray fluorescence (XRF). Maximum potential acidity (MPA) then can be calculated from TS with assumption all of sulfur measured in the form of pyritic sulfur. The formula of MPA calculation is MPA (kg H_2SO_4/ton) = 30.625 x Total Sulfur (%).

Acid neutralizing capacity (ANC) test is determined with known amount of standardized hydrochloric acid (HCl) addition to the weighted powder sample which back-titrating afterwards with NaOH to calculate amount of acid consumption. This process aims to obtain quantification of the inherent acid buffering of sample after reacting the sample with strong acid. The acid consumption is reacted directly, with the aid from 1 to 2 hours heating to accelerate the reaction.

Based on the MPA and ANC results, NAPP is calculated by acid – base balance calculation method from the formula NAPP (kg H_2SO_4/t) = MPA – ANC

Net acid generation (NAG) test

The NAG measurement is carried out by adding hydrogen peroxide to the weighted pulverized sample. As a strong oxidizer, hydrogen peroxide forces the mineral to react, after allowing the reaction to happen for at least overnight then follow by heating to accelerate it. In the reaction, both acid generation and consumption simultaneously take place, therefore the measurement result of NAG pH indicates the net acid and/or base left in the rock sample after the acid producing and consuming occurred. Furthermore, after all of the reaction happens back-titrating to the pH 4.5 and 7.0 is carried out in order to know the residual acid amount. This value is expressed in unit kg H_2SO_4/t of rock sample.

Theoretically, NAPP and NAG test are complimentary to each other since NAPP informs the maximum of acid generation hypothetically while NAG test measures directly to the net result of both reactions.

Even though static test is really useful in geochemical characterization, it could not provide information about reaction rate of AMD generation since the characteristic of this test is one time measurement only. Therefore, in order to investigate the behavior of acidic water in the mine site, kinetic test could be an option. This test is intended to simulate the AMD generation, validate static test result and to determine reaction rate of AMD process and metal solubility, and AMD control technique simulation. The kinetic test usually consists of wetting, drying and flushing cycle, which are important to make sure unsaturated porous in the sample and oxygen can be available. The common

methods of kinetic test are column leach tests, humidity cell test, shake flask and Soxhlet reactor test.

1.2.3 Prevention and treatment method

AMD generation is a threat that should be avoided, because when it starts to generate the process could last for a long time. Theoretically, the process will be stopped when at least one of the reactants is depleted or not available anymore. Even though the AMD reaction certainly will stop, identification of when and how this reaction finish is difficult. Therefore, the best method for AMD management is to prevent the generation. This method is reliable, especially for AMD long-term management.

Even though prevention is the logical option, the lack of negative environmental awareness in the mine has been caused AMD treatment still broadly needed to control the acidic water. AMD treatment usually divided into two main methods, an active treatment and a passive treatment. An active treatment is where human power still needed to maintain the process of acidic water improvement, in the daily or regular basis. The example of active treatments are carbonate addition, pebble quick lime, etc. Meanwhile, a passive treatment generally does not need human intervention to control or manage the improvement process, this includes vertical flow pond, anoxic limestone drainage, anaerobic wetland, aerobic wetland and oxic limestone.

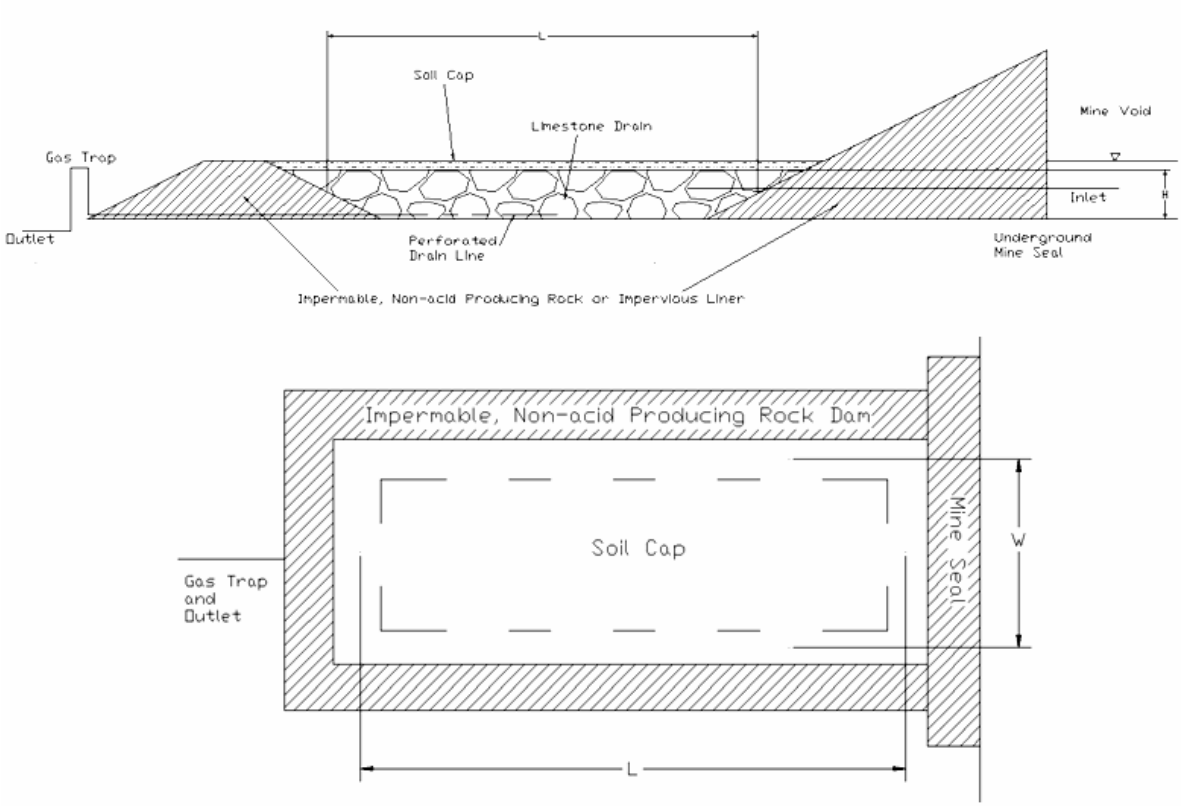

Fig. 1.5 Anoxic limestone design (INAP, 2012)

In the prevention and mitigation strategy of AMD, the basic approach is to reduce oxygen ingress and reduce the flow of water. As explained before, water acts as a transport medium for oxidation products, therefore it could pollute the water body and soil in the surrounding mine. In the coal mine, several techniques could be applied to prevent the AMD. This includes the use of low permeability covers or mixing the material with high pyrite content with alkaline material to neutralize the acid. Regarding the activity of mining, further prevention can be done to avoid AMD. Segregation of rock based on their acid producing capacity is a common method in surface coal mine. Based on the segregation, several prevention strategies can be constructed: dry cover, wet cover, encapsulation, etc. The prevention method can be chosen in term of several factors, from the availability of material, geochemical condition, engineering judgment until economical consideration. Fig. 1.6 shows an example of waste rock encapsulation strategy in mine site.

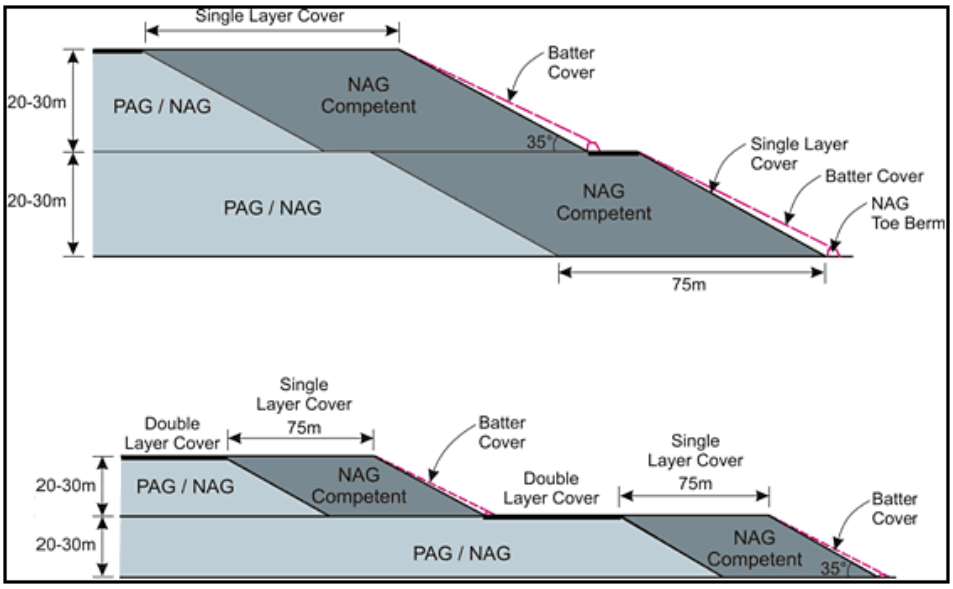

Fig. 1.6 Example of waste rock encapsulation strategy (INAP, 2012)

1.2.4 Dry cover system in overburden dumping area

The practice to prevent AMD generation in dumping material has been variously carried out in Indonesia mine. Generally, in ore mining, encapsulation and blending methods are favorable method. Gold mine in Mt. Muro is one example of mines that used encapsulation method. In Freeport Indonesia gold mine, has utilized the blending of acid-producing rock with limestone to prevent AMD in overburden and tailing management. Meanwhile, in the coal mining, KPC as one of the biggest coal mine in Indonesia has developed the dumping method based on the geochemical characterization. This consists of three main designs: low effort, medium effort and high effort, which vary based on the compaction and material segregation. Similar to KPC, PT Bukit Asam and Berau Coal have been also developing the prevention method that appropriates with their condition. However, numerous mining companies in Indonesia have not been considered the prevention method yet and constructed the waste dumping area without the geochemical characterization. In this case, it is important to have techniques to prevent AMD without rehandling the material, since it seems impossible based on the economical consideration. Dry cover method, as the common AMD prevention in the world, could serve a solution for this problem.

Dry cover is a protective layer placed over mine waste. This term as “dry” is in contrast with water or “wet” cover (INAP, 2012). The main objective of this cover layer

is to reduce AMD generation and its transport to the receiving environment. Due to the characteristic of a material that is constructed in the dry cover, this method should be developed on a case-by-case basis, with consideration of the short-term and long-term impacts. Based on the type of cover layer, dry cover is divided into soil cover, alkaline cover, organic cover, cover of sulfide-bearing but net neutralizing material and synthetic cover. Moreover, the multi-layer cover also can be constructed to increase the performance of the prevention. This variation depends on the material cost and availability within the mine. The illustration of this concept is provided in the Fig. 1.7.

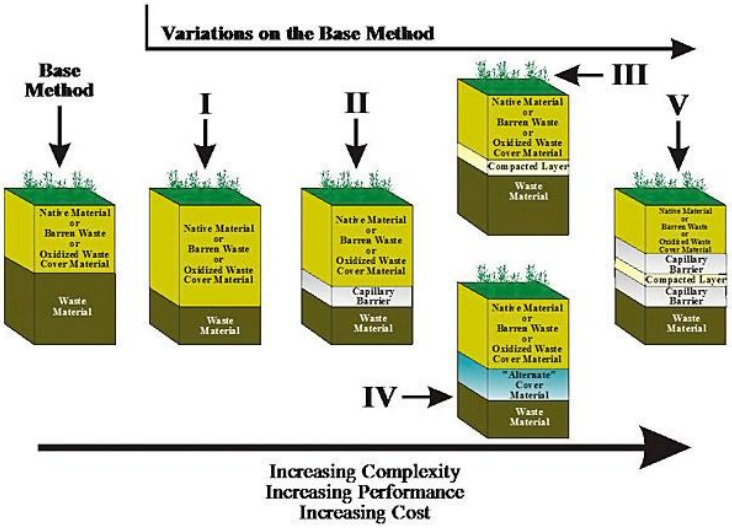

Fig. 1.7 Variations of cover layer design (Hogan & Tremblay, 2010)

1.3 Problem statement and objectives

Due to the need of preventing AMD generation in the coal mining area, this study is proposed. Furthermore, the situation of Indonesia coal mine that has problems with large volume of potential acid producing rock than non-acid producing rock make the prevention strategy more challenging. Therefore, this research is intended to acknowledge the effective use of new cover layer on the coal mine, fly ash and organic material combination, as the long-term prevention strategy to deal with the AMD formation in regard to the excessive of potentially acid producing capacity. Comprehensive review of the overburden dumping area will be conducted, in order to understand the oxidation of sulfide minerals in the dump, which greatly depend on the reacting agents: water and oxygen. The attempt to comprehend both reactants

distribution and flow will be carried out and utilize for long-standing prediction of this cover layer strategy.

Since the amount of coal mines that already near to the closure stage escalate, concern of AMD prevention and control also increase as the pollution from the high dissolved metal concentration with acidic mine effluent likely occurring. Therefore, with a better understanding of the configuration of the overburden dumping site, includes the design construction, the oxidation of sulfides, the distribution and flow pattern of reacting agents, the prevention strategy might be more efficient and effective. Moreover, by studying the new material which is economical and appropriate the prevention of AMD in the mine site could be more feasible to be applied.

1.4 Dissertation outline

This dissertation consists of 6 chapters which briefly describe as follows:

Chapter 1 includes the introductory part of this study, explains about the background of Indonesia current coal mining situation, AMD generation process within the mine especially overburden dumping area, and the prevention method of AMD. The problem statements and objectives of the studies, as well as an outline of the dissertation are also introduced in this chapter.

Chapter 2 explains about the current condition of Indonesia coal mine that related to AMD issues. One of Indonesian coal mines is selected and investigated for its AMD problem, including the sulfide mineral and geochemical capacities of coal-bearing rocks. Dry cover method that is applied in this mine also investigated for its effectiveness to reduce oxygen and water infiltration.

Chapter 3 discusses about the selected materials that can be used to overcome AMD issues on dry cover method: coal ash and organic material. Due to the various materials availability and also coal mining that different in characteristics of coal-bearing capacity, which make the dry cover system varies from one site to another site, different types of coal ash and organic material are compared. Furthermore, coal ash is classified into groups that can be useful in determining the dry cover method based on the coal-bearing rock characterization..

Chapter 4 studies about the applicability of those materials in the dry cover system by mainly utilizing column leach test in the laboratory. Leachate water behavior of this simulation then analyzed to understand the effect of those material additions to the coal-bearing rock. In addition, the organic material is also studied for long-term placement in dry cover system.

Chapter 5 discusses about the iron-oxidizing bacteria existence and inhibition due to the application of dry cover layer. The same leaching test as describe in the previous chapter is utilized in order to understand the behavior of leachate water and metals dissolution that related to the iron-oxidizing bacteria.

Chapter 6 summarized the conclusions of each chapter, including the recommendations.

References

Akcil, A., & Koldas, S. (2006). Acid Mine Drainage (AMD): causes, treatment and case studies. *Journal of Cleaner Production*, *14*(12–13 SPEC. ISS.), 1139–1145. https://doi.org/10.1016/j.jclepro.2004.09.006

Betz, M. R., Partridge, M. D., Farren, M., & Lobao, L. (2015). Coal mining, economic development, and the natural resources curse. *Energy Economics*, *50*, 105–116. https://doi.org/10.1016/j.eneco.2015.04.005

Ciccu, R., Ghiani, M., Serci, A., Fadda, S., Peretti, R., & Zucca, A. (2003). Heavy metal immobilization in the mining-contaminated soils using various industrial wastes. *Minerals Engineering*, *16*(3), 187–192. https://doi.org/10.1016/S0892-6875(03)00003-7

Ferguson, K., Borden, R., Verburg, R., & Bezuidenhout, N. (2009). INAP ' s Global Acid Rock Drainage Guide 1, (2), 1–14.

Hogan, C. M., & Tremblay, G. A. (2010). The Canadian MEND program. *AusIMM Bulletin*, (3), 50–51.

INAP. (2012). Global Acid Rock Drainage Guide, INAP: The International Network for Acid Prevention. Retrieved from http://www.gardguide.com

J. Kusuma, G. (2012). An Evaluation on the Physical and Chemical Composition of Coal Combustion Ash and Its Co-Placement with Coal-Mine Waste Rock. *Journal of Environmental Protection*, *03*(07), 589–596. https://doi.org/10.4236/jep.2012.37071

Lottermoser, B. (2010). *Mine Wastes*. https://doi.org/10.1007/978-3-642-12419-8

Natural Resources Canada. (2004). Design, construction and performance monitoring of cover systems for waste rock and tailings: Volume 2 - Theory and background. *OKC Report No. 702-01, MEND 2.21*.(July).

Peppas, A., Komnitsas, K., & Halikia, I. (2000). Use of organic covers for acid mine drainage control. *Minerals Engineering*, *13*(5), 563–574. https://doi.org/10.1016/S0892-6875(00)00036-4

Pérez-López, R., Nieto, J. M., & de Almodóvar, G. R. (2007). Utilization of fly ash to improve the quality of the acid mine drainage generated by oxidation of a sulphide-rich mining waste: Column experiments. *Chemosphere*, *67*(8), 1637–1646. https://doi.org/10.1016/j.chemosphere.2006.10.009

Soares, A. B., Possa, M. V., de Souza, V. P., Soares, P. S. M., Barbosa, M. C., de Oliveira Ubaldo, M., … Borma, L. S. (2010). Design of a Dry Cover Pilot Test for Acid Mine Drainage Abatement in Southern Brazil, Part II: Pilot Unit Construction and Initial Monitoring. *Mine Water and the Environment*, *29*(4), 277–284. https://doi.org/10.1007/s10230-010-0126-0

Sobek, A. A., Schuller, W. A., Freeman, J. R., & Smith, R. M. (1978). Field and Laboratory Methods Applicable to Overburdens and Minesoils.

Söderholm, P., & Svahn, N. (2015). Mining, regional development and benefit-sharing in developed countries. *Resources Policy*, *45*, 78–91. https://doi.org/10.1016/j.resourpol.2015.03.003

U.S. Energy Information Administration. (2015). Annual Energy Outlook 2015. *Office of Integrated and International Energy Analysis*, *1*, 1–244. https://doi.org/DOE/EIA-0383(2013)

Yeheyis, M. B., Shang, J. Q., & Yanful, E. K. (2009). Long-term evaluation of coal fly ash and mine tailings co-placement: A site-specific study. *Journal of Environmental Management*, *91*(1), 237–244. https://doi.org/10.1016/j.jenvman.2009.08.010

Broughton, L. M., & Robertson, A. M. (1992). Acid Rock Drainage from Mines - Where We Are Now. *IMM Minerals, Metals and Environment Conference*. Manchester.

Miller, S., Robertson, A., & Donahue, T. (1997). Advances in acid drainage prediction using the net acid generating (NAG) test. *Proceedings Fourth International Conference on acid rock drainage, II*, hal. 533–547. Vancouver, B. C. Canada.

Nordstrom, D., & Southam, G. (1997). Geomicrobiology of sulfide mineral oxidation. (J. Banfield, & K. Nealson, Penyunt.) *Geomicrobiology: Interactions Between Microbes and Minerals, 35*, hal. 361-390.

Stumm, W. M., & Morgan, J. J. (1981). *Aquatic Chemistry: An Introduction Emphasizing Chemical Equilibria in Natural Waters.* New York: John Wiley & Sons.

Yeheyis, M. B., Shang, J. Q., & Yanful, E. K. (2008). Characterization and environmental evaluation of Atikokan coal fly ash for environmental applications. *Journal of Environmental Engineering and Science, 7*(5), pp. 481-498.

CHAPTER 2

AMD issue in Indonesian coal mine and its current prevention countermeasure

2.1 Background

Coal mining is a prominent economic sector in Indonesia that gives a significant contribution to the national income. In the worldwide market, Indonesia is considered as one of the largest coal producer and exporter of thermal coal in the world. Start from early 1990's coal mining in Indonesia has grown rapidly that was able to surpass Australia's coal production, the global leading coal producer country over decades, in 2005. Currently, in term of exported thermal coal, Indonesia is in the stable position as the second exporter country after Australia. Fig. 2.1 provides the current and projected condition of coal export in the world based on the data of U.S. Energy Information Administration report, The Annual Energy Outlook. Exported thermal coal from Indonesia includes the intermediate rank coal (5,100 – 6,100 kcal/kg) and low rank coal (under 5,100 kcal/kg) which mostly demanded from India and China.

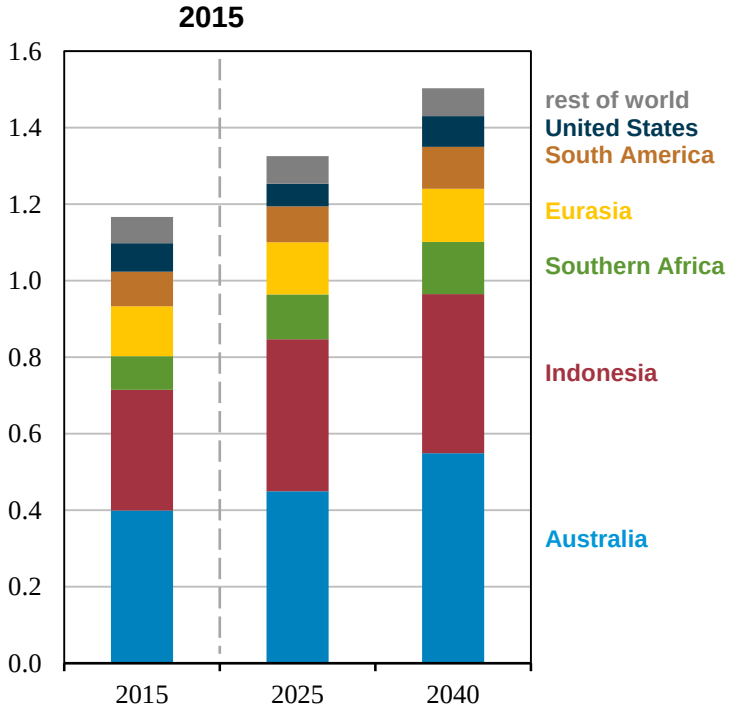

Fig. 2.1 Thermal coal exports (EIA, 2017)
Table 2.1 Indonesia details of coal production and usage

	2014	2015	2016	2017	2018	2019
Production (in million tonnes)	458	461	456	461	425[1]	400[1]
Export (in million tonnes)	382	375	365	364	311[1]	160[1]
Domestic (in million tonnes)	76	86	91	97	114[1]	240[1]
Price (USD/ton)	72.6	60.1	61.8	n.a.	n.a.	n.a.

[1]predicted

Furthermore, not only Indonesia coal export, but also its domestic coal consumption increased from 49 million tonnes in 2007 to 76 million tonnes in 2014. Due to the domestic market obligation (DMO) from government, it is further increased to 97 million tonnes in 2017 as provided in Table 2.1.

Indonesia ranks in the 9th position of its global coal resources, which around 2.2% of total global coal resources based on BP Statistical Review of World Energy. Almost 60% of the coal resources in Indonesia are a low calorific value which classified as sub-bituminous, spread in small deposit all over the Indonesian area: Sumatera, Jawa, Kalimantan, Sulawesi and Papua Island (Indonesia 2011). However, a considerable amount of coal resources is concentrated in South Sumatera, South Kalimantan and East Kalimantan province (Belkin, Tewalt, Hower, Stucker, & O'Keefe, 2009).

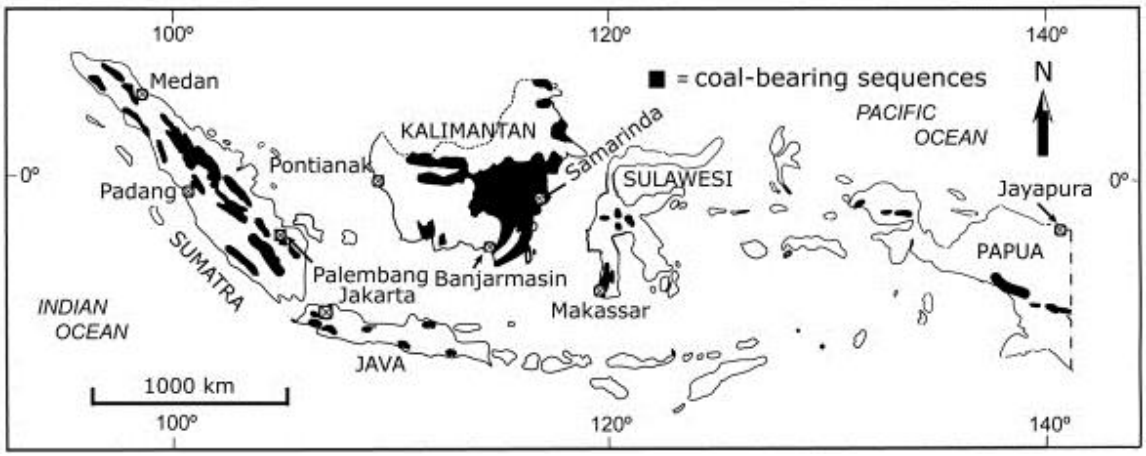

Fig. 2.2 Map showing the generalized location of coal-bearing sequences in Indonesia (after Belkin et al., 2009)

Indonesia has a tropical humid climate (Peel, Finlayson, & McMahon, 2007) and relatively high rainfall. Correspondingly, rapid wet and dry cycle caused by that condition will influence the rate of physical rock weathering (Sadisun, Shimada, Ichinose, & Matsui, 2005). The high rate weathering process is expected which turns the

hard-rock to soft-rock and make it susceptible to further physical and chemical processes (Bienawaski, 1989; Kramadibrata, Matsui, Rai, & Shimada, 2002). Moreover, along with the large potential in generating AMD of coal-bearing rock in Indonesia as stated in Table 2.2 (Gautama & Kusuma, 2008) will increase the possibility of AMD to be generated.

Table 2.2 Distribution of coal basin based on the geochemical properties

Basin	Sample position	Total sample	Type	
			NAF	PAF
Central Sumatera	Roof	4	0	4
	Over/inter-burden	5	4	1
	Floor	6	4	2
South Sumatera	Roof	4	1	3
	Over/inter-burden	12	4	8
	Floor	1	0	1
Barito	Roof	11	4	7
	Over/inter-burden	6	3	3
	Floor	7	7	0
Kutai	Roof	3	1	2
	Over/inter-burden	0	0	0
	Floor	3	0	3
Tarakan	Roof	2	1	1
	Over/inter-burden	0	0	0
	Floor	9	6	3
TOTAL		73	35	38

Following the unique climate and high potential in producing acidic water in the coal mine, study of the AMD generation is needed to be carried out comprehensively. By understanding the process, the appropriate prevention method can be applied, which minimize the risk of acidic water to pollute the environment. Therefore, this chapter focuses on the site investigation on one of the significant coal mines in Indonesia. Existing acid mine problems, the causes, potential and current prevention method are investigated.

2.2 AMD in Indonesian coal mine

As explained in the previous section, one of main coal resources in Indonesia is located in South Sumatera Province. The largest coal mine company in this area is PT Bukit Asam that belongs to the Indonesia government under state-owned enterprise management. Details on the investigation result of this coal mining are explained as follows.

2.3 Site description: PT. Bukit Asam

2.3.1 Location and geological conditions

PT Bukit Asam that has been commenced since 1919, lies on the 103^{o} 45’ – 103^{o} 50’ East longitude and 3^{o} 42’ 30” – 4^{o} 47’ 30” South latitude. Its mine permit covers ± 7,700 ha, including Tanjung Enim area, in South Sumatera Province. Coal in Bukit Asam is deposited in the South Sumatera Tertiary sedimentary basin, belonging to the Muara Enim Formation as the main coal bearing formation. Currently, there are three active mines in PT Bukit Asam: Tanjung Air Laya (TAL), Muara Tiga Besar (MTB – Northern Part or MTBU and Southern Part or MTBS) and Bangko Barat (BB). Detail of the mine location is provided in Fig. 2.3.

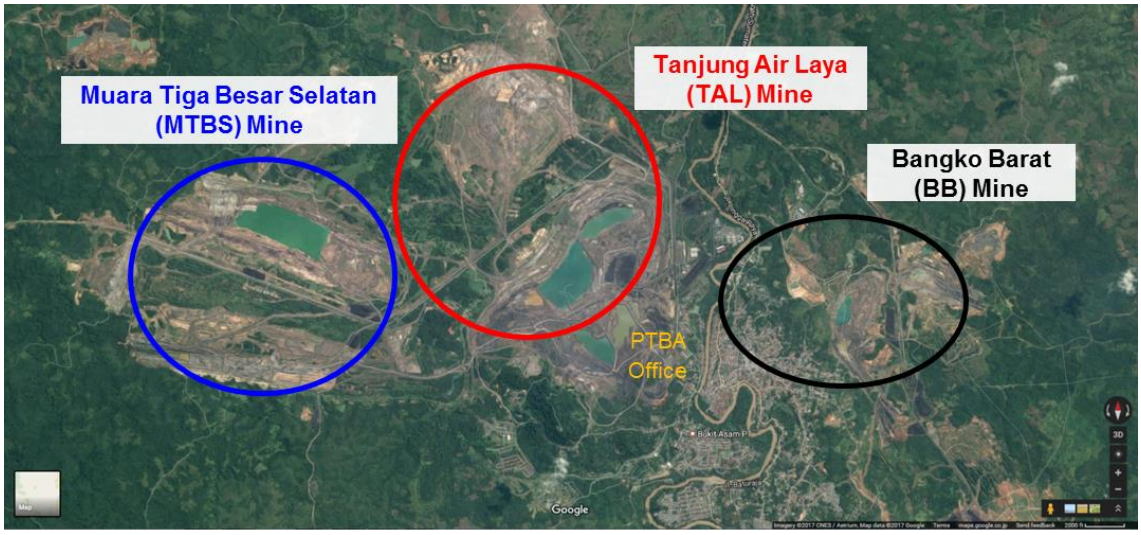

Satellite view, DigitalGlobe 2016, CNES / Astrium

Fig. 2.3 Bukit Asam mine location

The area of PT Bukit Asam is characterized by magmatic intrusion activity that improves the coal quality and controls the geological structural features (R. S. Gautama, 1994). Three coal seams are being mined in PT Bukit Asam, including Mangus or A seam (splits into two seams, A1 and A2), Suban or B seam (splits into two seams, B1 and B2) and lastly Petai or C seam (see Fig. 2.4). Overburden and interburden in Bukit Asam are mainly consisted of sandstone, siltstone, claystone and tuff.

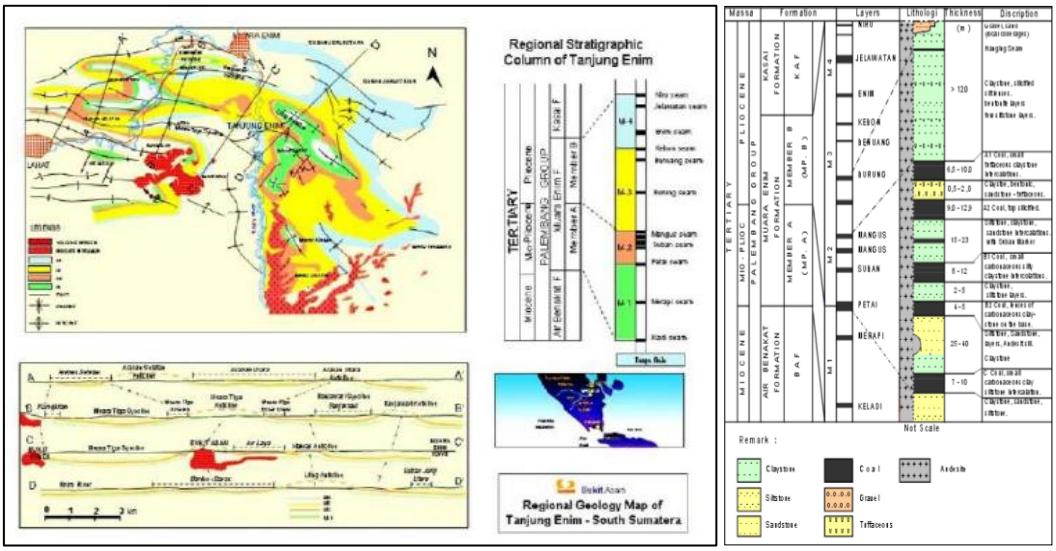

Fig. 2.4 Regional stratigraphy of Bukit Asam

Most of the coal in PT Bukit Asam is categorized as steam coal with intermediate calorific value. Table 2.3 explains the quality of coal in PT Bukit Asam. However, due to the intrusion activities, the distribution of coal is heavily influenced. As the consequences, anthracitic coal is also found in the surrounding intrusive bodies, and the calorific value decreased as the coal distance (R. S. Gautama, 1994). Therefore, a coal with higher calorific value (anthracite) is also mined in PT Bukit Asam.

Table 2.3 Mined coal quality in Bukit Asam

Parameter	BA 55	BA 59	BA 63	BA 67	BA 70
CV (kkal/kg, adb)	5,500 – 5,600	5,601 – 6,000	6,100 – 6,400	6,401 – 6,800	6,801 – 7,200
TM (%, ar)	23.76 – 29.64	23.54 – 29.51	19.47 – 28.52	13.57 – 20.32	9.44 – 15.89
IM (%, adb)	11.79 – 18.12	11.10 – 15.91	9.80 – 13.54	6.56 – 10.74	4.46 – 8.09
Ash (%, adb)	4.48 – 10.90	3.41 – 7.56	2.58 – 6.27	2.30 – 6.93	2.25 – 5.86
VM (%, adb)	36.67 – 40.70	38.34 – 42.06	39.61 – 42.76	39.86 – 42.99	40.17 – 41.00
FC (%, adb)	36.70 – 40.15	39.06 – 42.30	41.29 – 44.08	43.48 – 46.95	46.40 – 49.70
TS (%, adb)	0.12 – 1.01	0.08 – 0.94	0.53 – 1.87	0.21 – 0.93	0.17 – 1.18

2.3.2 Field investigation of current AMD problems

Since the operation started in 1919, the very first known AMD problem had been detected in 1992 which indicated by the acidic water in the East Klawas pond. Starting then, several AMD problems have been occurring in PT Bukit Asam up to now. The water quality measured in several places is very low in pH, for example in Bangko Barat. The water quality in Bangko Barat indicated that the water pH is less than 4, high

sulfate concentration of 600 – 3,000 mg/l, Fe concentration of 3 – 4 mg/l and Mn one is 4 – 8 mg/l (Gautama and Lindawati 1995). Similar problems could also be found in other mines, TAL and MTB, even though not as severe as in Bangko Barat. Hence, several methods to control AMD in those mines have been carried out. These methods include the addition of hydrated lime to the ponds in each coal mine in order to increase the water pH, the installation of settling ponds with several compartments that allow the solid particles to settle in the bottom part of the pond, and separation of waste rock based on the PAF and NAF rock (Rudy Sayoga Gautama, 2011). Currently, even though not evenly, there is an attempt to conduct dry cover method in the overburden dumping area by rock chemical segregation. Since this method is relatively new to be applied, detailed investigation of the impact of this method rarely to be conducted.

Site investigation carried out in 2016 found that most of the water in surrounding mine has a pH value below 5, which is very low and categorized as acidic water (see Fig. 2.5). Water in the several sampling points in the sump, accumulated water located on the face of mining activity, have pH value 3.90, 3.93 and 3.14 in MTBS, TAL and BB, respectively. Furthermore, the measurement of water in the outlet area of the overburden dumping area also shows the result of very acidic water. During the rainy season, volume of acidic water is large, hence the water in the treatment area after lime addition still acidic even if the number is slightly higher than the water on the site. Detail of the measurement result is presented in Table 4.

Fig. 2.5 Occurrence of AMD in the field

Table 2.4 Summary of sampling point measurement

Sampling Point	Measurement Date	On-site Measurement pH	EC (mS/cm)
Outflow water on revegetated dump area in Bangko Barat (BB) Mine	February 2016	3.6	0.65
Outflow water on revegetated dump area in BB Mine 2		3.8	1.10
Discharge water after lime addition in BB Mine		4.8	0.63
Pit sump in Muara Tiga Besar Selatan (MTBS)		3.9	1.00
Pit sump in Tanjung Air Laya (TAL)		3.9	1.05
Pit sump in Bangko Barat (BB)		3.1	1.50

2.4 Long-term potential of AMD generation

AMD generated during the life of mine is easier to be treated. Active treatment, such as lime addition, can solve the water pollution in the short-term due to readily resources as the company still exploits that area. However, when the area is mined out, the treatment of AMD can be difficult to be conducted. Therefore, potential of acid mine generation in the long-term is observed. One of the prominent sources of long-term acidic source is in the overburden dumping area. The availability of sulfide minerals, after excavated and re-dumped in certain area, will undergo a weathering process, and produce acid in a long period of time no prevention method is carried out.

2.4.1 Sulfide mineral existence in the coal bearing rock

Rock is collected from several boreholes of full coring and exposed area in the mine pits: MTBS, TAL and BB. Basically, the coal-bearing rock in PT Bukit Asam consists of overburden A1, interburden A1 – A2, interburden A2 – B1, interburden B1 – B2 and interburden B2 – C. Based on the polished thin-section of samples with magnification 100X, the samples are dominated by clay minerals, with also the presence of quartz, feldspar, iron oxide and carbonate that already weathered into the size similar to clay minerals. The sulfide mineral, pyrite, is also ubiquitous on the most of the samples.

Pyrite, as a main mineral to produce AMD, is found in the shape of euhedral with size less than 100μm (Fig. 2.6) and also framboidal with size less than 50μm (Fig. 2.7). The euhedral pyrite is in the single mineral occurrence while the framboidal looks agglomerated in the shape look like framboise. Hence, the surface reaction of framboise is larger, that make it easier to be oxidized and produce AMD. Based on the occurrence, euhedral shape is significantly less to be seen compared to the framboidal. Therefore, the AMD in the coal mine is reacted faster than in the ore mining, due to the mineral shape that differ in surface reaction.

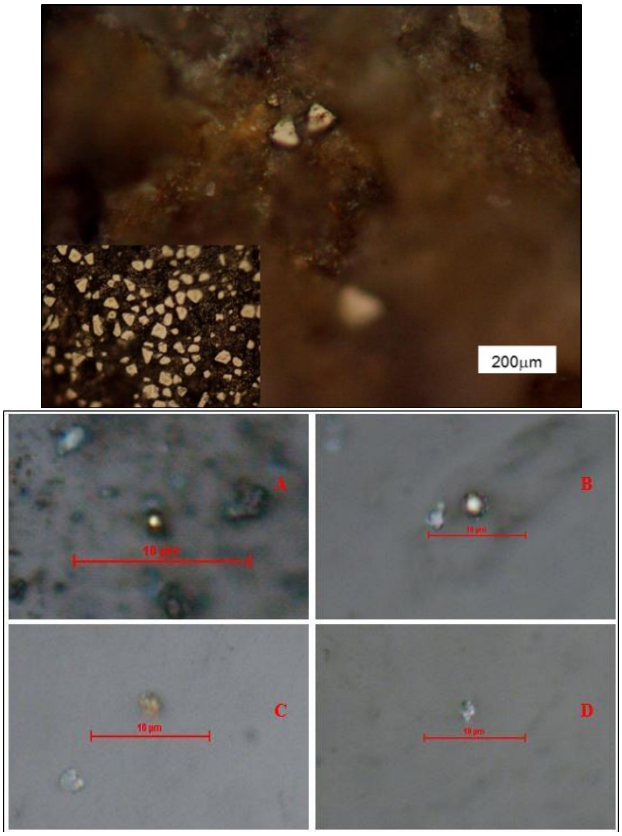

Fig. 2.6 Pyrite euhedral

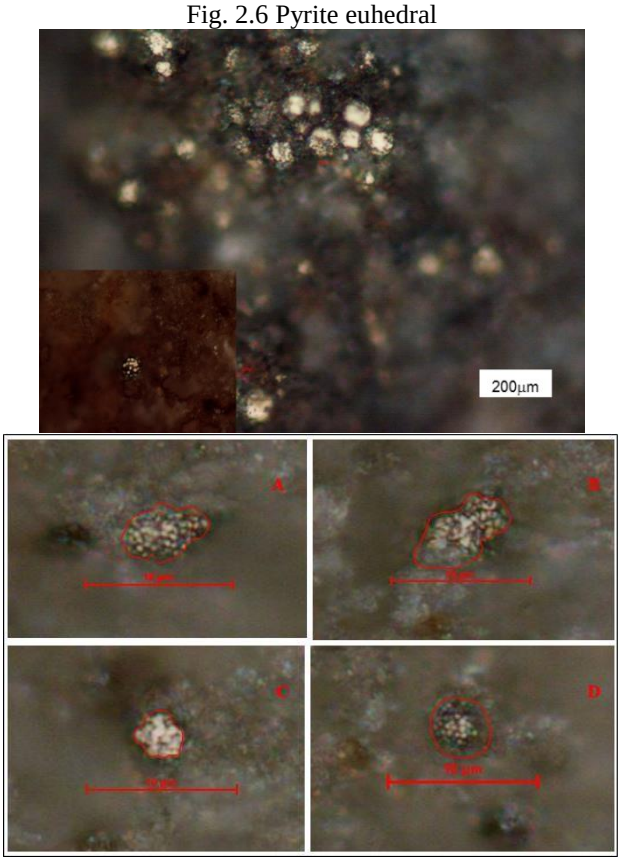

Fig. 2.7 Pyrite framboidal

Several past studies have been attempted to distinguish the difference of of euhedral and framboidal crystal minerals to the altered formation within the minerals. The interesting finding was shown from C.G. Weisener and P.A. Weber study (2010). In their work, the kinetic test (humidity cell test) was carried out for total 390 days to the sedimentary rocks that contained both crystal structures of pyrite. The alteration changes due the progressive oxidation was observed in time basis. Fig. 2.8 shows the result of the experiment.

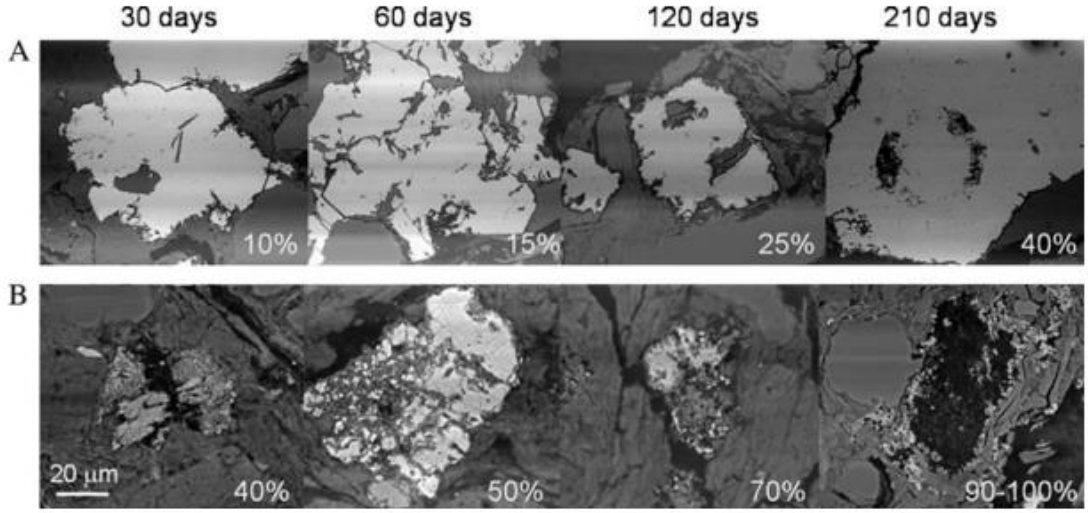

Fig. 2.8 Comparison of progressive oxidation with two pyrite morphologies: A. euhedral pyrite; B. framboidal pyrite (C.G. Weisener and P.A. Weber, 2010)

Percentage of alteration was stated briefly in the figure. It can be seen that due to the continuous day and night simulation to the sedimentary rock, pyrite was altered as the consequence of oxidation. Weathering phenomenon is happened to the rock, thus changed the morphology of the crystal. However, crystal alteration happens in different rate to the each shape of pyrite. Framboidal pyrite undergone faster alteration compared to euhedral pyrite. In the final stage of the experiment, 100% of the framboidal pyrite had been replaced with alteration products while euhedral pyrite only 42±5% had altered. Therefore, in the AMD generation within the coal mine, this difference could affect acidic water production. Because of crystallographic defect, short term elevated acid generation rates are due to framboidal pyrite oxidation while long-term acid generation might be derived from euhedral pyrite oxidation. The continuous AMD generation in the long-term with relatively fast reaction is expected in Bukit Asam mine.

2.4.2 Geochemical characterization of rock on the Bukit Asam

Result of geochemical characterization of PT Bukit Asam was provided in the graph on Fig. 2.8. The rock samples were obtained from the core drilling of PT Bukit Asam from the surface until certain depth that represents lithology of each mine and tested on-site in Bukit Asam laboratory. After the static test is carried out, the data can produce geochemical model within the mine site. Thus, the geochemical model then can be used further for overburden excavation and placement planning (R.S. Gautama & Hartaji, 2004).

Results of static test were provided in the Fig. 2.9. It clearly shows the high capacity of acid production in the rocks, as the result categorized numerous rock samples to PAF area (Smart et al., 2002). Rock is classified as PAF if the NAG pH $\leq$ 4.5 and the NAPP $\geq$ 0 kg H_2SO_4 (Miller, Robertson and Donahue 1997). The rest of geochemical classification can be seen in the area division on the graph. The more positive value of NAPP of rock, indicates the higher capacity in producing acid while a more negative value informing that less capacity in producing acid and higher capacity in neutralizing the acidity within the system. Other classification (Dumble & Ruxton, 2003) further divides PAF and NAF to be low capacity and high capacity based on the NAPP results, by obtaining the ratio of Acid Neutralizing Capacity (ANC) divided by Maximum Potential Acidity (MPA). Subtraction of MPA and ANC results in NAPP value.

Rocks classified as PAF is dominant compared to others classification. 53% of rock samples are categorized as PAF, with 11% rocks have NAPP > 50 kg H_2SO_4/ton, 29% rocks have NAPP between 10 – 50 kg H_2SO_4/ton and 13% rocks have NAPP between 0 – 10 kg H_2SO_4/ton. Meanwhile, 41% rocks are uncertain and 6% rocks are NAF. It means, only 5 samples out of 80 samples are classified as NAF. Moreover, all of NAF rock samples have NAG pH $\leq$ 6.0 that show the less to no neutralizing capacity. In addition, 4 out 4 NAF samples were situated in Bangko Barat. Therefore, the severe AMD problem is expected from PT Bukit Asam mines. Shortage of NAF amount with a deficiency in neutralizing potential is also observed in all of mines. Thus, these mines will tend to produce acidity when react to water.

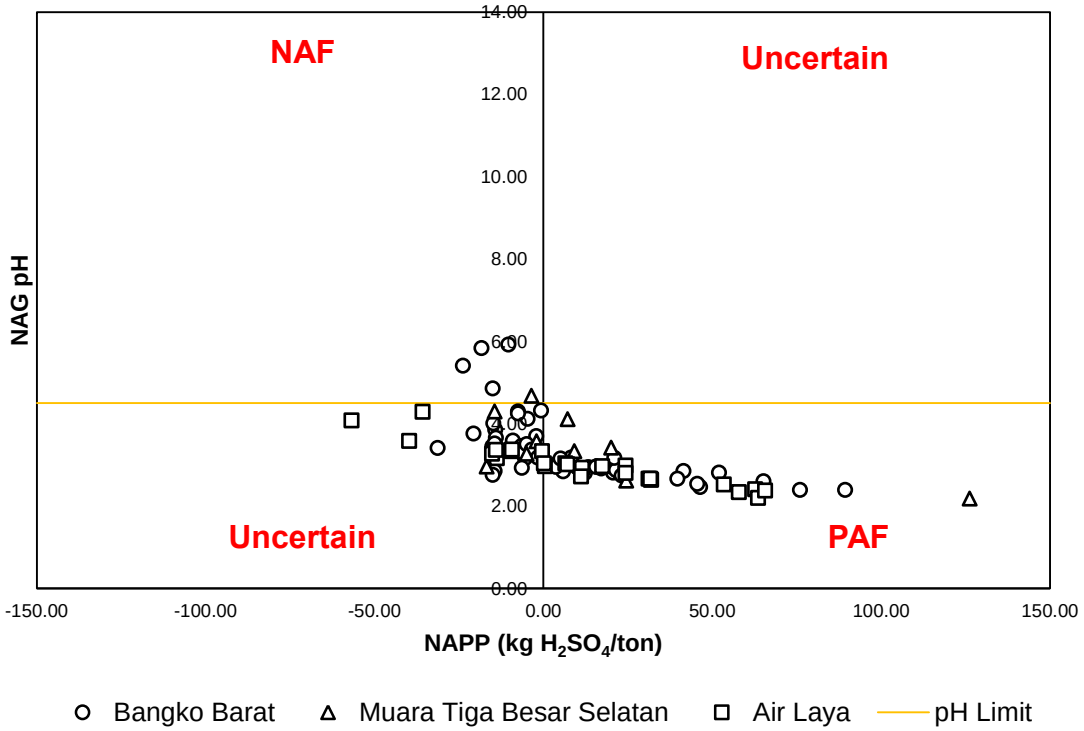

Fig. 2.9 Geochemical characterization of Bukit Asam coal-bearing rock

Fig.2.10 provides the result of rocks samples reactivity in each mine. Paste pH is observed by measuring the slurry mixture of fine rock sample after diluted with deionized water and rested overnight. Therefore, the measured pH value implies the available acidity and salinity in short-term effects due to the immediate reaction of acid and alkaline production. In contrary, NAG pH is the result of measured pH where all of sulfide minerals are forced to be oxidized hence prediction of maximum acid generating capacity obtained, by reacting the fine rock sample with strong oxidizing chemical, hydrogen peroxide. Therefore, the simultaneous reaction of acid and alkaline production occur during the process of the test.

Generally, rock samples in Bukit Asam have higher pH values of the paste pH test result than its value of NAG test. This implies the lack of neutralizing minerals to buffer AMD generation. Even though Muara Tiga Besar Selatan and Air Laya results confirm similar value where the rock in NAG test were lower than the threshold, ≤ 4.5, and the paste pH value was higher, several samples of Bangko Barat showed a different result where NAG pH values were higher than it. It means in Bangko Barat, rocks with neutralizing capacity were found. It is also supported by the previous result of rock

geochemical characterization. Moreover, several samples also showed the paste pH results that were below threshold, implies the excessive readily acidity that allows the samples to react immediately and produce AMD. The various capacities of rock samples in Bangko Barat then becomes the reason to conduct field measurement in Bangko Barat, especially for its occurrence of PAF and NAF rocks. The greatest potential in generating AMD among three mine sites in Bukit Asam and the various capacities of geochemical becomes the reasons for Bangko Barat selection of further measurement of oxygen and moisture concentration in PAF and NAF layer.

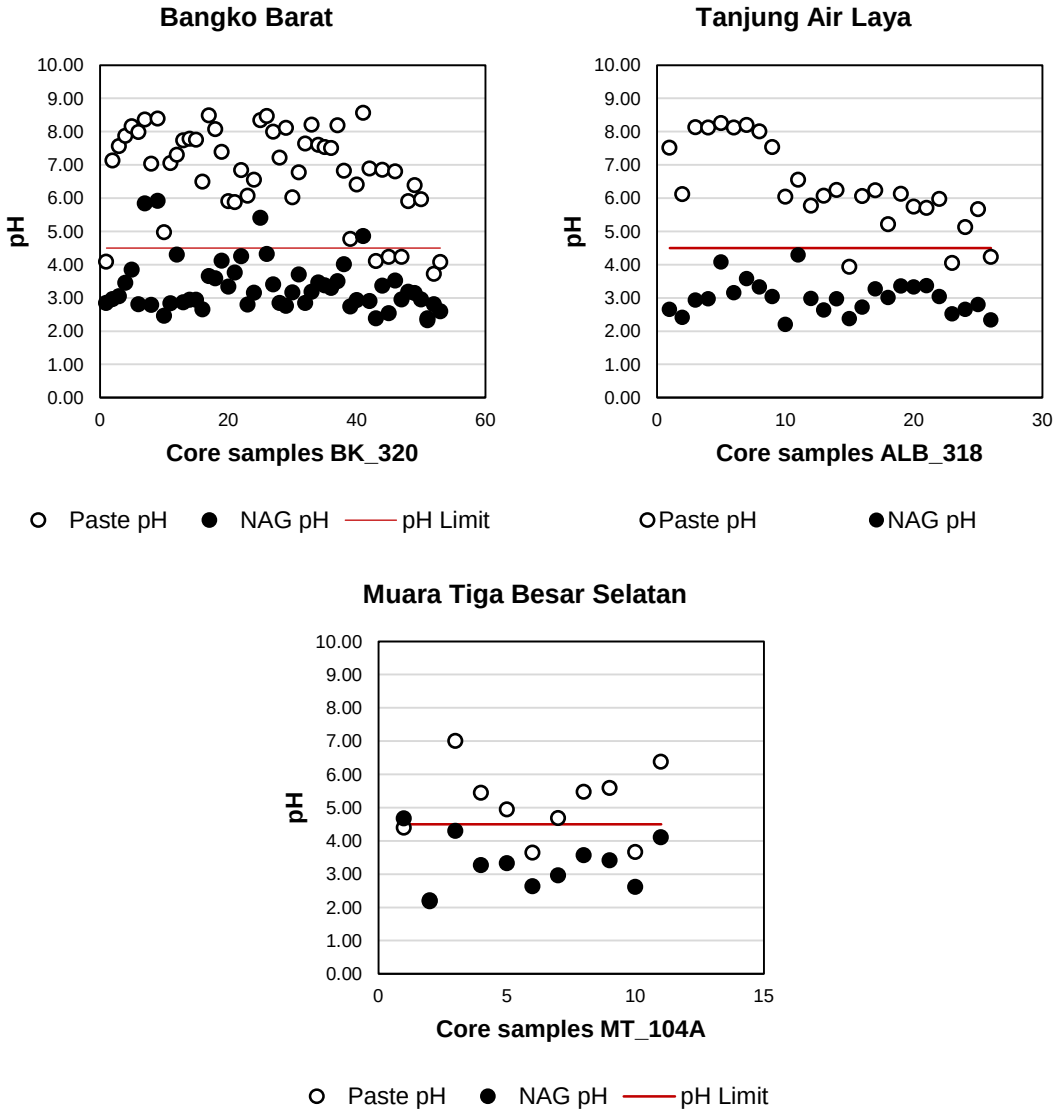

Fig. 2.10 Result of paste pH vs NAG pH

2.4.3 Kinetic test study for predicting net acid producing potential reaction

Several rock samples are collected at the mine site to be carried out the kinetic test in order to validate the previous result of sulfide mineral existence and geochemical properties. Free draining column leach test is chosen to be conducted to the samples. 500 g of rock sample that has size pass 4 mm and retain in 75 µm sifter is used in the experiment. The rock is then set in the Buchner funnel and placed under a heat lamp. 12 hours of heating with the rock surface has temperature around 35^{o}C and natural drying without lamp is carried out on the daily basis. This is performed in order to simulate the wet and dry condition within the mine site. Furthermore, daily spraying of 300 ml deionized water is conducted to the rock sample. The leachate water is collected and measured for its water quality. Four samples were selected for kinetic test. These samples were collected from the drilling bore samples, that represents PAF rocks from each mine site. The results of kinetic test are presented in Fig. 2.11.

The kinetic test confirms the potential of rock samples in producing acidic water. Generally, rock samples have a constant acid producing during the measurements. Furthermore, based on the reaction of acidic water that is produced, it supports the previous result where the dominant existence of framboidal pyrite will cause a fast reaction in acid generation.

Interestingly, the kinetic result of Muara Tiga Besar Selatan has the neutral pH phase at the initial time of experiment. The first stage of measurement has increased pH from 4.0 to around 7.0. After 30 days, the result shows decreasing value from neutral to acidic, with pH around 2.0. The rest of measurement then shows a similar trend of acid generation of rock samples. The leachate water behavior of Muara Tiga Besar Selatan explains the carbonate minerals that also exist in the rock samples, which able to buffering the leachate water. However, when the carbonate mineral is finished, the acid generation reaction still occurring due to remaining pyrite in the rock sample. Therefore, this result confirms the previous experimental result where the lack of neutralizing minerals capacity to neutralize the acid producing from PAF rock samples.

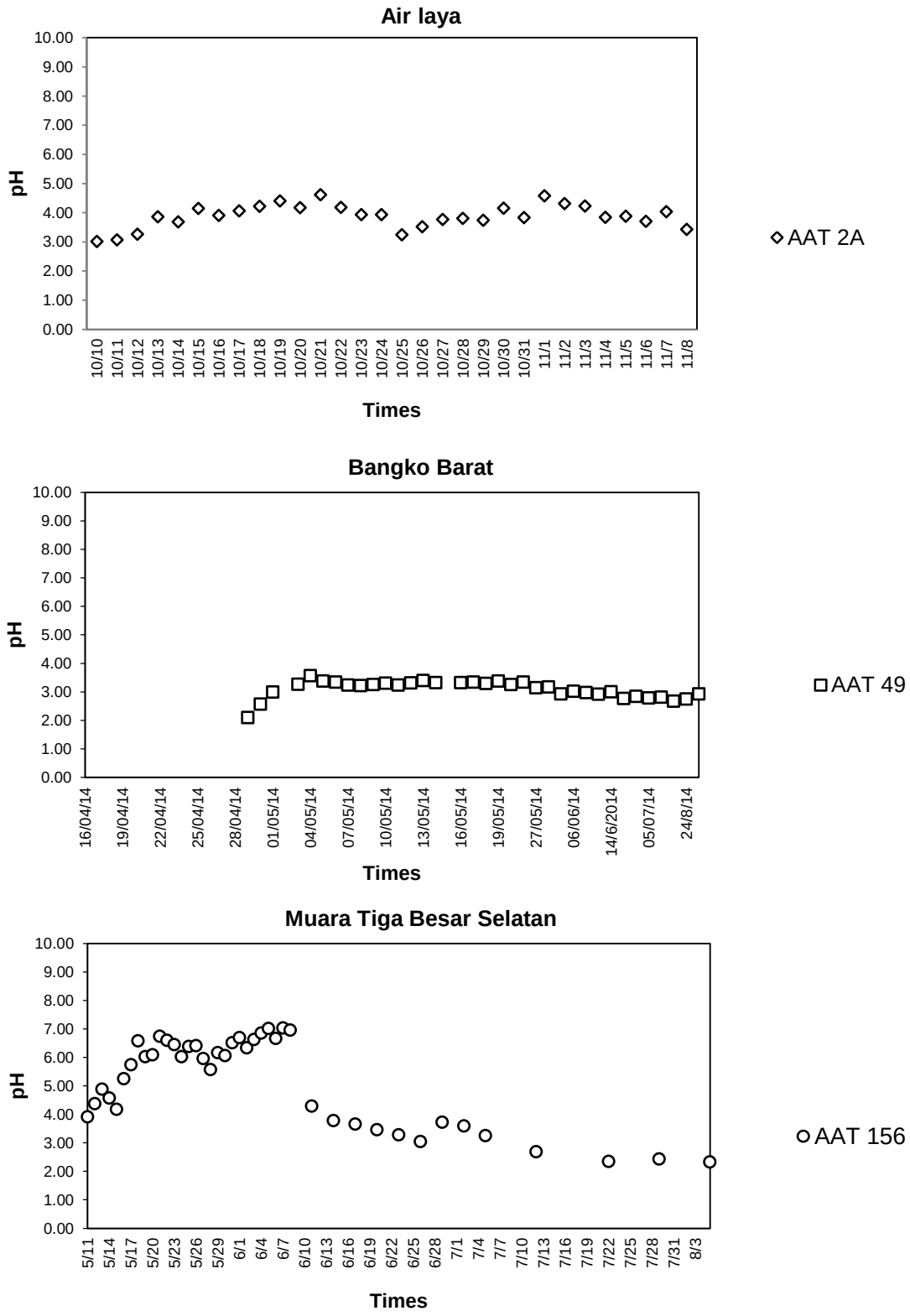

Fig. 2.11 Kinetic test results

2.5 Practice of AMD management: prevention method

Site investigation provides the information of high potential of an acid mine generation of mine site in the long-term. Therefore, it is important to evaluate the effectiveness of dumping area in order to know the effectiveness of the prevention method. A dry cover method constructed as a strategy to manage and prevent AMD is evaluated for its ability to minimize the oxygen and water infiltration to PAF layer.

2.5.1 Evaluation of dry cover strategies in overburden dumping to minimize oxygen ingress and water infiltration

Water is one of the reactants in sulfide oxidation, which the volume of water that is available within the rock waste dumping as moisture and/or water flow contribute the rate of oxidation. On the small scale of kinetic test, it was found out that the flushing rate of water will either increase or decrease the rate of AMD generation (J. Kusuma, 2012). Water, despite its role as the reactant, also influence the physical-hydraulic properties in the rock system, thus control the geochemical characteristic of leachate water. Deterioration of rock occurs due to the water, and decrease the rock particle size (Birkeland 1999). It increases the total area of the fresh surface area of sulfide minerals, which mean the reactive surface is available for further contact with oxygen and water, then accelerate the AMD generation, both of acid producing and neutralizing reaction (Davis, Doherty, & Ritchie, 1986; Song & Yanful, 2010). Moreover, it was also found out that in the field scale of partially covered waste rock pile (pilot test), produced less acid than an uncovered one which indicate the role of volume of water flushing to the sulfide oxidation. Furthermore, in the constant water content of the study from Hollings et al. 2001, the pyrite oxidation reaches a maximum value at certain water content where the oxygen was preserved adequately.

Oxygen, in the respect of water role, is also a key parameter in controlling the sulfide mineral oxidation. Its flux in the dumping profile is often used to evaluate the effectiveness of cover performance, since the sulfide oxidation rate can be calculated from the consumption of oxygen, either from direct measurement (Mbonimpa, Aubertin, Aachib, & Bussière, 2003) and the modified Fick’s Law (Collin 1987). In the laboratory scale, the oxygen diffusion coefficient can be measured in the chamber or column

(Yanful & ASCE, 2012). From the direct measurement of field scale, the attempts to observe the consumption of oxygen within the dump have already been carried out in the ore mine (Miller, Schumann, Smart, & Rusdinar, 2009). The results show the unconformity of oxygen consumption between the results of laboratory and the field which means effort to conduct study for understanding the oxygen consumption as a measure of sulfide oxidation rate still need to be carried out.

This part attempts to investigate the behavior of oxygen in both PAF and NAF layer on the on-going dry cover construction, especially its relationship with the moisture in both layers. As a preliminary study, observation was conducted in the coal overburden dumping site in order to find out the oxygen concentration within the layer as well as the water moisture. Both of PAF and NAF layer were measured from the surface and 150 cm depth, where the layer has not been covered. Hence, the behavior of oxygen and moisture highly depend on the physical and chemical reaction of rocks. Furthermore, the field data on the geochemical capacity of rock is also provided to understand the relationship between rocks, oxygen and water moisture.

Fig. 2.12 Overburden dumping construction in Bukit Asam mine

Previous studies already discussed the overburden dumping characterization in Indonesia coal mine (Chandra, 2009; Kusuma, 2012). The site observation also confirms the result, where the bottom-up and/or end-tipping dumping method is utilized as a method in dumping the overburden rocks. This results in segregation heterogenous materials based on the size of particles (see Fig. 2.12). Due to the gravity force, larger size of the rocks will accumulate on the tip of the dumping area while the finer stays at the higher location. Preferential flow will occur due to the difference of rock size sorting in the dumping area.

Currently, Bukit Asam coal mine attempts to conduct prevention method by applying dry cover strategy, as well as most coal mining in Indonesia. So far, there are two types of dumping strategy in Bukit Asam: without segregation of PAF and NAF layer and the encapsulation of PAF rock with NAF rocks (see Fig. 2.13). However, due to the lack of NAF rock, only 2-m thickness of NAF rocks that able to be layered on the PAF layer which usually more than 10 m in thickness. In the case of no segregation, dumping area will surely generate AMD because of the PAF rocks can react freely to the air and water within the overburden dumping area. The effectiveness of dumping method to prevent AMD generation is investigated by water quality measurement in surrounding overburden dumping rock.

Eight sampling points were chosen based on engineering consideration to represent all of the area in the dump (see Table. Point 1 – 6 are located in leachate water outlet directly from overburden dump. Meanwhile, point 7 – 8 are located in the area of sedimentation pond, where the accumulated water is originated from the water channel of overburden dump. Based on the measurement results, generally all of the sampling points have acidic water. Moreover, the dissolved concentrations of sulfate, and selected metal concentrations show an extremely high concentrations compared to the threshold of wastewater quality of the Indonesian government and also EPA. Therefore, the AMD generation in the overburden dumping without encapsulation not only will keep producing AMD but also has elevated concentrations of elements, likely dissolved from gangue minerals in the rocks.

Table 2.5 Measurement results of several sampling points in surrounding overburden dumping area

Points	pH	EC (mS/cm)	ORP (mV)	SO_4^{2-} (mg/l)	As (mg/l)	Al (mg/l)	Fe (mg/l)
1	4.1	0.5	472	264.0	2.5	1.7	3.1
2	5.8	3.0	588	7321.9	3.1	2.3	72.8
3	3.7	1.5	575	1031.3	2.9	10.1	1.3
4	3.6	1.3	569	860.7	3.5	4.7	1.5
5	3.7	0.7	567	708.8	0.8	4.7	2.4
6	3.6	0.7	568	578.2	0.0	2.3	2.2
7	3.6	1.1	565	859.8	0.6	7.2	2.9
8	4.8	0.6	510	394.2	0.4	0.9	3.8

However, in the case of PAF encapsulation with a thin layer of NAF, dry cover performance is still not understandable. The capability of NAF layer which deficit in the amount compared to PAF, to minimize oxygen ingress and water percolation still need to be understood. Therefore, this method is further measured in the next sub-chapter.

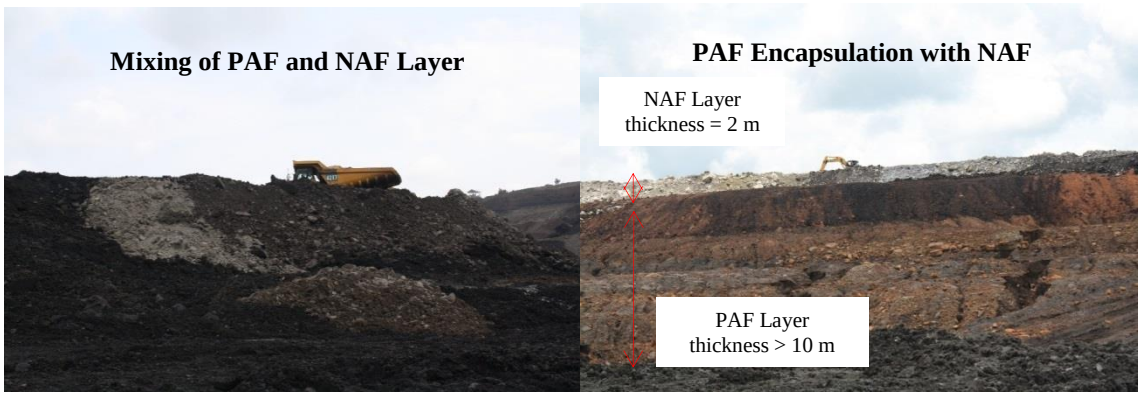

Fig. 2.13 Current dry cover strategies practice on Bukit Asam

2.5.2 Materials and methods

In order to know the efficiency of NAF cover to reduce water and oxygen infiltration, the field measurement was carried out. This field measurement was based on the available data and investigation of the surrounding are in the mine. The most importance is the significant AMD problem caused by the coal-bearing rock as well as the large amount of PAF and NAF capacity in producing and non-producing acid. Therefore, static test was conducted to each layer to know the capacity of acid producing and neutralizing within the rock. After understand, the measurement of oxygen and moisture behavior was observed with oxygen and soil water sensor and data logger measurement in the layer. Bangko Barat was selected as the location of field investigation due to its high capacity in acid producing.

2.5.2.1 Materials

The observation was conducted in the interburden and overburden dumping area, where the segregation based on the capacity of the rock to generate AMD. The rock materials consist of various types of rocks, such as claystone, siltstone, sandstone and tuff. The mixture of various rocks creates homogeneous physical geochemical properties, thus the only difference was the acid producing of each layer, depends on the PAF or NAF layer rocks were observed.

2.5.2.2 Methods

Data collection was firstly acquired from the chemical laboratory, belongs to Geology division, of PT Bukit Asam. After that, the oxygen and soil moisture were measured by using MIJ 03 (E.M.J. Co. Ltd) and SM 300 (Delta-T) sensor, respectively. The data then was recorded with MIJ 01 data logger which is portable and can be used for long-term measurement with specified interval time. Following configuration is the sensor installment in the field (see Fig. 2.14).

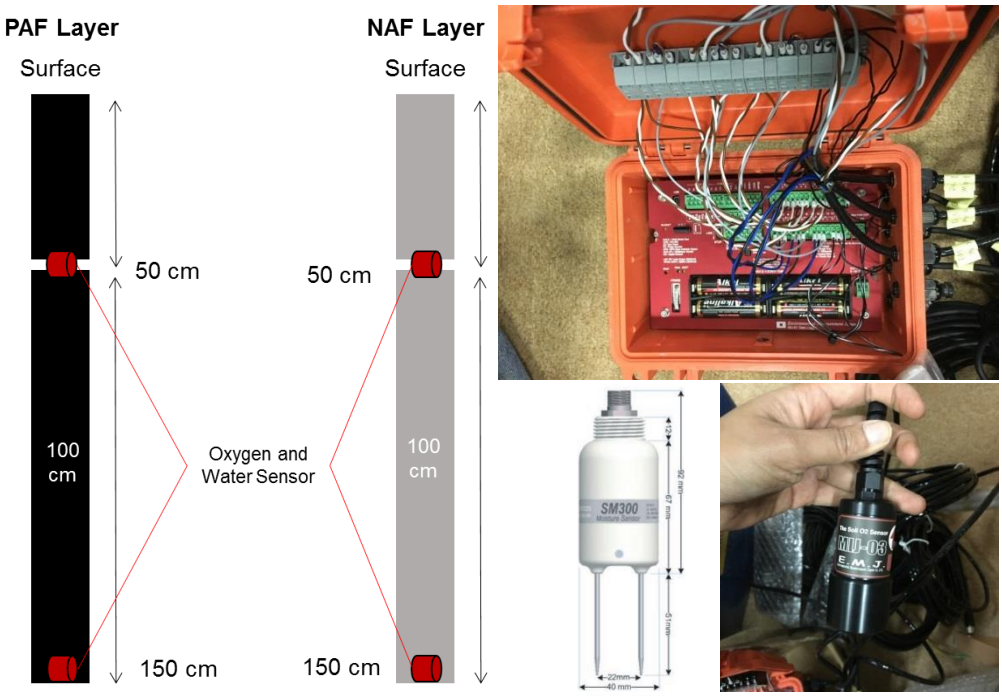

Fig. 2.14 Installation of oxygen and soil moisture sensor in PAF and NAF layer

The measurement was conducted for 24 hours of each layer. The oxygen and moisture result is supposed to highly depend on the diffusion and advection behavior, as well as the oxygen reaction within the rock. The weather condition of measurement time

was also affected the behavior of oxygen, therefore, the result was analyzed simultaneously with the moisture content of the rock. Rocks were also sampled from each point of measurement of oxygen and moisture in order to investigate its acid producing capacity. The static test was conducted to the rock samples by following the AMIRA from EGI static test method. Fig. 2.15 shows the field measurement and location of measurement points in PAF and NAF layer.

Fig. 2.15 Bangko Barat dumping site; NAF and PAF layer; point measurement of investigation

2.5.3 Results and discussions

Fig. 2.16 shows the characteristics of geochemical capacity of rock in sampling location that consists of two points (50 cm and 150 cm depth) for each PAF and NAF layer. Rock in 100 cm depth was also measured in order to know the variation of geochemical capacity in the layer. The measurement result of geochemical capacity in PAF layers showed an irregular value order as the depth increases. This happens due to the dumping method which do not separate PAF rock in detail, such as low PAF and high PAF. Therefore, various acid producing capacity Based on the measurement, PAF 50 cm and PAF 150 cm show large potential in producing acid while PAF 100 cm has low NAG pH result even though NAPP value is high.

NAG pH measurement results of PAF 50 cm and PAF 150 cm values are 1.21 and 1.47, respectively. These values are categorized as very low pH, likely to produce strong acidic water. This is also supported by the NAPP values, where PAF 50 cm and PAF 150 cm measurement results are 132.05 kg H_2SO_4/ton and 111.90 kg H_2SO_4/ton, respectively. It means PAF layer with a depth of 50 cm and 150 cm will produce strong acidic water if reacted with oxygen and water. Meanwhile, the NAG pH value of PAF

100 cm is 4.89, slightly over the pH 4.50. However, NAPP value is very high, 111.90 kg H_2SO_4/ton. This suggests the potential of producing acid in PAF layer with 100 cm depth although not as strong as 50 cm and 150 cm depth.

A different trend is shown by NAF layer, as the increasing depth seems to affect neutralizing capacity order. Deeper points seem to have higher capacity in neutralization. This may happen as the result of leaching process, where the carbonates are transported and accumulated in deeper location. The value of NAG pH of NAF 50 cm, NAF 100cm and NAF 150 cm are 5.11, 6.10 and 6.82, respectively. Meanwhile, the NAPP result also in the same order with NAG pH, which are 10.69 kg H_2SO_4/ton, -9.39 kg H_2SO_4/ton and -23.48 kg H_2SO_4/ton for NAF 50 cm, NAF 100 cm and NAF 150 cm, respectively.

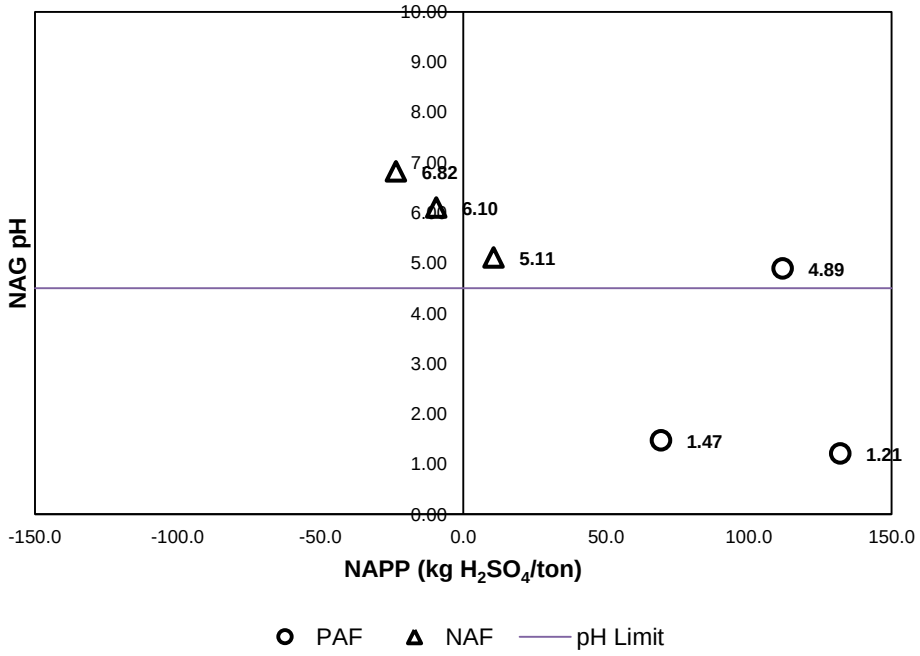

Fig. 2.16 Geochemical characterizations of rocks in sampling point

The result of 24 hours measurement in Bangko Barat overburden dumping site is provided in the Fig. 2.17. Generally, there is a large gap of oxygen measurement between NAF and PAF layer. NAF 50 cm and NAF 150 cm have value of oxygen around 13 % and 17%, respectively. Meanwhile, PAF 50 cm and PAF 150 cm have a value around 0 – 3 %. Therefore, with the similar condition, as both of the layer directly exposed to the surface, the drastic difference suggests that the oxidation process

happens in PAF layer. Due to the rapid oxidation process of sulfide mineral, oxygen is decreased in the PAF layer. Moreover, the difference of the oxygen level in PAF layer is significant compared to NAF, when both of oxygen level is compared to the oxygen on the surface layer. Atmospheric oxygen value is 20.9%. Therefore, acid production in PAF layer is expected to be excessive and high.

Water moisture in PAF layer is considerably low, as the value of the initial measurement is near 0 m^3/m^3 (lower than 0.1 m^3/m^3). However, during the measurement the level of water moisture increased drastically, which happened because of the rain that poured down at that time. After the rainfall, the water generally decreased. However, high water moisture is maintained in 50 cm depth of the PAF layer while on the deeper level, 150 cm depth, the water moisture decreases rapidly. It implies the PAF rock characteristic to retain on water near surface. This happens because of the slow movement of water to penetrate into the deeper level while rapid infiltration of rain is constantly took place. The water will accumulate mostly in the level near the surface, and partially becomes runoff water.

In NAF layer, the expected result is observed. Higher level, PAF 50 cm, has more oxygen than deeper level. Meanwhile, the water moisture concentration in all of sampling points is similar. Moreover, rain also fell down during the measurement and the same behavior occurs. Water moisture in deeper level can decrease rapidly compared to the near surface level. Important behavior is observed in the NAF layer, where 100 cm layer seems to reduce the oxygen penetration even if not in drastic reduction. Therefore, without any further treatment or additional strategy, NAF layer capability to reduce oxygen penetration entirely depends on its thickness. As consequences, sufficient amount of NAF layer to reduce oxygen penetration into PAF layer is prominent key that needs to be underlined. Appropriate thickness of the NAF layer in dry cover method for AMD prevention is required because this study has found out that with the thickness 200 cm, AMD is still can be generated.

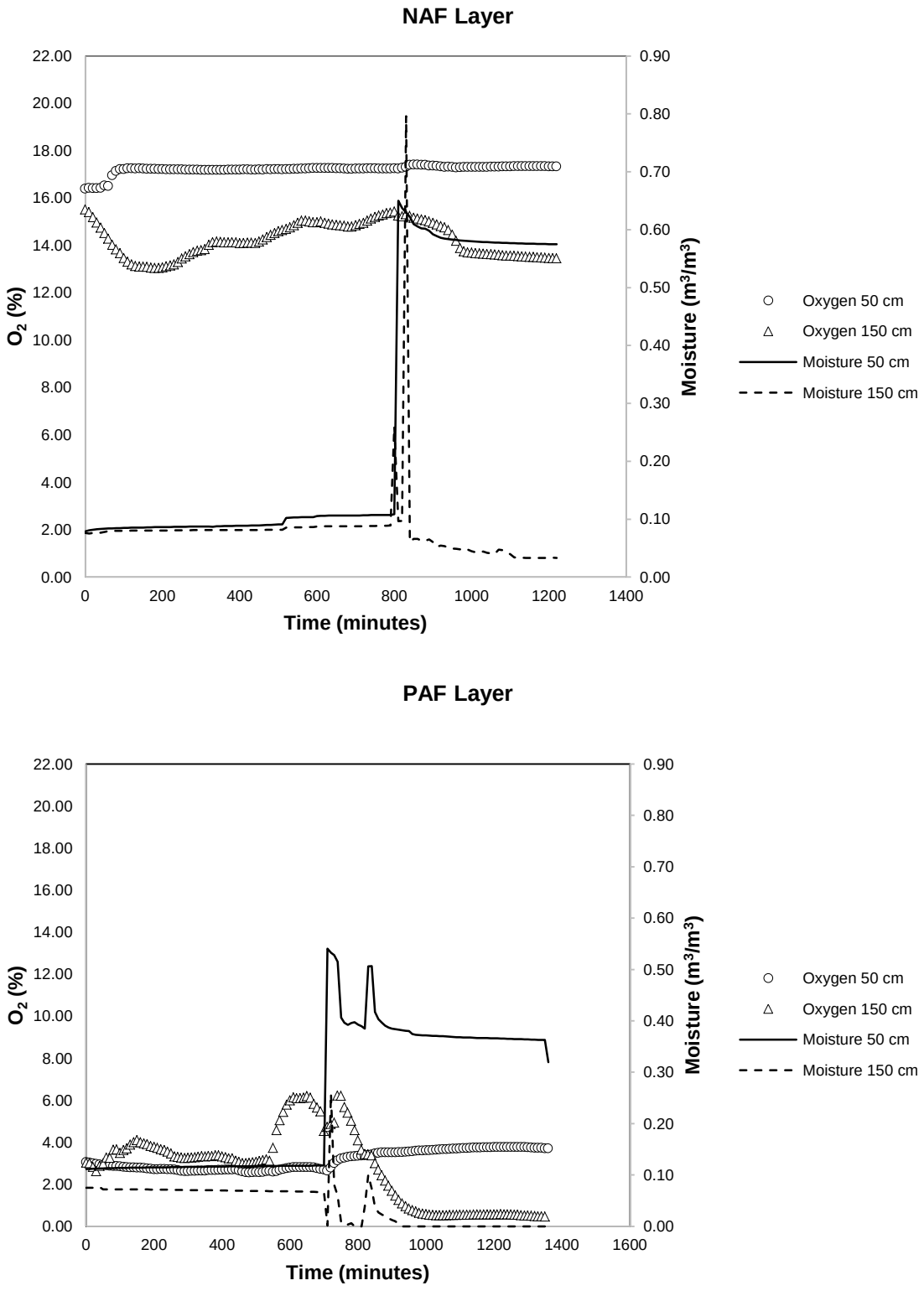

Fig. 2.17 Water moisture and oxygen measurement result of NAF and PAF layer

2.6 Conclusions

In this chapter, current AMD issues in Indonesian coal mine and its countermeasure were investigated through field observation, measurement on-site, sampling of coal-bearing rocks and overburden rocks, and sample analysis in order to know the problems in the long-term source of AMD as well as the effectiveness of a countermeasure that is carried out. The findings can be summarized as follows:

1. AMD issues in Indonesian coal mine are in severe condition, as acidic water can be easily found in surrounding mine site. Even though active treatment is already conducted by the company, the observation results show that in some conditions AMD still occurs. Therefore, in order to minimize this issue, prevention method is better to be carried out, especially in the high risk generation of AMD. Overburden dumping area is one of the sources of AMD that need to be studied for its prevention method due to the large scale and the long-term storage of waste rock thus the construction should be planned carefully.

2. Geochemical characterization of coal-bearing rock in Bukit Asam shows the high capacity in producing acid while the neutralizing capacity from rock is low. Even in several geochemical measurements results show no neutralizing capacity within NAF rock. Moreover, lack of NAF in volume compared to PAF rocks also become an important issue to be solved. Only 6 of NAF rock is available in the Bukit Asam, with NAG pH value is less than 6. The Kinetic result from 3 rocks in the coal mine shows the AMD generation will occur in the long-term duration.

3. Pyrite mineral shapes found in this coal mine consist of pyrite framboidal and pyrite euhedral. Those shapes of pyrite have a high surface reaction compared to pyrite with cuboid shape. Therefore, the reaction of AMD generation is expected to be rapid. Moreover, in Bangko Barat, paste the pH value is lower than NAG pH that indicates the reactivity of rock to be oxidized in the fast reaction.

4. Overburden dumping area is constructed with the end-tipping dumping. This has the consequence of the separation particle size of rocks due to gravitational force. Coarser rock will accumulate in the lower part of the overburden dumping while the

smaller size will be detained in the higher position. Therefore, this condition will establish the preferential flow of fluid within the dumping, which follows the air-filled porosity constructed by material segregation.

5. NAF thickness in this coal mine is proven to be ineffective to reduce the AMD generation on dry cover strategies. Oxygen in the PAF layer is decreased significantly as the depth increased while in NAF layer insignificant reduction of oxygen through the increase of depth is observed. Therefore, an appropriate dry cover strategy needs to be studied further in order to effectively reduce AMD generation.

References

Belkin, H. E., Tewalt, S. J., Hower, J. C., Stucker, J. D., & O'Keefe, J. M. K. (2009). Geochemistry and petrology of selected coal samples from Sumatra, Kalimantan, Sulawesi, and Papua, Indonesia. *International Journal of Coal Geology*, *77*(3–4), 260–268. https://doi.org/10.1016/j.coal.2008.08.001

Bienawaski, Z. T. (1989). *Engineering rock mass classification*. *Geology*. New York: Wiley.

Davis, G. B., Doherty, G., & Ritchie, A. I. M. (1986). A model of oxidation in pyritic mine wastes: part 2: comparison of numerical and approximate solutions. *Applied Mathematical Modelling*, *10*(5), 323–329. https://doi.org/10.1016/0307-904X(86)90091-0

Dumble, P., & Ruxton, C. (2003). Guidance on Monitoring of Landfill Leachate, Groundwater and Surfact Water v 2. *Sepa*, (July).

Gautama, R. S. (1994). Acid Water Problem in Bukit Asam Coal Mine, South Sumatra, Indonesia. In *IMWA Proceedings* (pp. 533–542).

Gautama, R. S. (2011). Acid Mine Drainage Management in Indonesian Mines. *Proceedings of the Seventh Australian Workshop on Acid and Metalliferous Drainage, Darwin, Northern Territory. 21 *24 June 2011. (Eds LC Bell and B Braddock)*, 1–8.

Gautama, R. S., & Hartaji, S. (2004). Improving the accuracy of geochemical rock modelling for acid rock drainage prevention in coal mine. *Mine Water and the Environment*, *23*(2), 100–104. https://doi.org/10.1007/s10230-004-0047-x

Gautama, R. S., & Kusuma, G. J. (2008). Evaluation of Geochemical Tests in Predicting Acid Mine Drainage Potential in Coal Surface Mine. *Mine Water and the Environment*, 271–274.

Hollings, P., Hendry, M. J., Nicholson, R. V., & Kirkland, R. A. (2001). Quantification of oxygen consumption and sulphate release rates for waste rock piles using kinetic cells: Cluff Lake uranium mine, northern Saskatchewan, Canada. *Applied Geochemistry*, *16*(9–10), 1215–1230. https://doi.org/10.1016/S0883-2927(01)00005-1

J. Kusuma, G. (2012). An Evaluation on the Physical and Chemical Composition of Coal Combustion Ash and Its Co-Placement with Coal-Mine Waste Rock. *Journal of Environmental Protection*, *03*(07), 589–596. https://doi.org/10.4236/jep.2012.37071

Kramadibrata, S., Matsui, K., Rai, M. A., & Shimada, H. (2002). Properties of soft rocks with particular reference to Indonesian mining. In S. Wang, F. Bingjun, & L. Zhongkui (Eds.), *Proceedings of the 2001 ISRM International Symposium - 2nd Asian Rock Mechanics Symposium (ISRM 2001 - 2nd ARMS)*. Beijing.

Mbonimpa, M., Aubertin, M., Aachib, M., & Bussière, B. (2003). Diffusion and consumption of oxygen in unsaturated cover materials. *Canadian Geotechnical Journal*, *40*(5), 916–932. https://doi.org/10.1139/t03-040

Miller, S. D., Schumann, R., Smart, R. S. C., & Rusdinar, Y. (2009). ARD Control by Limestone Induced Armouring and Passivation of Pyrite Minerals Surfaces. *8th International Conference on Acid Rock Drainage*, 1–11. Retrieved from http://www.inap.com.au/documents/Stuart_Miller_B6_T4_ARD-Control-by-Limestone-Induced-Armouring-and-Passivation-of-Pyrite-Min.pdf

Peel, M. C., Finlayson, B. L., & McMahon, T. A. (2007). Updated World Map of the Koppen-Geiger Climate Classification Updated world map of the K ¨ oppen-Geiger climate classification. *Hydrology and Earth System Sciences*, (October 2007). https://doi.org/10.5194/hess-11-1633-2007

Sadisun, I. A., Shimada, H., Ichinose, M., & Matsui, K. (2005). Study on the physical disintegration characteristics of Subang claystone subjected to a modified slaking index test. *Geotechnical and Geological Engineering*, *23*(3), 199–218. https://doi.org/10.1007/s10706-003-6112-6

Smart, R., Skinner, B., Levay, G., Gerson, A., Thomas, J., Sobobieraj, H., Stewart, W. (2002). ARD test handbook: Project P387A prediction and kinetic control of acid mine drainage. *Project P387A, Prediction and Kinetic Control of Acid Mine Drainage*, (May), 42.

Song, Q., & Yanful, E. K. (2010). Effect of Water Addition Frequency on Oxygen Consumption in Acid Generating Waste Rock. *Journal of Environmental Engineering*, *136*(7), 691–700. https://doi.org/10.1061/(ASCE)EE.1943-7870.0000213

Yanful, E. K., & ASCE, A. M. (2012). Oxygen diffusion through soil covers on sulfidic mine tailings. *Journal of Geotechnical Engineering*, *119*(8), 1207–1228.

Belkin, H. E., Tewalt, S. J., Hower, J. C., Stucker, J. D., & O'Keefe, J. M. K. (2009).

Geochemistry and petrology of selected coal samples from Sumatra, Kalimantan, Sulawesi, and Papua, Indonesia. *International Journal of Coal Geology*, *77*(3–4), 260–268. https://doi.org/10.1016/j.coal.2008.08.001

Bienawaski, Z. T. (1989). *Engineering rock mass classification*. *Geology*. New York: Wiley.

Davis, G. B., Doherty, G., & Ritchie, A. I. M. (1986). A model of oxidation in pyritic mine wastes: part 2: comparison of numerical and approximate solutions. *Applied Mathematical Modelling*, *10*(5), 323–329. https://doi.org/10.1016/0307-904X(86)90091-0

Dumble, P., & Ruxton, C. (2003). Guidance on Monitoring of Landfill Leachate, Groundwater and Surfact Water v 2. *Sepa*, (July).

Gautama, R. S. (1994). Acid Water Problem in Bukit Asam Coal Mine, South Sumatra, Indonesia. In *IMWA Proceedings* (pp. 533–542).

Gautama, R. S. (2011). Acid Mine Drainage Management in Indonesian Mines. *Proceedings of the Seventh Australian Workshop on Acid and Metalliferous Drainage, Darwin, Northern Territory. 21 - 24 June 2011. (Eds LC Bell and B Braddock)*, 1–8.

Gautama, R. S., & Hartaji, S. (2004). Improving the accuracy of geochemical rock modelling for acid rock drainage prevention in coal mine. *Mine Water and the Environment*, *23*(2), 100–104. https://doi.org/10.1007/s10230-004-0047-x

Gautama, R. S., & Kusuma, G. J. (2008). Evaluation of Geochemical Tests in Predicting Acid Mine Drainage Potential in Coal Surface Mine. *Mine Water and the Environment*, 271–274.

Hollings, P., Hendry, M. J., Nicholson, R. V., & Kirkland, R. A. (2001). Quantification of oxygen consumption and sulphate release rates for waste rock piles using kinetic cells: Cluff lake uranium mine, northern Saskatchewan, Canada. *Applied Geochemistry*, *16*(9–10), 1215–1230. https://doi.org/10.1016/S0883-2927(01)00005-1

J. Kusuma, G. (2012). An Evaluation on the Physical and Chemical Composition of Coal Combustion Ash and Its Co-Placement with Coal-Mine Waste Rock. *Journal of Environmental Protection*, *03*(07), 589–596. https://doi.org/10.4236/jep.2012.37071

Kramadibrata, S., Matsui, K., Rai, M. A., & Shimada, H. (2002). Properties of soft rocks with particular reference to Indonesian mining. In S. Wang, F. Bingjun, & L. Zhongkui (Eds.), *Proceedings of the 2001 ISRM International Symposium - 2nd Asian Rock Mechanics Symposium (ISRM 2001 - 2nd ARMS)*. Beijing.

Mbonimpa, M., Aubertin, M., Aachib, M., & Bussière, B. (2003). Diffusion and consumption of oxygen in unsaturated cover materials. *Canadian Geotechnical Journal*, *40*(5), 916–932. https://doi.org/10.1139/t03-040

Miller, S. D., Schumann, R., Smart, R. S. C., & Rusdinar, Y. (2009). ARD Control by Limestone Induced Armouring and Passivation of Pyrite Minerals Surfaces. *8th International Conference on Acid Rock Drainage*, 1–11. Retrieved from http://www.inap.com.au/documents/Stuart_Miller_B6_T4_ARD-Control-by-Limestone-Induced-Armouring-and-Passivation-of-Pyrite-Min.pdf

Peel, M. C., Finlayson, B. L., & McMahon, T. A. (2007). Updated World Map of the Koppen-Geiger Climate Classification Updated world map of the K ¨ oppen-Geiger climate classification. *Hydrology and Earth System Sciences*, (October 2007). https://doi.org/10.5194/hess-11-1633-2007

Sadisun, I. A., Shimada, H., Ichinose, M., & Matsui, K. (2005). Study on the physical disintegration characteristics of Subang claystone subjected to a modified slaking index test. *Geotechnical and Geological Engineering*, *23*(3), 199–218. https://doi.org/10.1007/s10706-003-6112-6

Smart, R., Skinner, B., Levay, G., Gerson, A., Thomas, J., Sobobieraj, H., … Stewart, W. (2002). ARD test handbook: Project P387A prediction and kinetic control of acid mine drainage. *Project P387A, Prediction and Kinetic Control of Acid Mine Drainage*, (May), 42.

Song, Q., & Yanful, E. K. (2010). Effect of Water Addition Frequency on Oxygen Consumption in Acid Generating Waste Rock. *Journal of Environmental Engineering*, *136*(7), 691–700. https://doi.org/10.1061/(ASCE)EE.1943-7870.0000213

Yanful, E. K., & ASCE, A. M. (2012). Oxygen diffusion through soil covers on sulfidic mine tailings. *Journal of Geotechnical Engineering*, *119*(8), 1207–1228.

Birkeland, P. W. *Soils and geomorphology*. New York: Oxford University Press, 1999.

Collin, M. *Mathematical modeling of water and oxygen transport in layered soil covers for deposits of pyritic mine tailings.* Stockholm: Royal Insitute of Technology, Department of Chemical Engineering, 1987.

Gautama, Rudy S., and Lindawati. "Acid mine drainage in surface coal mine: case study from South Sumatera." *The 1995 Indonesian Mining Conference.* 1995.

Indonesia, Geological Agency. "Map Location of Resource Deployment and Coal Reserves." *Ministry of Energy and Mineral Resources Republic of Indonesia*, 2011.

Miller, S, A Robertson, and T Donahue. "Advances in acid drainage prediction using the net acid generating (NAG) test." *Proceedings Fourth International Conference on acid rock drainage.* Vancouver, B. C. Canada, 1997. 533–547.

CHAPTER 3

Fundamental study of coal ash and organic material composition and individual role to prevent AMD generation

3.1 Introduction

Dry cover can be ineffective to prevent AMD if there is not enough NAF material available to cover PAF material as investigated in the previous chapter, resulting in oxygen and water can infiltrate to the NAF layer and reach PAF layer where AMD process is taken place. Additionally, when the lack neutralization capacity within NAF rocks occurs, alternative materials to improve the dry cover method need to be found out. However, this also heavily depends on the material available on the main site which is site specific, can be different from one site to another mining site.

Various alkaline materials have been widely investigated in order to improve dry cover, as an additional layer that has an ability to reduce AMD generation. This includes limestone, lime, sodium bicarbonate, etc. that prospectively might control the pyrite oxidation, as the main sulfide minerals in AMD generation. However, those materials can be not economical to be applied, due to the high amount that is needed, which make it expensive, or because of unavailability of those materials around the mining site, which increase the transportation cost thus impossible to be used. In coal mines, one of interesting material to be applied as an additional cover layer is coal ash, as a by-product of thermal combustion of coal in power stations that has high alkalinity (Adriano, Page, Elseewi, Chang, & Straughn, 1980). Moreover, coal ash also has solidifying properties that can harden after addition of water (Steenari, Karlsson, & Lindqvist, 1999) and creating firm layer (Neuschütz & Greger, 2010)

Oxygen also plays important role in generating AMD. Therefore, the organic material can be used as an active filter against the oxygen that penetrates the covering material (Hallberg, Granhagen, & Liljemark, 2005; Neuschütz, Stoltz, & Greger, 2006; Peppas, Komnitsas, & Halikia, 2000). Furthermore, organic material contains nutrients and organic matter and can be used as an organic amendment, supporting the establishment of vegetation. Various types of organic material are applied to cover layer,

such as paper mill sludge and sewage sludge, depends on the material that is available to be used in the mine. The most commonly used organic material is the sewage sludge, due to the availability of this material in the sludge treatment facility. However, Indonesia has difficulty in supplying this material in the remote area of the mine. Therefore, alternative of organic material with similar function should to be found.

In order to completely reduce AMD generation, the combination of those materials will be used to cutoff both water and oxygen source to the PAF layering and also alter the leachate water that still able to penetrate the cover layering. However, refer to the previous studies, those materials usage in the mine always site specific that heavily depend on the material availability and also the problems on the adjacent mine. It is worrisome to apply the similar strategy to another mine site due to the lack of study that focus on the characterization of various types of materials. Therefore, this chapter focuses on the characterization of both materials and finally proposing guideline (Chapter 4) that can make this material have comprehensive consideration before finally chosen and utilized on the dry cover strategies.

3.2 Fundamental studies of coal ash from coal-fired power plant

3.2.1 Materials and experimental method

In the attempt to observe the differences between various fly ash and bottom ash based on physical and geochemical properties, several samples are collected from Indonesia and Japan coal-fired power plant. The description of materials and methods used in this chapter is explained as follows.

3.2.1.1 Materials

Six fly ashes and two bottom ashes from various parent coal and locations are sampled in various locations. Six samples are based in Indonesia coal-fired power plant while one sample that is originally sourced from Fukuoka coal-fired power plant, Japan. However, the coal source of Japan coal-fired power plant is from Indonesia and Australia. Further details about the coal ash samples can be seen in Table 3.1.

Table 3.1 Coal ash samples

Sample	Source	Feed Coal Type
FA AI	Coal-fired power plant, South Kalimantan	Sub-bituminous
FA ADR	Coal-fired power plant, East Kalimantan	Sub-bituminous
FA KYU	Coal-fired power plant, Fukuoka	Sub-bituminous
FA KPC	Coal-fired power plant, East Kalimantan	Sub-bituminous
FA ICA	Coal-fired power plant, West Kalimantan	Sub-bituminous
BA ICA	Coal-fired power plant, West Kalimantan	Sub-bituminous
FA BA	Coal-fired power plant, South Sumatera	Sub-bituminous
BA BA	Coal-fired power plant, South Sumatera	Sub-bituminous

3.2.1.2 Experimental methods

All of the samples received similar treatment prior the experiments. Fly ash and bottom ash were dried in the oven completely for 24 hours before starting analysis at 105^{o}C. After that, the certified amount of samples was analyzed for its physical characterization while the other amount was analyzed for geochemical characterization. Physical characterization is carried out by conducting several experiments, including experiments for analyzing specific gravity, particle size distribution, and morphology of particles by using method of water pycnometer following the ASTM D854 (ASTM, 2000) , the sieve analysis (for particle size above 0.075 mm) and hydrometer analysis (for particle size below 0.075 mm) by following JIS A1204, and scanning electron microscopy energy dispersive X-ray (SEM-EDX).

Geochemical characterization was carried out together with chemical characterization, by conducting static tests follows AMIRA standard (Smart et al., 2002), bulk chemical analysis X-ray Fluorescence (XRF) and elemental digestion with acid sequential extraction as explained in method by (Sasaki, Haga, Hirajima, Kurosawa, & Tsunekawa, 2002) The experimental procedure is described as follows:

1 2.5 g of dried samples were added to a Teflon vessel and then 20 ml of 1 mol/L HCL was mixed
2 The solution was shaken for 16 hours at 30^{o}C, and then centrifuged at 3,000 rpm for 20 minutes and decanted
3 The residue was washed with 10 ml of deionized water 3 times and the supernatant solutions were mixed. The supernatant solutions were analyzed by Seiko ICP-AES to measure the concentration of leached metal

4 The residue was added to a plastic with 30 ml of 10 ml/l HF. And the solution was shaken for 1 hour at 30^{o}C, then centrifuged at 3,000 rpm for 20 minutes and decanted
5 The supernatant solutions were sampled and the residue was added to 30 ml of 10 mol/l HF again, and the solution was shaken for 16 hours at 30^{o}C
6 5.0 g of boric acid was added to the solution and shaken for 8 hours at 30^{o}C, then centrifuged under the same condition before and decanted
7 The residue was washed three times with 10 ml of boiling deionized water, and all of the supernatant solutions were mixed for the ICP-AES analysis
8 The residue was added to 10 ml of concentrated HNO_3, and then shaken for 6 hours at 30^{o}C and centrifuged and decanted
9 The residue was washed with 15 l of deionized water three times, and then centrifuged and decanted. All of the supernatant solutions were mixed and measured by ICP-AES

In order to support the result, mineralogical analysis was also conducted by using X-ray diffraction (XRD) technique. The XRD analysis was conducted using wide angle goniometer RINT 2100 XRD under the conditions: radiation CuKα, operating voltage 40 kV, current 26 mA, divergence slid 1 deg., anti-scatter 1 deg., receiving slit 0.3 mm, step scanning 0.050^{o}, scan speed 2,000^{o}/min, scan range 2,000 – 65,000^{o}.

Static test that is used in here, including Acid Base Accounting (ABA) method consists of the calculation of Maximum Potential Acidity (MPA) derived from Total Sulfur test and Acid Neutralization Capacity (ANC) test, resulting Net Acid Production Potential (NAPP) as already previously explained. Furthermore, by conducting Net Acid Generating (NAG) test with an increasing ratio of mixture of fly ash and also potentially acid forming (PAF) rocks in order to predict the net acid production potential in reality, the behavior of the addition fly ash to PAF rocks can be predicted.

3.2.2 The characterization of coal ash

3.2.2.1 Physical properties

Table 3.2 provides the result of specific gravity from coal ash. Generally, the relative density of fly ash ranges between 1.9 to 2.8 g/cm3, with the color is gray or tan (H.Kosmatka & L.wilson, 2011) which in accordance with the result of this experiment. The lowest specific gravity is FA KPC, with value 2.136, while the highest specific gravity is FA ADR, with value 2.739. The low unit weight due to the low specific

gravity of coal ash is an attractive property for its use in geotechnical application (Pandian, 1998). The variation of specific gravity of coal ash is due to the combination of various factors like gradation, particle shape, and chemical composition.

Table 3.2 Specific gravity of coal ash

Sample	SG (g/cm^3)
FA AI	2.635
FA KPC	2.136
FA ADR	2.739
FA ICA	2.497
BA ICA	2.611
FA BA	2.338
BA BA	2.474
FA KYU	2.283

3.2.2.2 Particle size distribution

Prior the sieving and hydrometer measurement of particle size distribution, the size of coal ash is observed under transmitted-light microscope with 100x and 300x magnification. Bottom ash and fly ash are compared from the difference of the size. Based on the observation, it can be seen in the Fig. 3.1 that generally bottom ash has a bigger size than the fly ash.

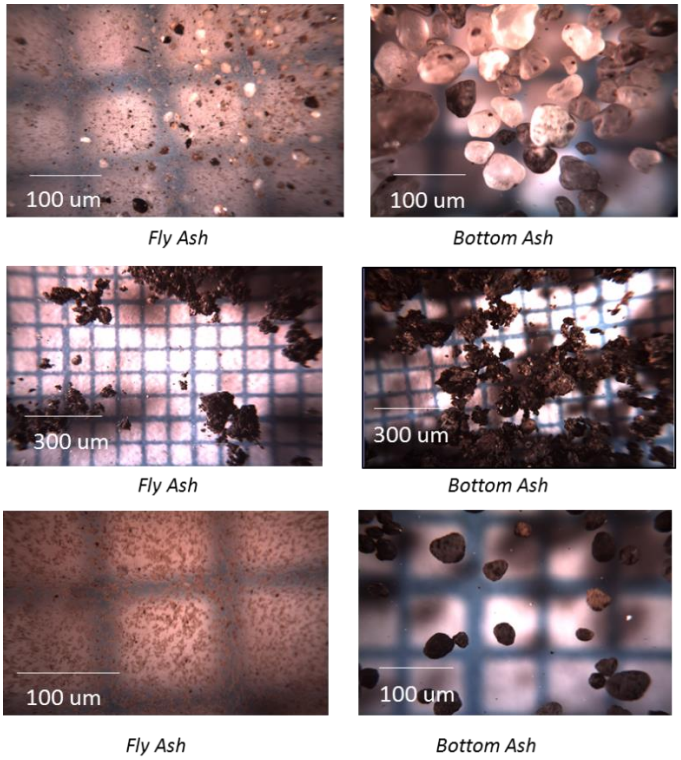

Fig. 3.1 Transmitted-light microscopy result of coal ash

Particle size distribution was analyzed by two methods, for the particle size above 0.075 mm using sieve analysis and particle size below 0.075 mm using hydrometer analysis. The result can be seen in Fig. 3.2. From the result, it can be seen that finer particle size was owned by mostly fly ash, except for FA KPC. This result is understandable since fly ash is coal combustion product that are driven out of the boiler with the flue gases, while ash that falls to the bottom of the boiler is called as bottom ash. The difference in size is the reason why such segregation happens.

However, in FA KPC, it gives different trend of particle size. This might happen because of the handling during the storage where agglomeration of particle occurs and affect the overall particle size. This could happen with the addition and/or contact with water during the storage which make the coal ash is hardening. In order to understand this, further analysis is conducted by using the SEM-EDX measurement.

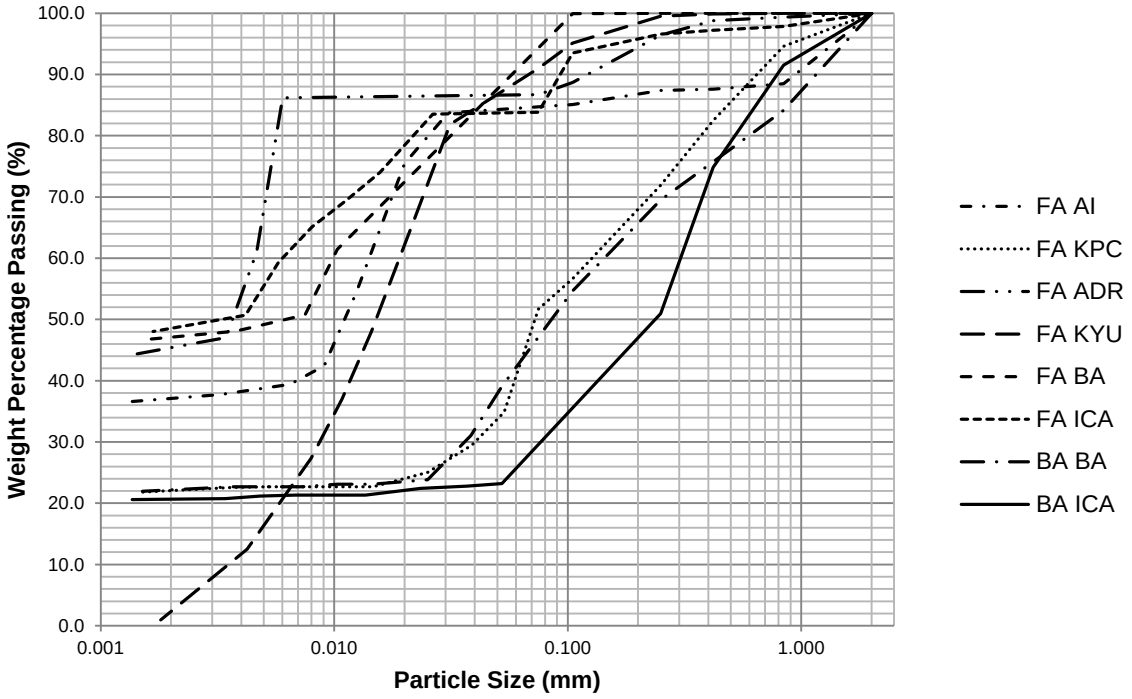

Fig. 3.2 Particle size distribution of coal ash

3.2.2.3 Shape and morphology by direct observation of micro-structure

Microstructure of fly ash and bottom ash is observed from the result of SEM-EDX techniques. Based on its optical morphology, the particles of fly ash can be defined into 11 classes: (1) amorphous, nonopaque; (2) amorphous, opaque; (3) amorphous, mixed

opaque and nonopaque; (4) rounded, vesicular, nonopaque; (5) rounded, vesicular, mixed opaque and nonopaque; (6) angular, lacy opaque; (7) nonopaque, cenosphere (hollow sphere); (8) nonopaque, pleroshpere – sphere packed with other spheres; (9) nonopaque, solid sphere; (10) opaque, sphere; and (11) nonopaque sphere with either surface or internal crystals (Fisher et al., 1978). Therefore, based on SEM-EDX result, for simplification, coal ash according to their shapes and structures can also be classified spherical particles, plerosphere and irregular particles (Chengfeng, Qiang, & Junming, 2005).

Generally, spherical particles existed in all coal ash samples (see Fig. 3.3). However, there are significant differences in the structure that can differ fly ash into two groups. Firstly, FA KYU, FA ADR and FA AI were dominantly consisting of spherical particles and also plerosphere. Moreover, the spherical particles were also seen to be attached to the bigger sphere, or sometimes agglomerated between similar sizes of particles. This is due to the very high temperature when the burning process of coal carried out. Certain temperature, usually higher than 600^{o}C, will melt most of the clay minerals and organic carbon. It allows the process of reshaping of the remaining minerals, coated by the melted part when the cooling down takes place and then taking shape into a sphere.

Meanwhile, the second group consists of FA KPC, FA ICA and FA BA that shared the similar particle shape that dominantly have an irregular shape with small amount of spherical particles. Furthermore, all of the irregular particles have coarser surface due to the un-burned part because the lower burning temperature than the first group. Some irregular particles in this research look like solids (FA ICA and FA BA). Meanwhile, several holes can be observed on the surfaces of fly ash as can be seen in FA KPC. Interestingly, the hollow surface in FA KPC was seen obviously porous that indicates its high capacity in holding the water.

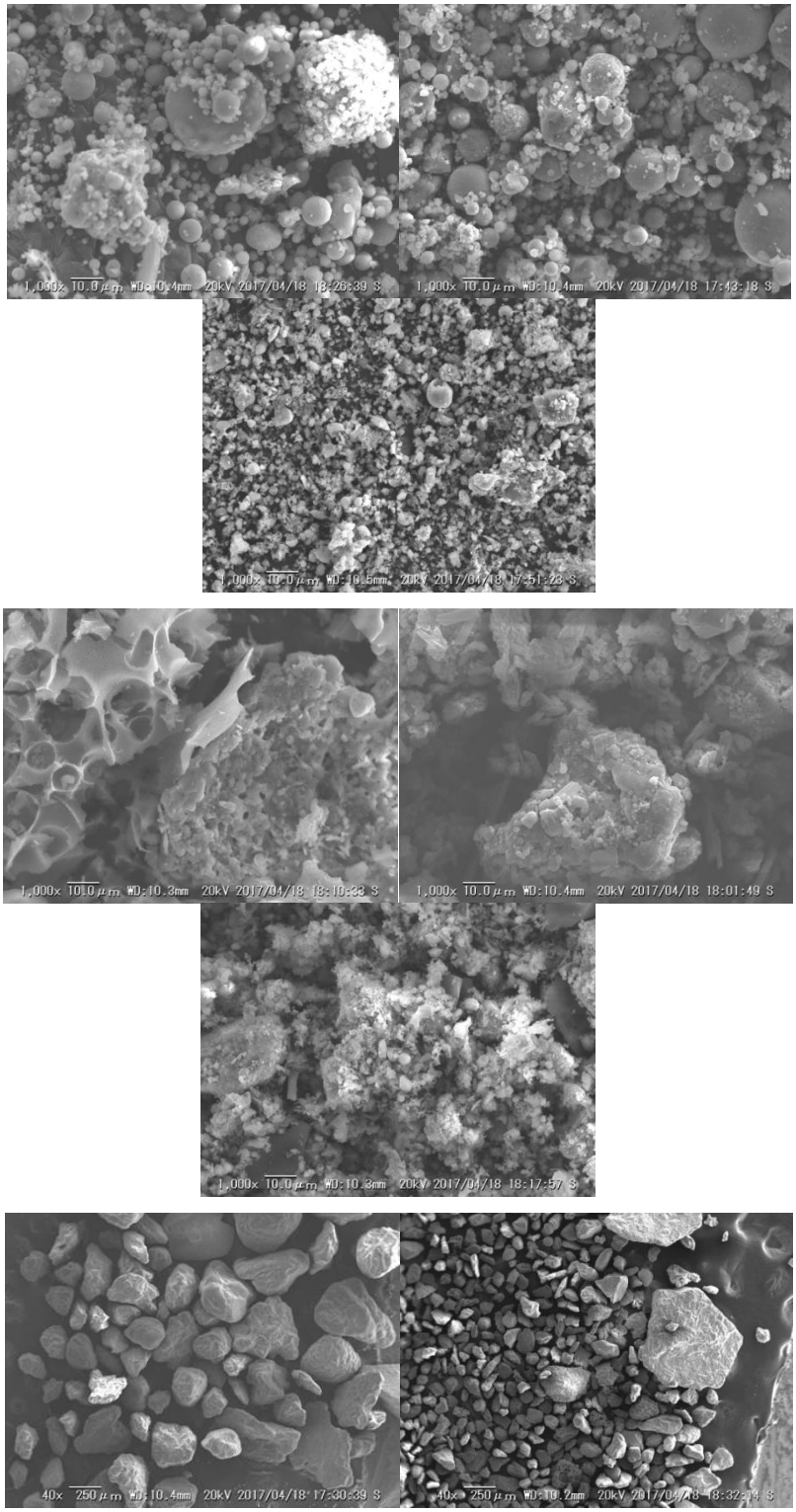

Fig. 3.3 SEM-EDX result of coal ash (top, left to right, 1000x: FA KYU, FA ADR and FA AI – middle, left to right, 1000x: FA KPC, FA ICA and FA BA – bottom, left to right, 40x: BA BA and BA ICA)

So far, the studies of fly ash conclude that difference in boiler types may be the main reason for different particle types, resulting in different formation of particles.

Spherical particles are formed after combustion, when the temperature decrease and mineral compounds condense onto the tiny nucleuses and grow up to form spheres (Chengfeng et al., 2005). Bigger particles might also not completely combusted, thus result in broken sphere. Moreover, if there are un-burned carbon and mineral substance, it could produce irregular particles, that can be distinguished based on their light microscopy, whether it is opaque or nonopaque.

Bottom ash microstructure observation shows that with different magnification, the particle size is obviously bigger than fly ash. The result also shows that no spherical particles exist, while the irregular particles mainly have a smooth surface that on contrary to the fly ash condition.

3.2.2.4 Mineralogical characterization

Bulk chemical analysis was measured by using the XRF technique for total 6 samples of fly ash and 2 bottom ash. The result of XRF measurement is provided in Table 3.3. As can be seen, the primary chemical components were SiO_2, Al_2O_3, FeO, CaO and LoI (loss on ignition). All of samples are mainly composed by SiO_2, indicates that most of un-burned material from coal is the silicate minerals. Moreover, samples of FA ADR, FA KYU, FA BA and FA AI were high in the CaO concentration; suggest its higher capacity in producing alkalinity compare to the rest of the samples. The main inorganic elements found in samples are Si and Al, suggesting the high amount of quartz and aluminosilicates.

Table 3.3 XRF result of coal ash

Sample	SiO_2 (%)	TiO_2 (%)	Al_2O_3 (%)	FeO (%)	MnO (%)	MgO (%)	CaO (%)	Na_2O (%)	K_2O (%)	P_2O_5 (%)	LoI (%)	Total (%)
FA ADR	36.2	1.1	20.4	21.4	0.3	4.9	10.7	0.6	0.8	0.3	1.4	98.1
FA KPC	33.1	0.8	14.3	5.8	0.1	1.4	1.7	0.7	1.5	0.1	39.8	99.2
FA ICA	50.6	1.2	23.3	10.9	0.1	1.9	1.9	0.6	2.0	0.1	5.3	97.9
BA ICA	73.5	0.8	15.6	5.5	0.0	1.1	1.4	0.5	1.0	0.1	0.2	99.7
FA KYU	67.4	1.1	18.7	4.2	0.0	1.1	2.9	0.7	1.2	0.3	2.0	99.5
FA BA	46.5	0.9	21.1	5.3	0.1	2.8	3.0	0.9	0.8	0.2	16.4	98.0
BA BA	68.8	0.7	18.5	3.9	0.0	2.1	1.7	0.9	0.8	0.1	2.5	99.9
FA AI	42.1	0.6	9.9	25.0	0.4	7.7	11.5	0.5	0.5	0.0	0.2	98.6

LoI value shows the value of unburned carbon of the coal ash. Based on the result, it can be seen that the coal ash that has high value of LoI (FA ADR, FA KYU, FA AI) has a lower value of CaO and vice versa. Coal ashes that have a lower value of LoI (FA KPC, FA ICA, BA ICA, FA BA and BA BA) have a higher value of CaO. Calcium

concentration on the coal ash has relation to its neutralization therefore this significant difference is expected to affect the capacity in buffering AMD generation when used as cover layer. Interestingly, this differentiation is similar with the group that is found in the SEM-EDX. The group that has found to have spherical shape dominant is observed to have high CaO content and lower LoI. Meanwhile, the group which irregular shape dominant seen to have higher LoI and lower CaO. This finding suggest the burning process has a significant role in determining the shape of coal ash as well as the dominant elemental concentration remain in coal ash.

Except for FA KPC, based on ASTM C-618 (standard specification for coal fly ash and raw or calcined natural pozzolan for use in concrete, see Table 3.4 (Astm, 2010)) all of samples are classified into class F, ASTM C-618 classification. Class F in this classification means that the number of silicon dioxide, aluminum oxide and iron oxide has minimum 70% in mass percentage, while class C only 50%. Class N is also available, however this class specific only for raw of calcined natural pozzolan. Even though can be referred to, this classification is difficult to be implemented in AMD prevention since no further explanation for the capacity in neutralizing, therefore it is important to observe its neutralization as well as acid production potential and also further physical characteristic that has beneficial to the prevention of AMD.

Table 3.4 Fly ash classification by ASTM C-618

	Mineral admixture class		
	N	**F**	**C**
$SiO_2+Al_2O_3+Fe_2O_3$,	70.0	70.0	50.0
SO_3, max, %	4.0	5.0	5.0
Moisture content, max, %	3.0	3.0	3.0
Loss on ignition, max, %	10.0	6.0	6.0

The result of sequential extraction has the ability to distinguish several elements based on its form of minerals. Soluble elements, such as sulfate and oxidative compounds, are dissolved in the stage of HCl extraction. Silicate minerals are extracted in the stage of HF, and refractory elements such as sulfides are dissolved in the stage of HNO_3. Based on the data of sequential extraction in Fig. 3.4, it is observed that all of coal ash does not contain any sulfide mineral. It becomes one of the reasons of net producing capacity of coal ash will not be acidic. Moreover, in the stage of HCl extraction, only element S that has a significant amount in coal ash, means that sulfate minerals in the coal ash are quite high. This suggests the existence of sulfate minerals,

such as $CaSO_4.2H_2O$, that contributes to alkalinity producing when react with water. In the stage of HF extraction, all of the elements are extracted. This means that silicate minerals are major in the coal ash that contributes to quartz mineral as a major mineral in the silicate group.

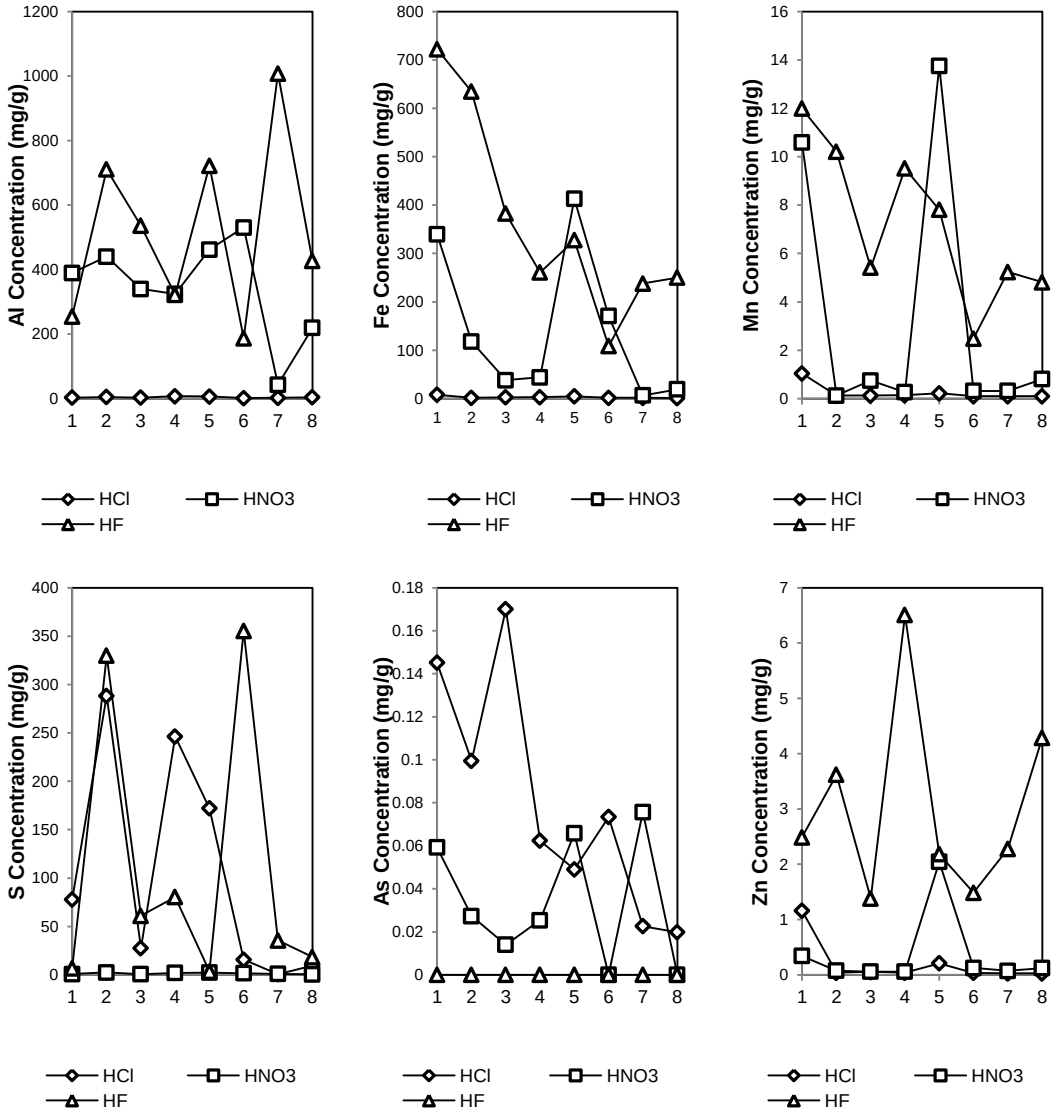

Legend: 1. FA AI 2. FA ICA 3. FA KYU 4. FA BA 5. FA ADR 6. FA KPC 7. BA ICA 8.BA BA

Fig. 3.4 Sequential extraction of coal ash

To support the result of acid digestion, XRD measurement is conducted. Table 3.5 provides the summary of XRD analysis measurement. As already known from sequential extraction, quartz mineral can be found in all of coal ash. Magnetite and hematite are also existed in most of coal ash, suggest its durability to undergo the

burning process, from low to high temperature. Interestingly, carbonate minerals (in this case are calcite and dolomite) mainly appear in the coal ash that shows high burning temperature.

The XRD result shows that both fly ash and bottom ash have a similar mineral composition. It mainly consists of quartz and aluminosilicate minerals, which understandable since the property of those two mineral groups have high maximum temperature, up to 800^{o}C therefore, can exist after burn in the boiler, which usually has temperature 400 – 600^{o}C. This is also the similar situation with magnetite and hematite that consists of Fe and O in their chemical composition that will melt at temperatures above 950^{o}C. Several fly ashes show the presence of carbonate minerals that likely will contribute to alkalinity properties of fly ash and bottom ash. It can be observed in the FA AI, FA ADR and FA KYU samples contain calcite and dolomite mineral, that belong to carbonate group.

Table 3.5 XRD result of coal ash

Samples	Minerals								
	Quartz	**Mullite**	**Aragonite**	**Magnetite**	**Hematite**	**Siderite**	**Calcite**	**Dolomite**	**Albite**
FA AI	x		x	x	x			x	
FA KYU	x			x	x	x	x		
FA ADR	x			x	x	x	x		
FA KPC	x	x	x	x	x		x		
FA BA	x		x	x	x				
FA ICA	x		x		x				
BA BA	x		x	x	x	x			x
BA ICA	x		x	x			x		

Result of mineralogy characterization of coal ash can be explained by referring to Table 3.6 (Pansu, M and Gautheyrou, 2006). Dehydroxylation of major minerals in coal ash, iron oxide and carbonate, happen in the high temperature, more than 800^{o}C. This explains the occurrence of those minerals in the coal ash even after the burning process finish.

To summarize, based on the physical characterization, it can be seen that the coal ash can be classified into two groups. The first group, consists of FA ADR, FA KPC and FA AI has dominant shape of spherical, high concentrations of Ca and low concentration of LoI. The carbonate minerals are also found to be significant in this group. Meanwhile, the second group, consists of FA KPC, FA BA, BA BA, FA ICA and BA ICA has irregular shape dominant, high concentration of LoI and also low

concentration of Ca. Sulphur content in this group is also observed higher compared to the first group.

Table 3.6 Dehydration and dehydroxylation of some clays, oxides and salts as a function of temperature in ^{o}C

Type	Name	Dehydration[a] (^{o}C)	Dehydroxylation[b] (^{o}C)
clays 1:1	Kaolinite–halloysite	350	1000
clays 2:1	smectites – montmorillonite	370	1000
clays 2:1	Illite – micas	350–370	1000
clays 2:1	vermiculite	700	1000
clays 2:1:1	chlorite	600	800
fibrous clays	Sepiolite–	300	800–900
	palygorskite allophane	200	900–1,000
iron oxides	Hematite α Fe_2O_3	(flat spectrum)	1000
	goethite α FeO–OH	100	370
	magnetite Fe_2O_3	375	650
Al oxides	gibbsite γ-$Al(OH)_3$	100	350
Ca carbonate	Calcite–aragonite $CaCO_3$	–	950–1,000
Mg carbonate	magnesite $MgCO_3$	–	710
Ca–Mg carbonate	dolomie $CaMg(CO_3)_2$	–	800–940
halogenous compounds	sodium chloride NaCl	–	800 (fusion)
sulphate	gypsum $CaSO_4 2H_2O$	–	300
sulphide	pyrite FeS_2	–	615
organic compounds	free or linked organic matter	–	300–500

[a] Dehydration: loss of water adsorbed on outer or inner surfaces, with or without reversible change in the lattice depending on the types of clay, water organized in monomolecular film on surface oxygen atoms or around exchangeable cations.

[b] dehydroxylation (+ decarbonatation and desulphurization reactions), loss of water linked to lattice (OH^-), irreversible reaction or destruction of the structure, water present in the cavities, O forming the base of the tetrahedrons

(modified from Pansu et al., 2006)

3.2.3 The neutralization capacity of coal ash

In this section, the neutralizing capacity of coal ash will be analyzed that can be used for covering layer purposes in AMD prevention. Several static tests from AMIRA standard (Smart et al., 2002), derived from Sobek et al. 1978 and modified by Skousen et al. 1998 are used and further modified in order to understand the coal ash behavior in neutralizing acidic water from PAF.

Acid neutralizing capacity is carried out to the coal ash samples. As explained in the previous chapter, the method of this test is listed as follows.

1. Fizz rating determination

   Several drops of HCl 8% are added to a small amount of pulverized sample. Observation of reaction is carried out in order to determine the fizz rating, based on bubbling reaction that occur due to the presence of calcium carbonate. The fizz rating

will determine the concentration and quantity of HCl and NaOH in further steps of the test.

2. After determining the HCl and NaOH, prepare 2.0 g of pulverized sample into a 250 ml flask or beaker, then add the required amount of HCl and 20 ml of deionized water. Blank sample is also prepared by adding the same volume and concentration of acid and 20 ml of deionized water in separate flask.
3. Heat the flask or beaker with hot plate until the reaction is complete. It is shown by no bubbling reaction occurring in the solution.
4. Cool down the flask or beaker to room temperature. After that, add deionized water to give a total volume of 125 ml. Measure the pH of solution. If the pH is between 0.8 to 1.5, titration is is conducted as explained in the step 5. When the measured pH is higher than 1.5, additional acid is added to the sample so that the total amount added is equivalent to the next highest fizz rating.
5. Titrate the solution with determined NaOH from step 1. Continue the titration to pH 7.0 and record the volume of added NaOH.
6. ANC is then calculated with the following equation:

$$ANC = \left[\frac{Y \times M_{HCl}}{w_t}\right] \times C$$

Where Y *is* $[(volume\ of\ HCl\ added) - (volume\ of\ NaOH\ titrated\ x\ B)]$, B *is* $[volume\ of\ HCl\ in\ blank)/(volume\ of\ NaOH\ titrated\ in\ blank)]$, M_{HCl} *is the of* HCl, w_t *is the weight of sample* g, C *is the conversion factor* $= 49.0\ kg\ H_2SO_4/ton$

Furthermore, net acid generating (NAG test) is also utilized in this experiment. The process of NAG test is explained in the following steps:

1. Measured 2.5 g of pulverized samples into a 500 ml conical flask
2. Add 250 ml of 15% H_2O_2 to the flask and store the it in a fume hood after place the watch glass on top of the flask. Allow the sample to react until effervescence ceases, overnight at longest.
3. Place the flask on a hot plate until effervescence stops or a minimum of 2 hours
4. Allow the sample to cool to room temperature, rinse the adhered samples on the side of flask by adding deionized water to give a final volume of 250 ml
5. Record the pH of the solution. This measurement is NAG pH.

Result of static test shows an interesting result that able to differ the fly ash into two main groups. ANC test (see Fig. 3.5) shows a significant result of neutralization from FA AI, FA ADR and FA KYU, which reached until more than 100 kg H_2SO_4/ton. It is

also supported by the result of NAG pH of those 3 samples that have high value, for FA AI, FA ADR and FA KYU, 11.93, 11.01 and 11.77, respectively. On the contrary, FA BA, FA ICA and FA KPC have a low result of the ANC and also NAG pH. This suggests that the latter group has the insignificant capacity in producing alkalinity. Meanwhile, bottom ash samples show inconsiderable value of ANC. It suggests that the addition of bottom ash based on this result will not increase the pH due to the lack of acid neutralizing capacity.

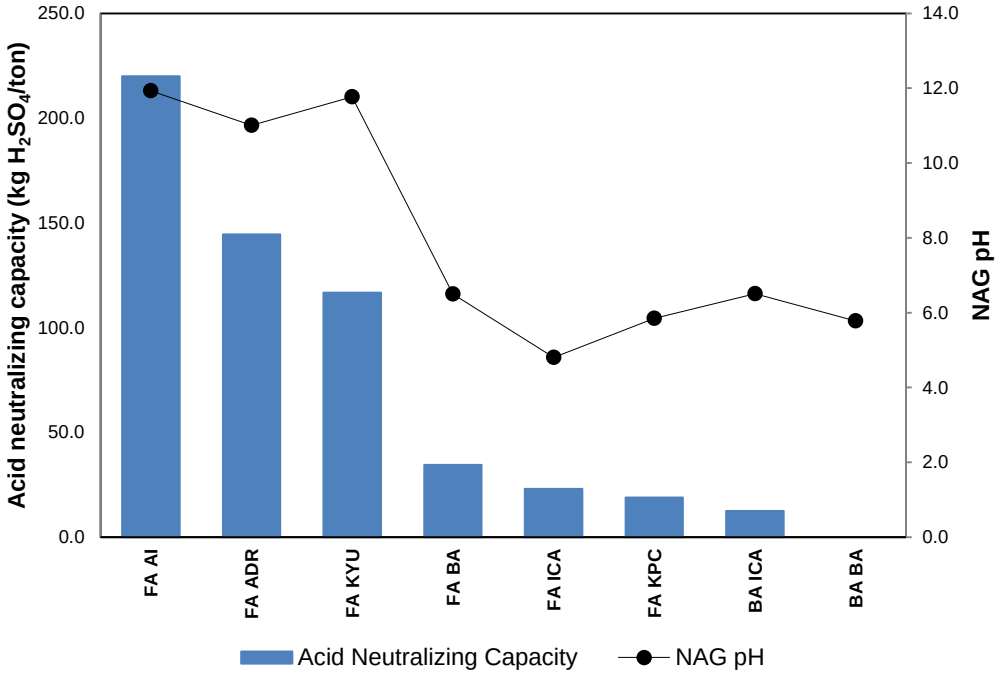

Fig. 3.5 Geochemical characterization of coal ash

From the NAG test result and paste pH test, it can be observed that in the first group (that has higher alkalinity potential) shows higher paste pH test value than NAG pH (Fig. 3.6). It means, the alkalinity in fly ash group 1 is readily to be reacted at the immediate time. This could be happened due to the remaining left after coal burning process minerals in group 1 only carbonate and also iron oxide, thus alkalinity could be readily reacted. This will be an advantage when this kind of fly ash is used to prevent the PAF rock material that will produce acidity in the short time.

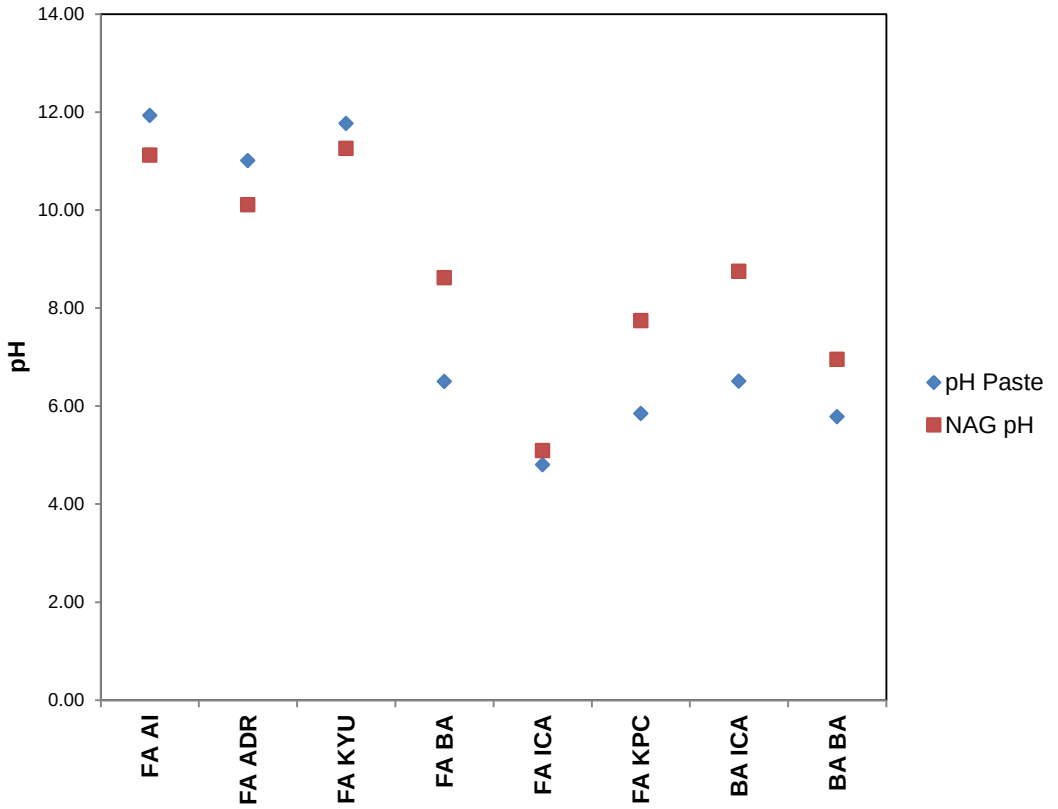

Fig. 3.6 Paste pH vs NAG pH result of coal ash

3.3 Fundamental studies of organic material

Preventative remedial measure against AMD has been extensively studied globally, including the mitigation by using the covering method of PAF rock. Due to the elevated cost, demand to use alternative materials increases. One of the promising material is organic waste, that can originate from the paper pulp, water treatment and also municipal waste industries (Gootthardsson & Sundberg, 2005). In the world, paper pulp and sewage sludge (Neuschütz, 2009) is the most well studied organic material that can be utilized as an organic material cover layer. Intensive study has been conducted for those materials that applied directly to the mine site and proved able to prevent AMD generation.

The main function of organic material cover is as an oxygen barrier that able to cut off oxygen ingress to the PAF layer due to degradation process in aerobic condition. This will depend on the organic matter contains in the organic material.

Application of organic material in Indonesia is a rare study to be conducted. Moreover, it is extremely difficult to have an organic material sourced from water treatment or sewage sludge, or even paper waste, due to the remote location area of mining in Indonesia. Moreover, the transportation of the widely known organic material to mining site will be costly that is impossible to be carried out. Therefore, this study investigates the most common available organic material in Indonesia mining site, the plant waste, since the extensive amount of plant in the mining area. The empty bunches of palm oil from Indonesia coal mine site is chosen, and then compared to sewage sludge material from Japan. Characterization of material and also comparison in acting as an oxygen barrier is then conducted.

3.3.1 Materials and experimental method

3.3.1.1 Materials

Sewage sludge from SWING company (sample name SW-OM), Japan water treatment and the empty bunches of palm oil from PT Arutmin Indonesia (sample name AI-OM) is studied.

3.3.1.2 Experimental methods

In order to know the amount of water in the materials, the samples are oven dried for 48 hours in 105^{o}C. After that, the samples are analyzed for organic matter contents in the laboratory. Major element and mineralogical analysis were carried out by using XRF and XRD analysis, respectively. Rigaku 3100 X-ray fluorescence spectrometer was used for XRF analysis. Oxygen consumption experiment in the sealed chamber is conducted, by putting certain weight of samples and quantified water to the chamber. Oxygen concentration is then measured on a time basis by using GC (gas chromatography) SRI 300 that belongs to Safety and Resource production laboratory.

3.3.2 The characterization of organic material

The water loss in both samples shows that inherent moisture of SW-OM is very high compared to AI-OM, which is more than 3-fold larger. From 2 times measurement each, percentage of AI-OM is 26.81% and 33.25%, while SW-OM is 81.77% and 83.05%. Fig. 3.7 below describes the average value of water loss in the organic material. Based

on this result, less than 20% of sewage sludge that is readily decomposed and can be used for oxygen consuming barrier in the same weight basis of EFB. Therefore, the total amount that is needed of sewage sludge a lot higher than EFB, which not beneficial.

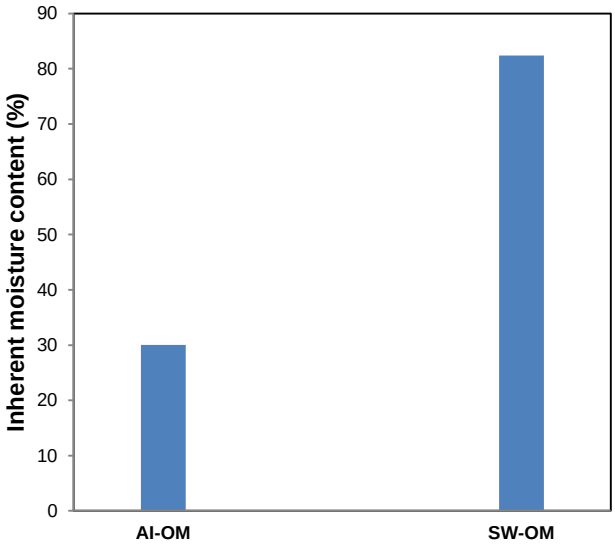

Fig. 3.7 Inherent moisture content of organic material

As an organic layer when saturated with water, sewage sludge can be useful because it will the limiting factor for the rate of oxygen diffusion into waste rock. The layer with high moisture content can also act as a physical barrier against oxygen diffusion. Given that oxygen diffusion coefficient (2 x 10^{-9} m^2s^{-1}) and oxygen solubility (8.6 g m^{-3} at 25°C) in water are very low (Nicholson, et al., 1989; He, et al., 1992), the establishment of organic covers is considered as one of the best oxygen limiting factors, that are readily available for acid production control measures. In the absence of convective transport, the rate of oxygen transport through water is too slow to be of any significance for acid generation (Reardon, et al., 1985; Broman, et al., 1991; Loomis, et al., 1984).

However, in Indonesia coal mine with tropical climate where the temperature daily can be very high especially during the summer or dry season, this function is inefficient. Therefore, in the application of cover layer EFB is better to be applied in Indonesia compared to sewage sludge.

Organic matter measurement of H, C and N percentage shows the result of similar value between AI-OM and SW-OM (see Table 3.7). This means, both of organic

material will have an oxygen barrier function from the consumption during the organic material decomposition in the aerobic condition.

Table 3.7 Organic matter measurement result of organic material

Sample's Name	Weight of Sample (µg)	H (%)	C (%)	N (%)	Ash contents (µg)	Ash (%)	100 - Ash (%)
	824.90	5.39	42.62	1.44	85.90	10.41	89.59
AI-OM2	689.70	5.41	42.71	1.37	69.30	10.05	89.95
	813.80	5.67	44.03	0.82	58.50	7.19	92.81
	705.60	5.39	42.80	1.27	62.90	8.91	91.09
AI-OM1	752.60	5.82	44.85	0.68	31.60	4.20	95.80
	818.90	5.64	44.27	1.10	59.60	7.28	92.72
	795.00	6.18	39.48	5.91	163.70	20.59	79.41
SW-OM2	790.90	6.21	40.00	5.93	150.60	19.04	80.96
	790.00	6.20	39.94	5.86	159.90	20.24	79.76
	667.30	6.12	39.65	5.71	137.10	20.55	79.45
SW-OM1	745.90	6.29	40.45	6.01	143.60	19.25	80.75
	733.30	6.52	42.08	5.72	135.00	18.41	81.59

XRF measurement shows similar results of elemental composition, except for silicate elements that noticeably high number is owned by AI-OM. This might belong to the uptake of minerals during the growth of EFB. However, SiO_2 is generally will have a stable form as mineral therefore, its existence gives insignificant impact to the dry cover system.

Table 3.8 XRF measurement result of organic material

Sample	SiO_2 mass %	Al_2O_3 mass %	FeO mass %	MnO mass %	MgO mass %	CaO mass %	Na_2O mass %	K_2O mass %	P_2O_5 mass %	S mass %	Cu mass %	Zn mass %
SW-OM	6.49	3.33	1.86	0.04	2.37	5.91	0.12	0.23	11.33	2.64	0.16	0.13
AI-OM	23.23	3.28	3.39	0.08	1.52	2.48	0.05	9.76	0.48	0.81	0.05	0.03

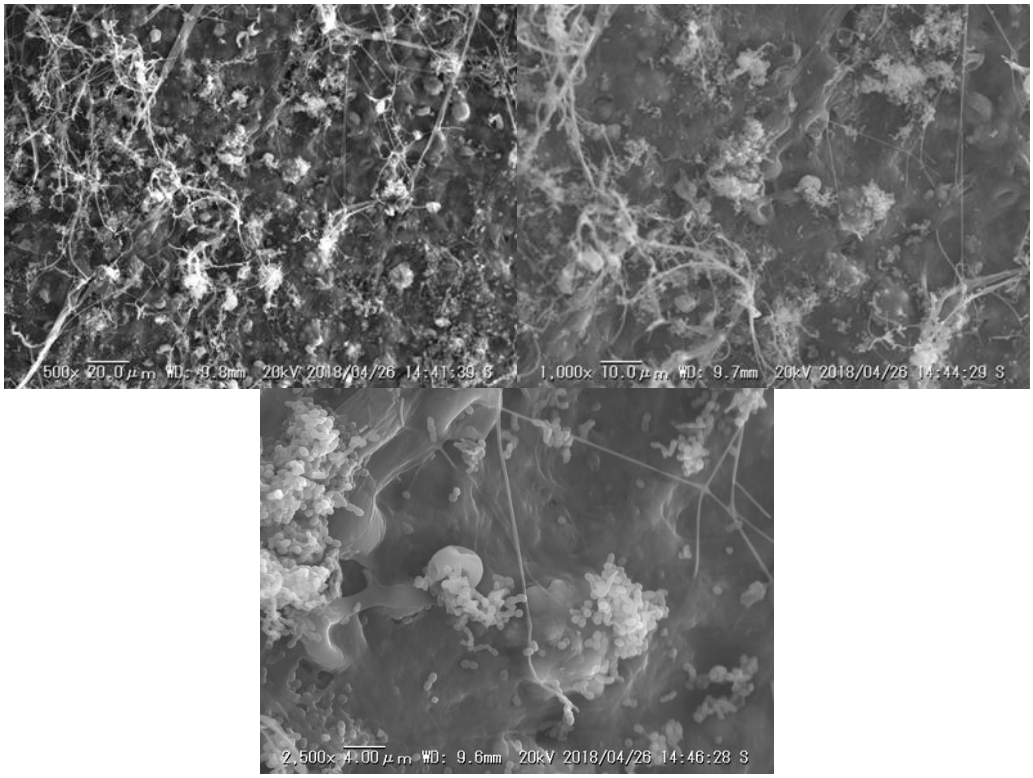

Fig. 3.8 SEM EDX result of AI-OM

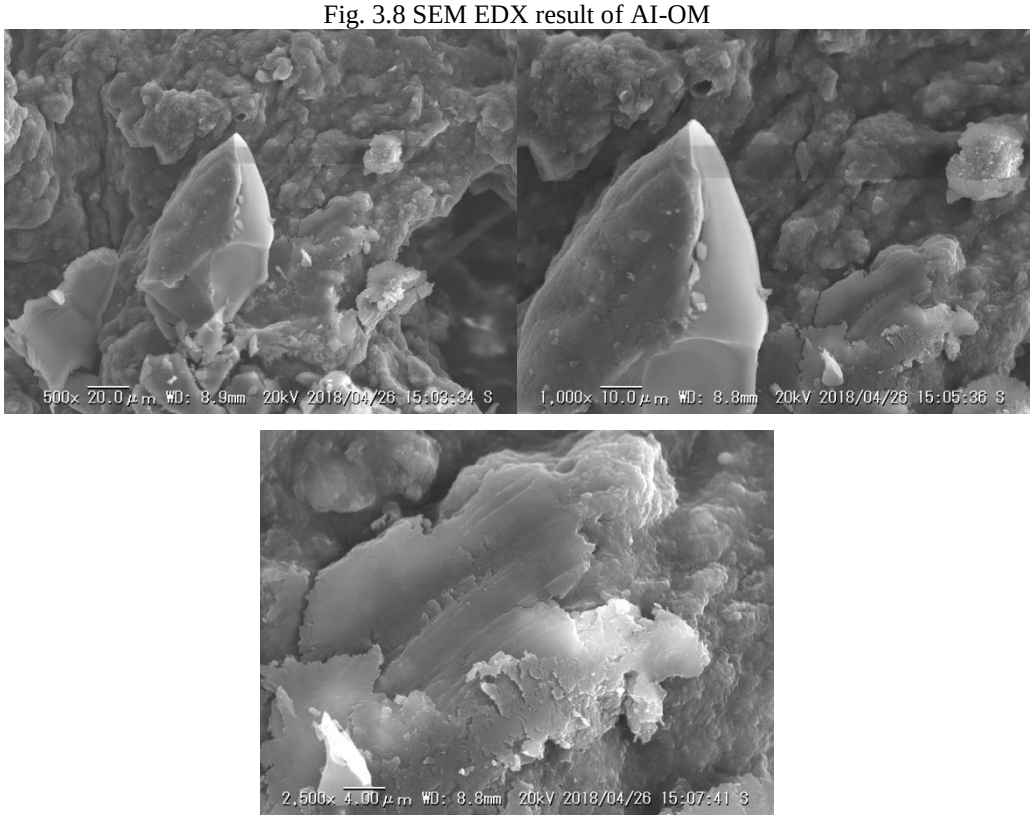

Fig. 3.9 SEM EDX result of SW-OM

SEM-EDS observation result shows that AI-OM has a fibrous structure while SW-OM has regular form, that almost similar to the crystal shape in mineral (see Fig. 3.8

and Fig. 3.9). This is due to the original source of AI-OM is a plantation that has fiber in its body. Breaking the long-chain of this material may take a longer time compared to the SW-OM, that in the observation result can be seen have various shapes with softer material thus easier to be reacted with oxygen during the decomposition process.

3.3.3 Oxygen consumption of organic material

The decomposition of organic matter ($C_6H_{12}O_6$) by biological action involves two processes, the anaerobic and aerobic degradation (Baker, et al., 1990). Anaerobic degradation takes place in nature, as in the decomposition of the organic muds at the bottom of marshes and in buried organic materials, to which oxygen does not have easy access. In that case, organic compounds break down by the action of living organisms that do not require air in the normal sense. These organisms require nitrogen, phosphorus and other nutrients to survive and develop cell protoplasm, and reduce the organic nitrogen to organic acids and ammonia (Elliot, 1986, Pierce, et al., 1995). Carbon from the organic compounds, which is not utilized in the cell protein, is liberated as methane (CH_4) and carbon dioxide (CO_2).

During aerobic degradation, living organisms which use oxygen, feed upon the organic matter and require nitrogen, phosphorus, carbon and nutrients. Most of the carbon consumed serves as a source of energy and is burned up as CO_2 (Glenn, Melchert, Eger, Kassa, & Dewar, 1997; Pierce, Belzile, Wiseman, & Winterbalder, 1994; Elliott, Liu, & W., 1996; Tasse, Germain, Dufour, & Tremblay, 1997).

In this section, aerobic degradation will be the main focus because those materials serve as the oxygen consumption barrier. Previous two organic materials, sewage sludge and EFB, compared to its ability in consuming the oxygen during its degradation process in the oxygen-rich condition. Experiment with tightly sealed chamber with rubber is conducted, in order to make sure no gas leak that can disturb the result of the experiment.

The chamber that is used in this experiment is made from acrylic that has two parts, the box part in the lower section and cylinder part that is used for sealing the chamber

with rubber and screw, thus make this chamber perfectly sealed, in the higher section. The detail dimension of the chamber is explained in Table 3.9.

Table 3.9 Box dimension

Box Part				Sylinder	
L (mm)	**W (mm)**	**T (mm)**	**Acry. T (mm**	**D (mm)**	**L Cyl. (mm)**
230.00	129.15	77.40	8.00	93.10	50.00
214.00	113.15	61.40		93.10	50.00

There are three boxes that are used in this experiment. Initial weight within the chamber is 101.88 g and 104.58 g of SW-OM and AI-OM, respectively. The third chamber is empty without sample, as a control column to represent free air. Each chamber is sprayed with 500 ml deionized water. The result of oxygen consumption measurement is shown in the Fig. 3.10.

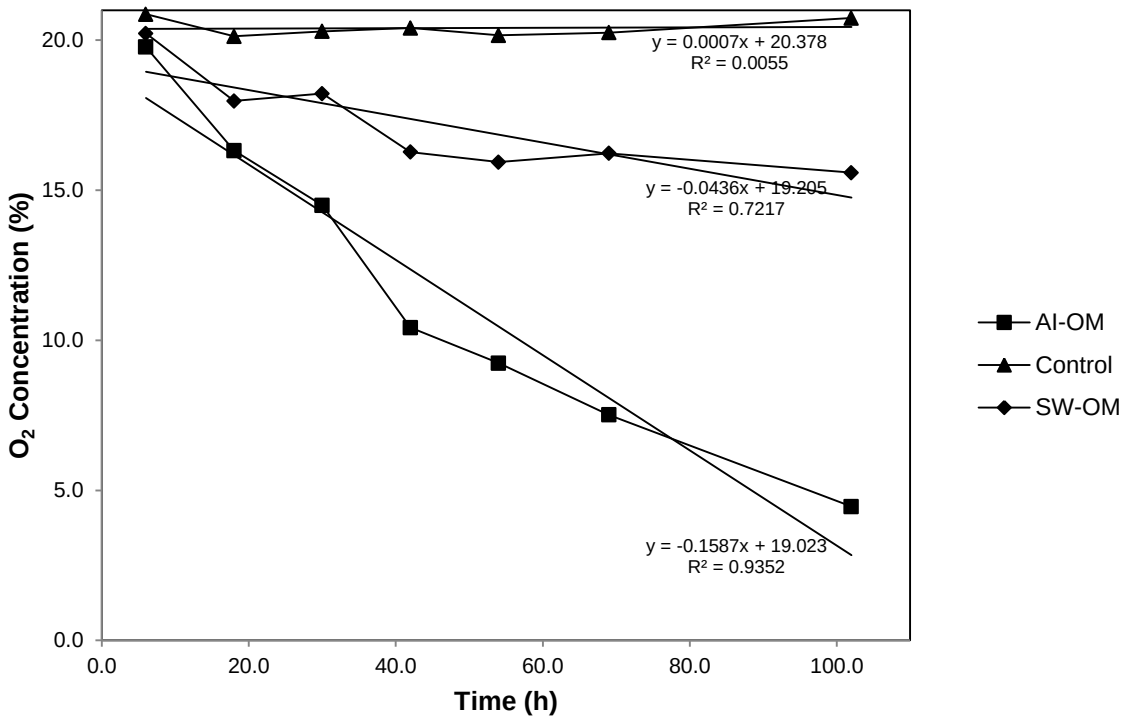

Fig. 3.10 Oxygen reduction of organic material

From the result of oxygen consumption, it can be seen that EFB in the AI-OM chamber can consume more oxygen compared to sewage sludge, in the SW-OM chamber. The reduction rate of oxygen from EFB can be up to 0.1587 (gradient of the trend line) for total 100 hours of measurement. Meanwhile, the reduction rate of oxygen from sewage sludge only around 0.0436, which is 3.6 times lower than EFB. Control column shows no significant change in the result of oxygen. Therefore, this result shows

that with the same weight, the plant based is able to consume the oxygen more rapidly compared to the sewage sludge, even with similar composition of organic matter. This is due to the extensive higher amount of water contained in SW-OM than AI-OM. Based on the characterization and the experiment, plant-based material, EFB is more beneficial to be used as an oxygen consuming barrier compared to AI-OM.

3.5 Conclusions

Based on the characterization of coal ash and organic material that have been carried out, it can be summarized as follows:

1. Similar value of specific gravity is owned by all of the coal ash, ranging around the value of 2.136 to 2.763 g/cm^3. This result means low unit weight that attractive for geotechnical uses.

2. Bottom ash has larger particle size distribution, comparing to fly ash.

3. From the different temperature during the coal burning process, fly ash is observed to be differentiated into two types of ash: 1.) The one with higher temperature that dominated by spherical particle shape, and 2.) The one with lower temperature that dominated by the irregular particle shape. Bottom ash has an irregular shape that difficult to be concluded.

4. Mineralogical observation confirms the existence of iron oxide, sulfate, silicate and carbonate minerals within coal ash, represented by hematite and magnetite, gypsum, quartz, and calcite and/or dolomite. Higher burning temperature coal ash group has more concentration of iron oxide, silicate, and carbonate mineral group as the rest of minerals already burned at lower temperature.

5. From the physical characterization result, it concluded that the most significant factor to determine the composition of coal ash is the temperature during the burning process of the coal.

6. Neutralizing capacity of coal ash has an interesting result, that can be summarized as follows:

- Fly ash and bottom ash is totally different in capacity of neutralization. Bottom ash shows insignificant potential to neutralize PAF rock, therefore fly ash is more beneficial to be used in the cover layer strategy.
- From the NAG pH and ANC test, fly ash can differentiate to two groups: Type 1 that has high alkalinity and Type 2 that has intermediate alkalinity. This result is in accordance with the segregation of coal ash based on physical and mineralogical properties.

7. Based on the characterization of organic materials, due to the high inherent moisture content, sewage sludge can also be used as the physical oxygen barrier as well as the oxygen consuming barrier. However, with the condition of tropical climate and high temperature at the mining site, especially during dry season, the physical barrier of oxygen function is unsuitable to be utilized in Indonesia.

8. Based on the oxygen consumption rate, plant-based organic material can consume more oxygen in weight basis compared to sewage sludge. The rate can differ into 3.6 folds higher than the sewage sludge.

References

ASTM. (2010). C618 - Standard Specification for Coal Fly Ash and Raw or Calcined Natural Pozzolan for Use. *Annual Book of ASTM Standards*, 3–6. https://doi.org/10.1520/C0618

ASTM. (2000). D854 - Standard Test Methods for Specific Gravity of Soil Solids by Water Pycnometer. *Astm D854*, *2458000*(C), 1–7. https://doi.org/10.1520/D0854-10.2

Chengfeng, Z., Qiang, Y., & Junming, S. (2005). Characteristics of particulate matter from emissions of four typical coal-fired power plants in China. *Fuel Processing Technology*, *86*(7), 757–768. https://doi.org/10.1016/j.fuproc.2004.08.006

Fisher, G. L., Prentice, B. A., Sllberman, D., Ondov, J. M., Biermann, A. H., Ragainl, R. C., & McFarl, A. R. (1978). Physical and Morphological Studies of Size-Classified Coal Fly Ash. *Environmental Science and Technology*, *12*(4), 447–451. https://doi.org/10.1021/es60140a008

H.Kosmatka, S., & L.wilson, M. (2011). *Design and Control of Concrete Mixtures*. *Construction*. Retrieved from http://www.cement.org/bookstore/supporting/cd100/EB001Frt.pdf

Hallberg, R. O., Granhagen, J. R., & Liljemark, A. (2005). A fly ash/biosludge dry cover for the mitigation of AMD at the falun mine. *Chemie Der Erde - Geochemistry*, *65*(SUPPL. 1), 43–63. https://doi.org/10.1016/j.chemer.2005.06.008

Neuschütz, C. (2009). *Phytostabilization of mine tailings covered with fly ash and sewage sludge*.

Neuschütz, C., & Greger, M. (2010). Stabilization of mine tailings using fly ash and sewage sludge planted with phalaris arundinacea L. *Water, Air, and Soil Pollution*, *207*(1–4), 357–367. https://doi.org/10.1007/s11270-009-0142-5

Neuschütz, C., Stoltz, E., & Greger, M. (2006). Root penetration of sealing layers made of fly ash and sewage sludge. *Journal of Environmental Quality*, *35*(4), 1260–1268. https://doi.org/10.2134/jeq2005.0229

Pansu, M and Gautheyrou, J. (2006). Water Content and Loss on Ignition. *Handbook of Soil Analysis*, *XIX*, 183. https://doi.org/10.1007/978-3-540-31211-6_1

Peppas, A., Komnitsas, K., & Halikia, I. (2000). Use of organic covers for acid mine drainage control. *Minerals Engineering*, *13*(5), 563–574. https://doi.org/10.1016/S0892-6875(00)00036-4

Sasaki, K., Haga, T., Hirajima, T., Kurosawa, K., & Tsunekawa, M. (2002). Distribution and transition of heavy metals in mine tailing dumps. *Materials Transactions*, *43*(11), 2778–2783. https://doi.org/10.2320/matertrans.43.2778

Skousen, J., Rose, a., Geidel, G., Foreman, J., Evans, R., & Hellier, W. (1998). Handbook of technologies for avoidance and remediation of acid mine drainage. *Reclamation of Drastically Disturbed Lands*, 140.

Smart, R., Skinner, B., Levay, G., Gerson, A., Thomas, J., Sobobieraj, H., … Stewart, W. (2002). ARD test handbook: Project P387A prediction and kinetic control of acid mine drainage. *Project P387A, Prediction and Kinetic Control of Acid Mine Drainage*, (May), 42.

Sobek, A. A., Schuller, W. A., Freeman, J. R., & Smith, R. M. (1978). Field and Laboratory Methods Applicable to Overburdens and Minesoils.

Steenari, B., Karlsson, L. G., & Lindqvist, O. (1999). Evaluation of the leaching characteristics of wood ash and the influence of ash agglomeration. *Biomass and Bioenergy*, *16*, 119–136.

Adriano, D. C., Page, A. L., Elseewi, A. A., Chang, A. C., & Straughn, I. (1980). Utilization and disposal of fly ash and other coal residues in terrestrial ecosystems: a review. *9*(No. 3).

Baker, M., Knoop, B., Quiring, S., Beard, A., Lesikar, B., Sweeten, J., & Burns, R. (1990). *Chapter 1: The decomposition process*. Texas: Texas Agricultureal Extension Service Solid and Hazardous Waste Management.

Broman, P. G., Haglund, P., & Mattsson, E. (1991). Use of sludge for sealing purposes in dry covers - development and field experiences. *Proceedings of the second international conference on the abatement of acidic drainage.* Quebec.

Elliot, H. A. (1986). Land application of municipal sewage sludge. *41*.

Elliott, L. C., Liu, L., & W., S. S. (1996). Organic cover materials for tailings: do they meet the requirements of an effective long term cover? *Proceedings of the 20th Annual British Columbia Mine Reclamation Symposium*, (hal. 196-209). Kamloops.

Glenn, D., Melchert, A., Eger, P., Kassa, Z., & Dewar, S. W. (1997). Reclaiming coarse taconite tailing with municipal solid waste compost. *Proceedings of the International Land Reclamation and Mine drainage Conference and in the Third International Conference on the Abatement of Acidic Drainage*, (hal. 813-824). Pittsburgh.

Gootthardsson, J., & Sundberg, A. (2005). Mine site reclamation using products from the pulp industry. *Securing the Future: International Conference on Mining and the Environment, metals and energy recovery.* Skelleftea.

He, X. T., Traina, S. J., & J., L. T. (1992). Chemical properties of municipal solid waste composts. *21*.

Loomis, E. C., & Hood, W. C. (1984). The effects of anaerobically digested sludge on the oxidation of pyrite and the formation of acid mine drainage. *Proc. 1984 Symposium on Surface Mining Hydrology, Sedimentology and Reclamation.* Lexington: Univ. of Kentucky.

Miller, S., Robertson, A., & Donahue, T. (1997). Advances in acid drainage prediction using the net acid generating (NAG) test. *Proceedings Fourth International Conference on acid rock drainage, II*, hal. 533–547. Vancouver, B. C. Canada.

Nicholson, R. V., Gillham, R. W., A., C. J., & Reardon, E. J. (1989). Reduction of acid generation in mine tailings through use of moisture-retaining cover layers as oxygen barriers. *26*.

Nordstrom, D., & Southam, G. (1997). Geomicrobiology of sulfide mineral oxidation. (J. Banfield, & K. Nealson, Penyunt.) *Geomicrobiology: Interactions Between Microbes and Minerals, 35*, hal. 361-390.

Pierce, W. G., Belzile, N., & Winterhalden, K. (1995). *Reclamation of sulphide tailings using municipal solid waste compost: laboratory studies.* Falconbridge Ltd.

Pierce, W. G., Belzile, N., Wiseman, M. E., & Winterbalder, K. (1994). Composted organic wastes as anaerobic reducing covers for long term abandonment of acid-generating tailing. *Proc. International Land Reclamation and Mine drainage Conference and in the Third International Conference on the Abatement of Acidic Drainage,*, (hal. 148-157). Pittsburgh.

Reardon, E. J., & Moddle, P. M. (1985). Suitability of peat as an oxygen interceptor material for the close-out of pyritic uranium tailings: column studies. *2*.

Stumm, W. M., & Morgan, J. J. (1981). *Aquatic Chemistry: An Introduction Emphasizing Chemical Equilibria in Natural Waters.* New York: John Wiley & Sons.

Tasse, N., Germain, D., Dufour, C., & Tremblay, R. (1997). Organic waste cover over the East Sullivan mine railings: beyond the oxygen barrier. *Proceedings of the 4th International Conference International on Acid Rock Drainage*, (hal. 1629-1642). Vancouver.

Yeheyis, M. B., Shang, J. Q., & Yanful, E. K. (2008). Characterization and environmental evaluation of Atikokan coal fly ash for environmental applications. *Journal of Environmental Engineering and Science, 7*(5), pp. 481-498.

CHAPTER 4

Study on the use of fly ash and organic material as a barrier cover on dry cover strategy

4.1 Introduction

Basic research on understanding the AMD generation and prevention strategies has been previously overviewed. As discussed in the Chapter 2, the potential of AMD generation is quite high in Indonesia coal mining site. A common problem that exists in Indonesia is the shortage amount of NAF material availability while the PAF material is abundant. It could be worsened when the NAF material is lacking in the capacity of acid neutralization. The neutralizing capacity of NAF has a significant role in the AMD generation process, by improving pH of the water thus immobilizing heavy metals. Both conditions, lack of NAF and insufficient neutralizing capacity, may affect the prevention method strategy since the conventional method in dumping overburden material is not effective in avoiding the AMD. Therefore, it is necessary to apply new technique for overcoming that problem in the dry cover method.

The alternate cover material to reduce AMD has been studied, especially for its capability in protecting sulfide minerals to react further with factors in generating AMD. In respect with that objective, dry cover materials can be generally classified in Table 4.1 (modified from MEND, 2004).

Table 4.1 Classification of dry cover material based on its function

Dry Cover Material Classification	Primary Role of Cover in Inhibition of AMD
Oxygen Transport Barriers	Act to retain moisture and hence provides a low diffusion barrier to atmospheric oxygen
Oxygen Consuming Barriers	Act as an oxygen consuming sink to provide low oxygen concentration at the interphase
Reaction Inhibiting Barriers	Act to inhibit reactions, neutralize pH

Coal ash and organic material has been studied for its characterization and possible use in dry cover strategies in an earlier chapter. Based on Table 4.1, the proposed material combination can be used as material for reaction inhibiting (coal ash) and oxygen consuming barriers. Consequently, the use of both materials as cover layer may have a more comprehensive inhibition process of AMD. In addition of the main

functions, the use of multilayer of organic material and fly ash than a single material layer of fly ash can be more beneficial for several reasons. Firstly, the availability of nutrient and organic matter in the organic material layer can act as a source of organic amendment for plant revegetation compared with the single layer coal ash that lack of those substances. Secondly, the plant uptake of heavy metals that contained in coal ash could be decreased by an additional layer above the coal ash that proved rich of metal concentrations. Lastly, the existence of organic material consumes the oxygen, which consequently provide an anaerobic condition that establish sulfate-oxidizing bacteria that advantageous to precipitate the dissolved metals, leached by coal ash and water reaction and/or during AMD generation.

Therefore, the possibility in using those materials as combination is studied in this chapter. Behavior of fly ash and organic material as cover layer is going to be investigated by using a column leach test with layering scenario was conducted in the laboratory scale. Furthermore, the additional tests and literature review are carried out to optimize those materials in dry cover strategies.

4.2 Addition of fly ash to PAF samples by using net acid generation (NAG) test

In this section, the similar fly ashes that are used in the previous chapter further investigate for theirs effect of neutralization to the PAF rock based on differentiation of group classification.

4.2.1 Materials and methods

5 fly ashes in this experiment are selected to represent the Type 1 and Type 2 coal ash. Type 1 coal ash consists of FA AI, FA ADR and FA KYU. Meanwhile, Type 2 coal ash consists of only FA KPC and FA BA. The same materials as the one in Chapter 3 of fly ash are used for this experiment.

PAF rock samples are collected from PT Bukit Asam, a coal mine company which is located in South Sumate, Indonesia. PAF rocks that are used in this experiment divided into PAF high capacity and PAF low capacity, as explained in the previous chapter. PAF high capacity has NAG pH<4.5 and NAPP>10 kg H_2SO_4/ton. Moreover, PAF low capacity has NAG pH<4.5 & NAPP<10 kg H_2SO_4/ton.

Table 4.2 XRF result of PAF rocks

Sample Name	SiO_2 (%)	Al_2O_3 (%)	Fe_2O_3 (%)	MgO (%)	CaO (%)	S (%)
PAF low capacity	60.1	17.8	3.3	1.1	0.3	0.1
PAF high capacity	40.9	16.7	5.4	1.2	0.3	2.1

Table 4.2 provides the result of XRF measurement from both PAF rocks. Significant differences can be seen from SiO_2 and measured total sulfur concentrations. In the coal bearing rocks, SiO_2 is considered as a stable crystal form and has an insignificant contribution in AMD process. Therefore, the difference of SiO_2 between PAF rocks can be ignored. Furthermore, sulfur content has noticeable difference. Total sulfur concentration has a positive relation to the acid producing capacity. Therefore, PAF high capacity is expected to have higher producing acidity compared to PAF low capacity. Further geochemical characterization, a static test, is carried out to understand the capability in producing acid of each rock.

Result of geochemical characterization of PAF rocks can be seen in Table 4.3. Based on the result, it can be observed that both of the rocks will produce AMD. Due to the large difference of sulfur contents, pyrite minerals, it will differ the amount of acid generated. PAF high capacity has NAPP 32.87 kg H_2SO_4/ton, compared to PAF low capacity that only 3.29 kg H_2SO_4/ton. These values suggest that more acidity is expected from PAF high capacity. It is confirmed from NAG pH value, where PAF high capacity has pH 1.34 that is lower than pH 3.80, the NAG pH value of PAF low capacity.

Table 4.3 Geochemical characterization of PAF rocks

Sample Name	TEST					
	Paste pH	TS (%)	ANC	MPA (kg H_2SO_4/ton)	NAPP	NAG pH
PAF low capacity	3.90	0.11	0.00	3.29	3.29	3.80
PAF high capacity	3.67	2.08	30.87	63.74	32.87	1.34

In order to know the effect of fly ash to the PAF rock, net acid generating test from AMIRA is carried out, as previously explained with modification. The amount of powdered rock in the NAG test consists of a mixture between PAF rock and fly ash, with a ratio of fly ash to PAF rock are 0%, 25%, 50% and 100%, to achieve a total weight of 2.50 g. The net final NAG pH is then recorded and compared.

4.2.2 Results

Fig. 4.1 and Fig 4.2 provides the result of the NAG pH test by adding fly ash to PAF rock. From the result of addition of fly ash addition to PAF high capacity, Type 1 fly ash can increase the final pH significantly after the 50% ratio. Neutral pH can be expected on this ratio. However, Type 2 fly ash is seen cannot increase the final NAG pH, even though 50% ratio is already used. This is understandable because 100% fly ash of Type 2 itself has around neutral pH value. Therefore, the low neutralizing capacity of Type 2 fly ash is not recommended to be used as cover material if the PAF rock has a high capacity. Meanwhile, based on this result, Type 1 fly ash is suggested to be utilized to neutralize PAF high capacity.

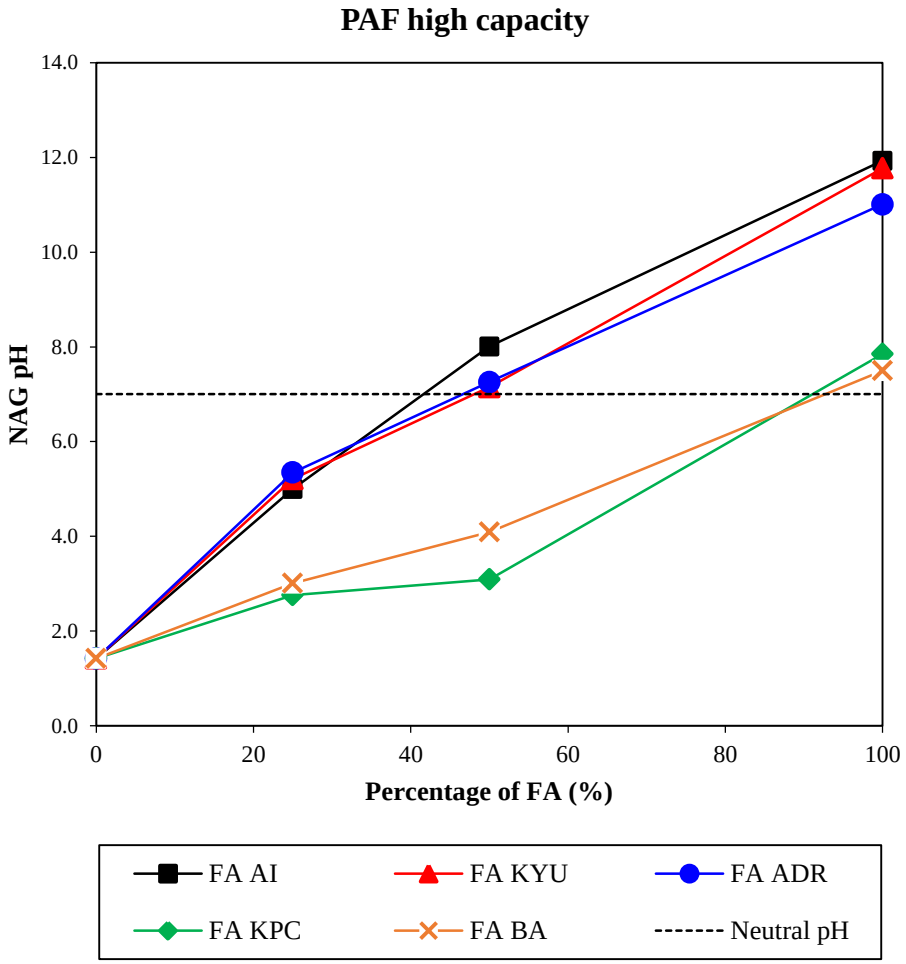

Fig. 4.1 Fly ash addition to PAF high capacity

Based on the result of fly ash addition to PAF low capacity, it can be seen that both of Type of fly ash can increase the final pH to neutral pH, around 7.0. Therefore, both Type 1 and Type 2 are can be utilized as cover material when the PAF rock has low capacity in producing acid.

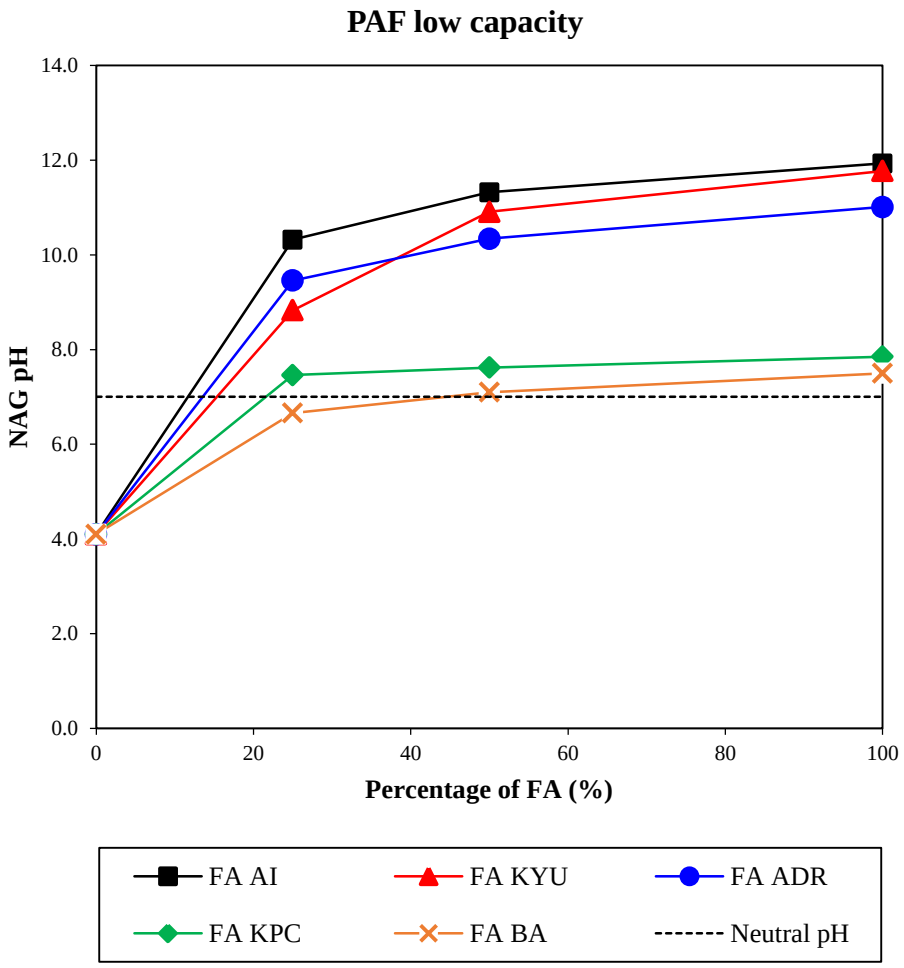

Fig. 4.2 Fly ash addition to PAF low capacity

4.3 Fly ash usage due to its neutralizing capacity classification based on the net acid generation in blending variation

In this section, two types of classification of fly ash are compared based on their neutralizing capacity classification. The neutralizing potential of fly ash in blending method to increase the pH of leachate water after interact with PAF will be analyzed on the pH parameter. Therefore, the use of fly ash based on their capacity regarding fly ash application in dry cover can be obtained.

4.3.1 Materials and experimental method

4.3.1.1 Materials

Two types of fly ash, Type 1 with high neutralizing capacity and Type 2 with an intermediate neutralizing capacity, are studied. Moreover, bottom ash from the same power plant of each type of fly ash is also observed in order to understand the leachate behavior of coal ash. Fly ash type 1 is fly ash from Adaro Mine (sample code=AD) while fly ash type 2 is fly ash from Bukit Asam Mine (sample code=BA). PAF material that is used sampled from each coal mine, as explained below.

Table 4.4 Geochemical characterization of Type 1

Sample Code	Paste pH	NAG pH	NAG (kg H_2SO_4/ton)		TS (%)	MPA	ANC	NAPP
			pH = 4.50	pH = 7.00		(kg H_2SO_4/ton)		
AD-BA	13.56	6.39	0.00	4.39	0.09	2.75	20.79	-18.04
AD-FA	11.90	9.20	0.00	0.00	0.24	7.34	51.33	-43.99
AD-P	2.55	2.65	37.43	60.56	0.94	28.76	0.00	28.76

*AD-BA=AD bottom ash; AD-FA=AD fly ash; AD-P=AD PAF

As can be seen from Table 4.4, fly ash of Type 1 has a very high neutralizing capacity with NAPP value equals to -43.99 kg H_2SO_4/ton and NAG pH is 9.20. Bottom ash of this coal mine also shares similar neutralizing capacity, with NAPP is -18.04 kg H_2SO_4/ton and NAG pH is 6.39, as compared to other bottom ash. The PAF rock sample has high acid producing capacity, with 2.65 and 28.76 kg H_2SO_4/ton of NAG pH and NAPP, respectively.

Table 4.5 Geochemical characterization of Type 2

Sample Code	paste pH	NAG pH	NAG (kg H_2SO_4/ton)		TS (%)	MPA	ANC	NAPP
			pH = 4.50	pH = 7.00		(kg H_2SO_4/ton)		
BA-P	3.86	2.90	14.04	27.00	0.95	29.09	0.00	29.09
BA-BA	6.90	4.92	0.00	8.79	0.11	3.37	2.73	0.64
BA-FA	9.64	6.59	0.00	2.53	0.28	8.58	17.13	-8.56

*BA-BA=BA bottom ash; BA-FA=BA fly ash; BA-P=BA PAF

Different with Type 1, Type 2 fly ash of BA has an intermediate neutralizing capacity with NAF pH 6.59 and NAPP -8.56 kg H_2SO_4/ton (see Table 4.5). This value is even lower compared to AD-BA. Moreover, the bottom ash of BA has near neutral NAPP, 0.64 kg H_2SO_4/ton, and slightly acidic NAG pH 4.92. Neutralization capacity of BA-BA is less expected compared to BA-FA, and also AD-BA. Moreover, BA-P has high acid producing capacity, with 29.09 kg H_2SO_4/ton and pH 2.90 of NAPP and NAG pH, respectively.

4.3.1.2 Experimental methods

As previously described, Free Draining Column Leach test from AMIRA P387A (Smart et al., 2002) with several modifications is used in this experiment. This test is carried out in order to simulate a certain scenario with the main objectives to understand sulfide mineral reactivity, rate of weathering and/or oxidation, metal solubility, and also the leachate water quality, based on the reactions happen within the column. The material is placed on the *Buchner* funnel, made from ceramic that high temperature resistance. Dry and wet phase are applied in the column that conducted on repeated cycle. Dry phase is consisted of natural and artificial drying. The latter utilizes the heat from a lamp that usually able to reach 35^{o}C on the surface material within the funnel. A daily cycle is applied in this experiment, so that the artificial drying is conducted for 12 hours and natural drying 12 hours. The wetting phase is carried out by spraying the *Buchner* funnel daily, for several minutes until the certain volume of deionized water is finished. Due to the quite high permeability, water able to flow out the funnel in only less than one hour. After that, the leachate water is collected and measured for pH value.

Table 4.6 Weight ratio of AD simulation column

Sample code	Weight (g)				NAPP (kg H_2SO_4/ton)	Sample code	Weight (g)				NAPP (kg H_2SO_4/ton)
	AD-Co-P	AD-Fi-P	AD-FA	AD-BA			BA-Co-P	BA-Fi-P	BA-FA	BA-BA	
AD-Co-B1		300		180	10.9	BA-Co-F1		400	800		3.99
AD-Co-B2		300		120	15.15	BA-Co-F2		400	400		10.27
AD-Co-B3		300		60	20.82	BA-Co-F3		400	200		16.54
AD-Fi-B1	300			180	10.9	BA-Fi-F1	400		800		3.99
AD-Fi-B2	300			120	15.15	BA-Fi-F2	400		400		10.27
AD-Fi-B3	300			60	20.82	BA-Fi-F3	400		200		16.54
AD-Co-F1		300	180		0.9	BA-Co-B1		400		800	8.98
AD-Co-F2		300	120		7.53	BA-Co-B2		400		400	14.01
AD-Co-F3		300	60		16.38	BA-Co-B3		400		200	19.03
AD-Fi-F1	300		180		0.9	BA-Fi-B1	400			800	8.98
AD-Fi-F2	300		120		7.53	BA-Fi-B2	400			400	14.01
AD-Fi-F3	300		60		16.38	BA-Fi-B3	400			200	19.03

*AD-Co-P=Adaro PAF Coarse; AD-Fi-P=Adaro PAF Fine; AD-FA=Adaro Fly Ash; AD-BA=Adaro Bottom Ash; BA-Co-P=Bukit Asam PAF Coarse; BA-Fi-P= Bukit Asam PAF Fine; BA-FA= Bukit Asam Fly Ash; BA-BA= Bukit Asam Bottom Ash

Blending of material between coal ash Type 1 and Type 2 to PAF that belong to each original mine is carried out. Different size of PAF, coarse (passes the 2.00 mm and retains the 0.75 mm) and finer (passes the 0.75 mm) is used in order to investigate FA behavior to different size of PAF, due to the size segregation found in the dumping situation. The weight ratio is further explained in following Table 4.6. The aim of the

ratio is to evaluate the effect of the NAPP ratio after coal ash and PAF mixing. Moreover, the column control observation of individual materials is also conducted.

4.3.2 Result and discussion

Graph in the Fig. 4.3 provides the result of column control simulation of AD. In the column of AD-Co-P and AD-Fi-P, columns that have a same PAF rock, but different particle size resulted in similar behavior of leachate water with slight gap between them. Generally, finer particle size column has lower pH value. In this experiment, the size of particle gives insignificant impact for individual behavior.

As predicted for bottom ash and fly ash, AD-BA has near-neutral pH in most measurements, except for the initial stage. However, the pH value is higher than its NAG pH measurement result. Meanwhile, the AD-FA gives high value of pH that after 40 days of measurement, shows decreasing value. This is due the reduction of neutralization capacity within the FA material. With the pH value of deionized water itself is around 7.00, the reduction value of pH for both coal ashes in the last stage will be around neutral pH, 7.00.

From the comparison between bottom ash and fly ash in Type 1 with blending method, it can be seen that bottom ash addition cannot increase the pH value of PAF (see Fig. 4.3) even though the final NAG pH of the mixture material is higher than fly ash mixture material. Therefore, in this type of coal ash, bottom ash is not recommended to be used as cover layer. Meanwhile, the final pH value measurement of leachate water gives significant improvement. Higher the mixture ratio between the materials that also means an increase value of NAG pH final mixture, higher pH of leachate water can be observed. This means, FA can effectively ameliorate the leachate water and prevent the acidic water to form.

Classification of NAPP that is between 0 to 10 kg H_2SO_4/ton actually considered as uncertain, still have potential to produce acidity (Stewart, Miller, & Smart, 2006). Positive NAPP means that the material will produce acidity. This is also confirmed with the blending ratio that has NAPP higher than 10 kg H_2SO_4/ton in the column (AD-Fi-F2, AD-Fi-F3, AD-Co-F2, and AD-Co-F3) has a tendency to still produce acid. Therefore,

it is recommended if NAPP calculation utilized to determine the amount of FA needed in dry cover strategy, the final blending value of NAPP should be less than 10 kg H_2SO_4/ton.

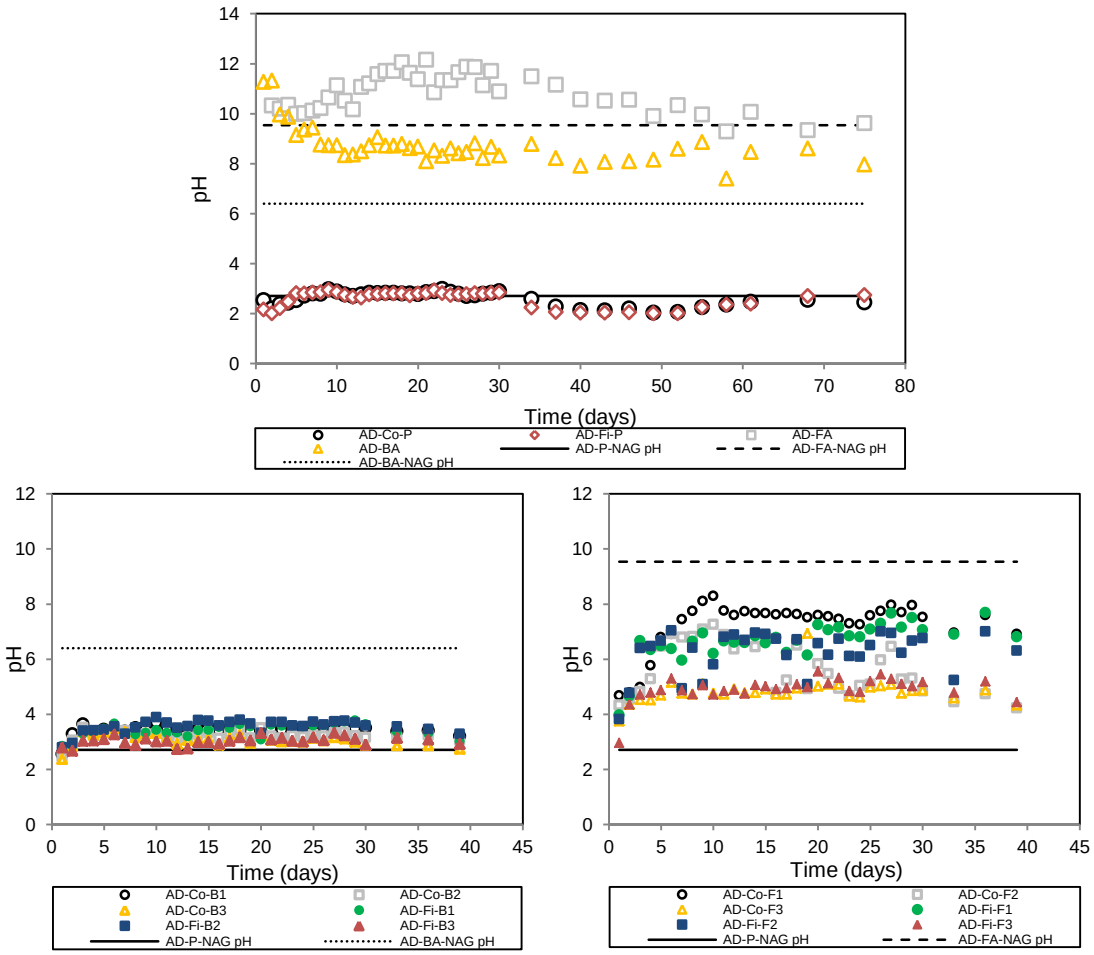

Fig. 4.3 Comparison result of AD bottom ash and fly ash

Result of control column of bottom ash and fly ash Type 2 in blending method is provided in Fig. 4.4, as well as the control column of PAF. The result of the control columns of BA has similar leachate water behavior with the previous coal ash and PAF in the previous discussion. The coal ash neutralization capacity is decreased after 30 days, that in a shorter duration than coal ash than AD. Fig. 4.4 also shows the leachate water behavior of BA, after bottom ash and fly ash are each mixed with the PAF materials with different particle size. The behavior of BA is not significant in improving leachate water in the simulation column. This validates the previous result of fly ash Type 1, which is better to use fly ash than bottom ash for dry cover strategy.

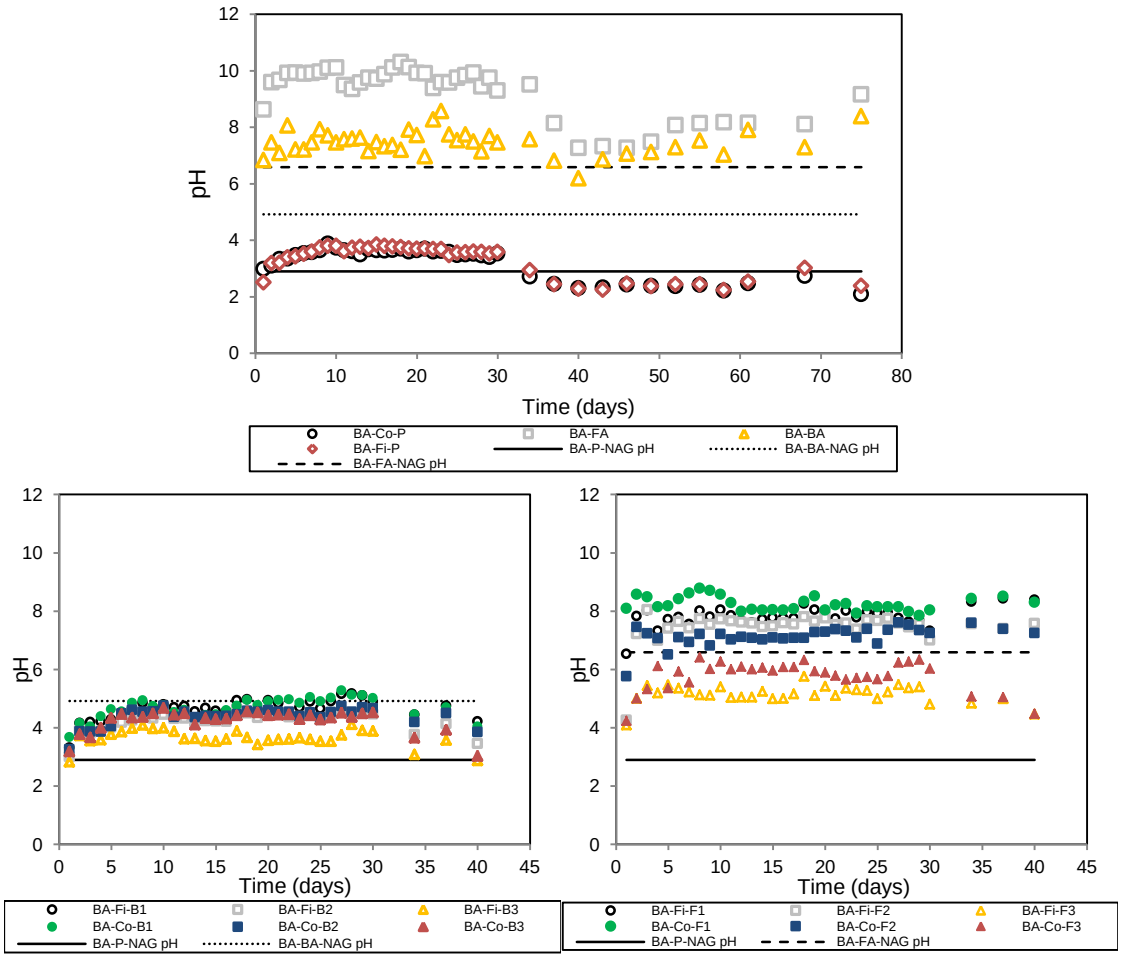

Fig. 4.4 Comparison result of BA bottom ash and fly ash columns

Fly ash mixture with PAF shows contrast result than bottom ash mixture result. In the simulation, only BA-Co-F3 and BA-Fi-F3 columns that have continuous acidic result, with average pH value is 5.77 and 5.15, respectively. From the NAPP value of blending materials, only those columns that have NAPP value more than 10 kg H_2SO_4/ton. Therefore, as it is also supported by the coal ash Type 2 result, it is better to use blending ratio with NAPP calculation between fly ash and PAF rocks with a value lower than 10 kg H_2SO_4/ton.

4.4 Mixing and layering scenario of fly ash with high neutralizing capacity

After obtaining the result of different type of fly ash leachate water behavior based on the geochemical classification, this section will discuss the effect of different type of fly ash utilization method on a dry cover strategy. Fly ash type 2 is chosen due to the better neutralization capacity for attenuate the PAF with high potential in producing acid, as found in Indonesia coal mine.

4.4.1 Materials and experimental method

4.4.1.1 Materials

Both materials used in this experiment are identical to the previous section, fly ash Type 1 and PAF samples from Adaro coal mine.

4.4.1.2 Experimental methods

This experiment is conducted with the same Buchner funnel as the previous chapter. The method also follows AMIRA, with modification in the daily cycle of wetting and drying that identical with previous explanation. The weight ratio between fly ash and material is listed in the Table 4.7.

Table 4.7 Weight ratio of fly ash and PAF rocks in the layering scenario

Column Code	Weight Ratio (g)		Column Code	Weight Ratio (g)	
	AD-LA-P	AD-LA-FA		AD-BL-P	AD-BL-FA
AD-LA-F1	300	180	AD-BL-F1	300	180
AD-LA-F2	300	120	AD-BL-F2	300	120
AD-LA-F3	300	60	AD-BL-F3	300	60

4.4.2 Result and discussion

Based on the pH measurement result, the control column has an expected result where the PAF rock has acidic water pH and the fly ash from Adaro has high pH measurement (see Fig. 4.5). Furthermore, in the result of pH measurement, it can be seen that if the layering method is used (AD-LA-F1, AD-LA-F2 and AD-LA-F3), the improvement is insignificant while if the blending is used, the significant improves in pH can be clearly seen. This result is in accordance with the past result that uses blending method for NAF layer with an intermediate neutralizing capacity (Nugraha et al., 2009) and also the utilization of fly ash Type 2 to the PAF (Kusuma et al., 2013). This is possibly due to the preferential flow that occurs after neutralization took place. Agglomeration that happens during a series of drying and wetting, result in slaking, will cause an air filled void within a column that resembles overburden dumping profile (Andrina, 2006; Song & Yanful, 2010; Newman, 1999). Therefore, generally in the fly ash, it is better to use blending method than layering one.

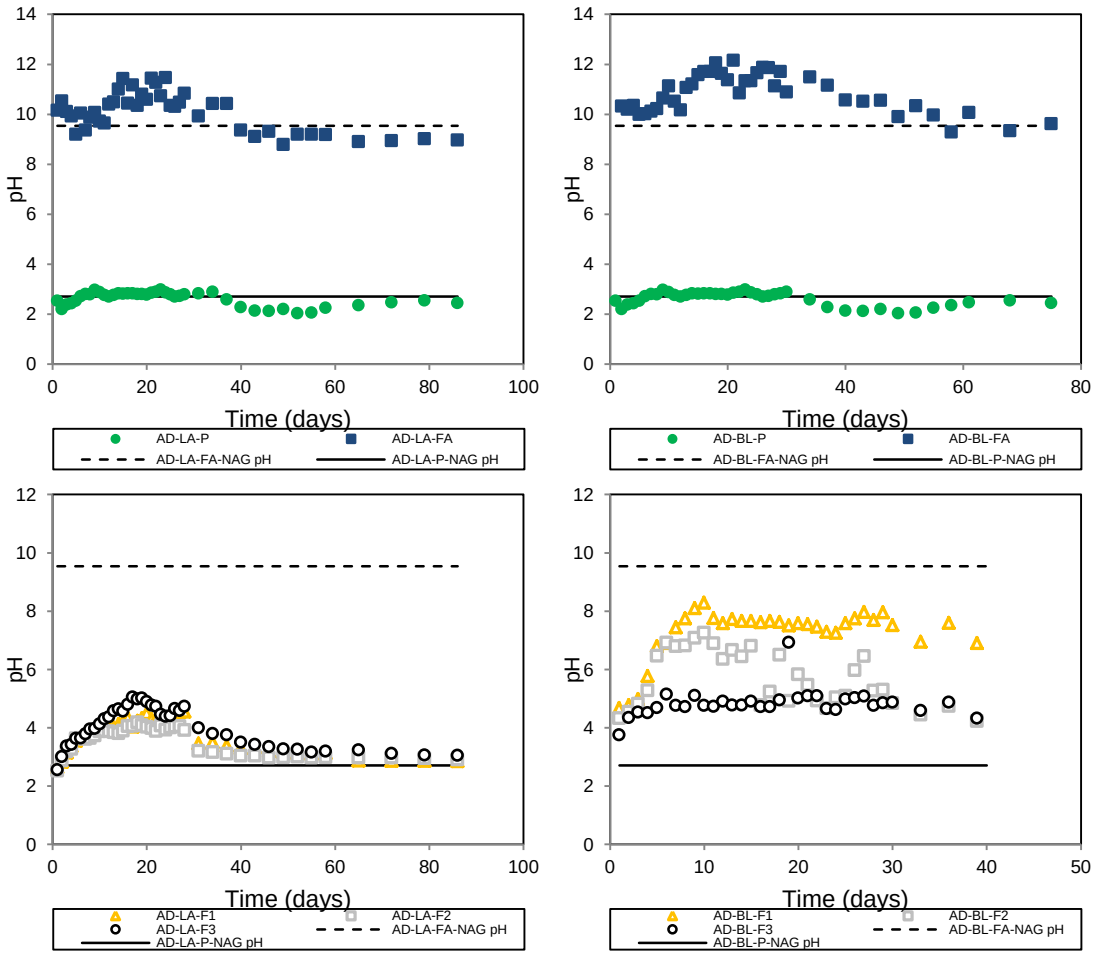

Fig. 4.5 The pH measurement result for control column (upper figure) and blending and layering scenario (lower figure)

4.5 Fly ash usage due to its neutralizing capacity classification based on thickness variation

This section will comprehend the needs of more applicable fly ash ratio based on thickness that is easier to be constructed at the coal mine. Similar like previous experiment, both fly ash Type 1 and Type 2 is used in this experiment. This section aims to find out the optimum thickness of fly ash from Type 1 and Type 2 that can be used in the mining to prevent AMD.

4.5.1 Materials and experimental method

4.5.1.1 Materials

Fly ash materials that are used in this section are each classified as Type 1 (AI-FA from Arutmin coal mine) and Type 2 (BA-FA from Bukit Asam). These materials were

already characterized in the previous Chapter 3. PAF that are used for this experiment sampled from Bukit Asam coal mine. Furthermore, geochemical characterization is provided in the Table 4.8 as follows.

Table 4.8 Geochemical characterization of AI-FA, BA-FA and PAF

Sample Code	Paste pH	NAG pH	MPA (kg H_2SO_4/t)	ANC (kg H_2SO_4/t)	NAPP (kg H_2SO_4/t)
PAF	5.35	3.71	94.9	67.3	27.6
AI-FA	11.58	11.87	18.4	249.9	-231.5
BA-FA	8.37	6.5	55.1	56.3	-1.2

4.5.1.2 Experimental methods

Different with previous experiments that use Buchner funnel, this experiment uses customized acrylic with dimension as can be seen in the Fig. 4.6. This is carried out due to the limitation of Buchner funnel in providing simulation with different thickness to be carried out. Table 4.9 explains the configuration of thickness difference in more detail. PAF samples that are used in this experiment have a particle size between 0.75 mm to 2.00 mm.

Table 4.9 Details of thickness within a column

Column name	Thickness of material (mm)		
	PAF	FA1	FA2
AI-2.5	200	25	
AI-5	200	50	
AI-10	200	100	
AI-20	200	200	
BA-2.5			25
BA-5	200		50
BA-10	200		100
BA-20	200		200
PAF	200		
AI-FA		100	
BA-FA			100

Prior the experiments, based on the result of the previous section, blending of both fly ash is carried out with the ratio 20:80 of fly ash and quartz sand. Quartz is chosen because it is a relatively stable mineral that not easily react with water to produce neither acidity nor alkalinity. The main parameters of this experiment are hydraulic conductivity and pH measurement. Hydraulic conductivity measurement is carried out with calculation of the difference of the falling head water when the water is released per time. The cock under the outlet of water is closed by the column saturated, maximum 1 hour after pouring the water. After saturated, the cock is opened and the debit of leachate water volume recorded per specified time. When the water is fully

released from the column, the leachate water, then collected for pH measurement. After the columns are completely dried out with natural and artificial drying similar like previous experiment, by measuring for its stable weight and compared to the initial weight in the column, water is poured again to the column. This process is counted as one cycle. On the total, this experiment is conducted for 8 cycles.

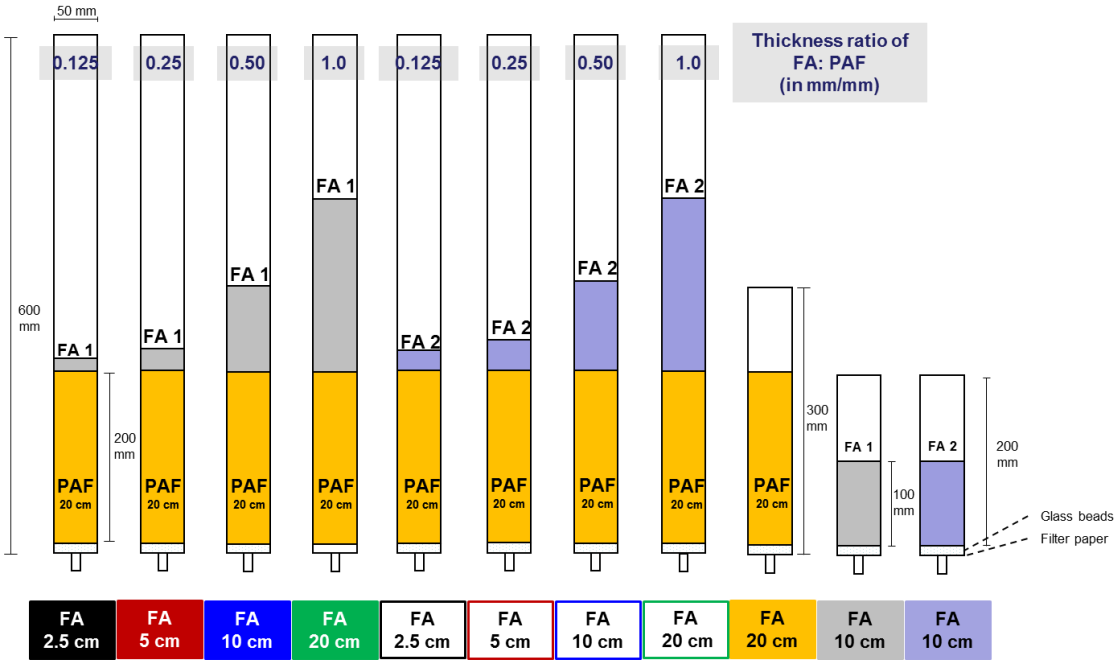

Fig. 4.6 Dimension of column and configuration of material within the column

4.5.2 Result and discussion

Fig. 4.7 provides the result of hydraulic conductivity measurement. From the control column, it can be seen that all of the materials decrease in permeability. Moreover, the permeability decrease in the PAF rocks is really high, as can be observed from the graphic and large value of positive gradient. This is happened due to the slaking behavior that happened because the continuously drying and wetting process within the column.

Fly ash from AI and BA also show decrease in permeability even though not as large as PAF material. The permeability decrease in the fly ash is possible to occur because of the cementation process that binds materials in fly ash and form an agglomeration. However, FA AI shows lower value in permeability and also higher

decrease of permeability reduction that indicates the cementation occurs rapidly in the Type 1 than Type 2 fly ash.

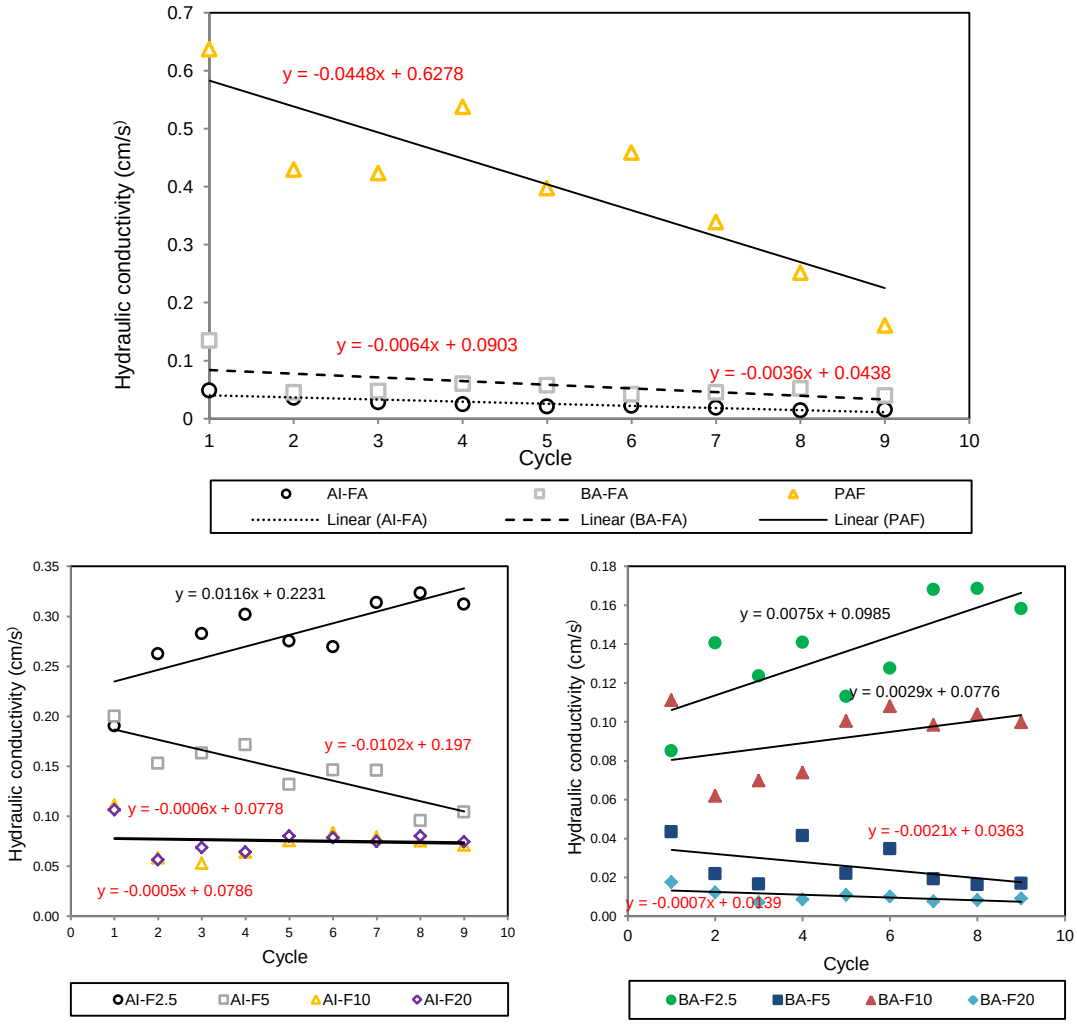

Fig. 4.7 Hydraulic conductivity result of the columns

Based on the simulation within the column, it can be observed that for fly ash Type 1, the thickness of 2.5 cm (AI-F2.5) will have an increase in hydraulic conductivity (see Fig. 4.7). This is an interesting phenomenon that might occur due to the layering of fly ash in this thickness can prevent the weathering in the PAF layer to happen, that should be prevented. Moreover, in the AI-F10, the decrease of permeability can be seen. In this case, Type 1 fly ash needs at the least thickness of more than 0.25 times of the PAF in order to have the effect of permeability reduction.

Interestingly, the Type 2 fly ash shows the increase of permeability even until the BA-F5 column. Permeability reduction can start to be observed from the column of BA-

F10. Therefore, in the Type 2 of fly ash it is better to be carried out at least for thickness of more than 0.5 times of the PAF to have the effect of permeability reduction.

The pH measurement result of each column is provided in the Fig. 4.11. From control column, it can be seen that the PAF that is used in the experiment PAF with low capacity has an increase pH to near-neutral in the cycle. Furthermore, the measurement of AI-FA and BA-FA confirm the fly ash classification where AI-FA as Type 1 has continuously higher pH than Type 2, BA-FA.

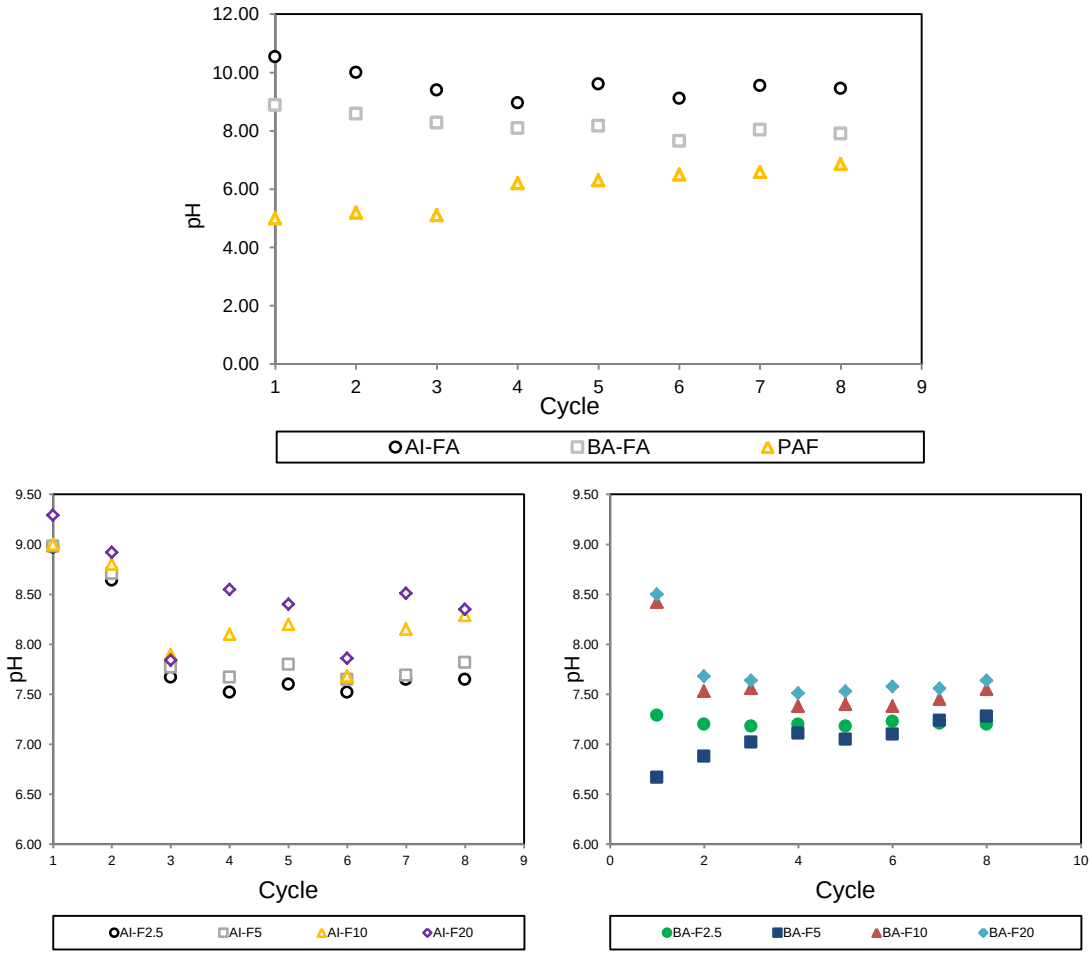

Fig. 4.8 pH measurement of simulation columns

From the simulation result of column with different thickness, Type 1 of FA shows its potential to improve the leachate water even though only 2.5 cm of FA is applied. In contrast, for the PAF that is in Type 2, thickness that needed in order to improve the leachate water is minimum 10 cm that equals to 0.5 times of PAF, even though the PAF that is used in the experiment is PAF low capacity. Therefore, for PAF with high

capacity in producing acid fly ash Type 2 is not recommended to be applied. Fly ash Type 1 is obviously a better option. However, if the PAF rock has low capacity in producing acid, fly ash Type 2 then can be utilized.

4.6 Organic material as oxygen consuming barrier on dry cover strategies

The primary function of organic material is the consumption of oxygen in the layer where the oxygen impedes. This process is happened due to the microbial degradation of the carbohydrate (CH_2O) fraction contained in the organic material. Common cover that utilizes organic material, usually consists of wood chips, wood wastes, peat, sewage sludge, hay, straw, silage and paper mill sludge (Sopper, 1993).

In this study, empty fruit bunches (EFB) of fruit palm oil is chosen as one of material for the cover layer due to its nutrient and organic matter content and also abundance in Indonesia. The well-known materials in the cover material are both wood fly ash and sewage sludge, due to its prominent availability to be utilized ubiquitously (Neuschütz & Greger, 2010; Peppas, Komnitsas, & Halikia, 2000). However, those materials contain metal (Steenari, et al., 1999; Wang, et al., 2011), and sewage sludge contains high levels of nitrogen and phosphorus (Petersen, et al., 2003). In addition, sewage sludges frequently contain bacteria, protozoa, viruses and ova of helminthes that are pathogenic, possibly harm the surrounding environment. These issues raise the awareness in using both organic materials as an oxygen consuming barrier. Therefore, the selection of EFB as an oxygen consuming barrier provides a promising usage.

As discussed in the chapter 3, aerobic oxidation of organic matter proceeds according the following equation 4.1 (Germain, et al., 1992). Based on that equation, the oxidation is occurred due to the two biochemical processes, first enzymatic hydrolysis to dissolve constituents. This is the breaking process of long chains of carbon from organic matter to the shorter one and easier to be digested. The second process is the uptake and metabolism of the dissolved mono-and diso-charides.

$$(CHO)_{106}2(NH_3)_{16}(H_3PO_4) + 138\ O_2 \rightarrow 106\ CO_2 + 16HNO_3 + H_3PO_4 + 122\ H_2O \qquad \text{Eq. 4.1}$$

Large amounts of oil palm biomass and wastes are generated in Indonesia each year (Astimar, 2014). Several examples of oil palm biomass are listed in the Table 4.10. EFB

property in this table is very similar like the characterization of EFB discussed in the previous chapter, thus indicate the similarity shared by both material of the same species. From these properties, the organic matter quality can characterized. Organic matter quality means how fast an organic material decomposes (Swift, et al., 1979); Brady & Weil, 2002). One of the most often used to understand organic matter quality is C/N ratio, where the lower this ratio, the higher the organic matter quality the organic material quality and the faster the material decomposes. EFB has the intermediate of organic material quality compared to the leaflet and trunk parts of the overall biomass.

Table 4.10 Property of several biomass of palm oil

Property	C (%)	N (%)	P (%)	K (%)	Ca (%)	Mg (%)	Lignin (%)	C/N	Lignin/ N	Moisture (%)
EFB	48.64	0.87	0.05	1.89	0.2	0.12	28.5	56.1	32.65	64.17
LFT	50.90	2.33	0.11	1.34	1.09	0.16	24.96	22.5	10.74	68.02
OPT	34.14	0.26	0.05	0.26	0.56	0.04	1.83	176	70.38	71.20

*LFT=oil palm leaflets; EFB=empty fruit bunches; OPT=trunk. All percentages are on a dry weight basis
Sources: (Moraidi (2012, 2015), UNEP (2012), Wan Razali, et al. (2012), Taqwan (2013)

Table 4.11 provides the decomposition rate constant (k) for oil palm biomass types. It can be seen that among three of biomasses, EFB has intermediate level of decomposition rate among the other oil palm biomass. Moreover, this is also comparable with the decomposition rate of sewage sludge that already observed. Francisca Gomez-Rico et al. (2008) found that during the usage for 0 – 9 months into limestone and sandstone, decomposition rate k of sewage sludge is 0.21 % of months^{-1} and 0.12 % of months^{-1}, respectively.

Table 4.11 Decomposition water for oil palm biomass types

Biomass types	k (% of months $^{-1}$)
Leaflets (LFT)	0.26
Empty fruit bunches (EFB)	0.20
Trunk (shredded)	0.11

Study about the simultaneous decomposition and nutrient release rate of EFB has been carried out by Moraidi, et al. (2012). The biomass is applied as a protective cover layer for soil, where EFB are heaped and covers approximately 30 m^2 land surface area. Temporal carbon and nutrient release (%) by the decomposition of EFB is presented in Table 4.12. Moraidi then reported in his paper that after 8 months of field decomposition, EFB had lost 79% and would reach 10% of its initial mass in 12 months.

Table 4.12 Release of measured parameter by decomposition of EFB

Decomposition (months)	Properties	EFB
3	C	57.4
	N	9.7
	C/N	26.0
	P	19.2
	K	55.5
	Ca	28.3
	Mg	36.6
6	C	82.7
	N	38.7
	C/N	15.4
	P	49.2
	K	87.3
	Ca	53.1
	Mg	61.9
8	C	87.6
	N	43.1
	C/N	20.1
	P	54.1
	K	86.0
	Ca	58.2
	Mg	55.7

Biomass weight loss of EFB follows an exponential decrease with time, by following equation of exponential. As consequences, the C/N ratios of EFB decrease with time and reduce its organic matter quality. Therefore, rapid decomposition is expected in the initial phase of the application then keeps decreasing in the matter of time. Moraidi reported that the mean monthly reduction in the C/N ratio of EFB was 5.4 units, which is similar result with study previously reported by Rosenani & Hoe (1996). In their paper, Rosenani and Hoe recorded that EFB's C/N ratio declined from 57 to 31 in 15 weeks of EFB decomposition. This equals to 6.9 units reduction of C/N every month.

Teh (2009) also conducted a similar study that has objectives to observe the physical changes of EFB during the composition in the field. On his paper, EFB thickness was reduced at the rate of 15.1 mm/month with graphic as shown in Fig 4.9. By fitting it to linear regression curves, it can be estimated the reduction to zero thickness can be achieved in about 9 months. Hence, this equation can be used in order to estimate the thickness of EFB that is needed for dry cover method which make use of decomposition of EFB process.

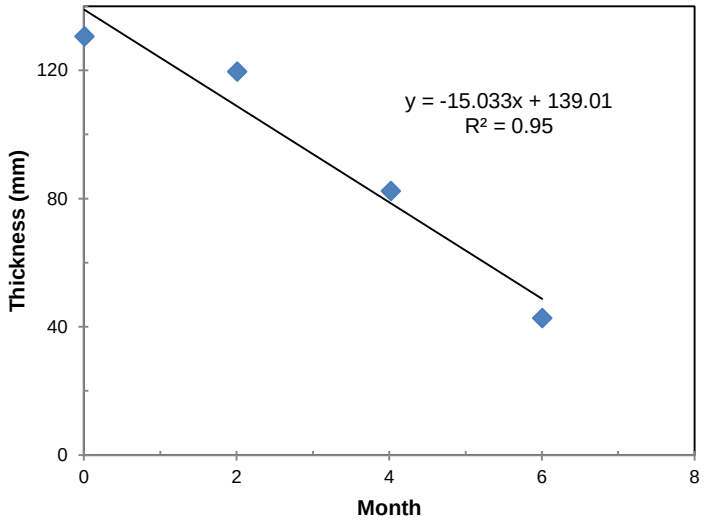

Fig. 4.9 Thickness reduction of EFB in the field

For long-term usage, based on the equation of EFB trend line in Fig. 4.9, minimum thickness of EFB should be not less than 762.97 mm in order to reach to zero thickness in 5 years. The reduction unit of C/N will follow as high as 6.9 units monthly. Moreover, if the long-term usage is expected to last until 10 years, the estimation of thickness needs to be increased not less than 1,664.95 mm. Therefore, estimated values for the thickness of EFB as a cover layer to consume the oxygen needs to be around 75 – 150 cm (number is rounded for easier construction on the field).

4.7 Simulation of fly ash (coal ash) and empty fruit bunches (EFB) of fruit palm oil as cover layer by Free Draining Column Leach test

After understanding the optimization of each material layer to be utilized in the mine, this section will try to understand the effect of both materials in the dry cover method. The study of combination of fly ash and EFB in dry cover simulation will be carried out. Free draining column leach test is conducted and analyzed further for the leachate water quality.

4.7.1 Materials and methods

4.7.1.1 Materials

In order to do the simulation, samples were obtained on the site, from Asam-asam Mine Pit 2 – 5, PT Arutmin Indonesia (PT AI) situated in South Kalimantan Province,

Indonesia. Samples consist of coal-bearing rock in surrounding mine, fly ash and also empty fruit bunches (EFB) of fruit palm oil.

Table 4.13 Geochemical characterization of samples

Sample Code	Lithology	TEST									Geochemical Classification *
		Paste pH	Paste EC	Total Sulfu	ANC	MPA	NAPP	NAG pH	NAG pH 4.5	NAG pH 7.0	
			(µS/cm)	(%)	(kg H_2SO_4/ton)				(kg H_2SO_4/ton)		
SS - 01	Sandston	4.80	260.00	0.11	0.00	3.27	3.27	4.40	0.30	7.30	PAF
CS - 02	Claystone	5.50	96.00	0.06	0.00	1.78	1.78	5.80	-	1.00	NAF
SS - 03	Sandston	3.20	813.00	0.17	0.00	5.14	5.14	4.00	1.20	4.70	PAF
SS - 04	Sandston	3.90	1098.00	0.11	0.00	3.29	3.29	3.80	1.60	6.10	PAF
CS - 05	Claystone	3.90	668.00	0.17	0.00	5.25	5.25	3.40	4.30	10.80	PAF
CS - 06	Claystone	3.90	538.00	0.14	0.00	4.13	4.13	4.10	1.20	10.70	PAF
SS - 07	Sandston	4.20	404.00	0.11	0.00	3.33	3.33	4.40	0.20	6.30	PAF
CS - 08	Claystone	4.50	376.00	0.09	0.00	2.66	2.66	4.60	-	5.90	NAF
SS - 09	Sandston	5.70	116.00	0.03	0.00	0.84	0.84	7.10	-	-	NAF
SS - 10	Sandston	5.60	203.00	0.04	0.00	1.13	1.13	6.70	-	0.20	NAF
SS - 11	Sandston	5.80	521.00	0.15	1.00	4.63	3.63	6.60	-	0.60	NAF

The rock was sampled by doing the grab sampling, after digging the rock material for around 15 cm in the depth to obtain fresh rock. Eleven rock samples were collected afterward and analyzed by static test to know the capacity in producing acid. The result of the rock sampling and static test is shown in Table 4.13. Based on the geochemical classification, 6 samples were categorized as potential acid forming (PAF) and 7 samples were non-acid forming (NAF).

Rock samples that were categorized as NAF then uniformly mixed together with the exact same weight and identical grain size. This procedure was carried out due to the consideration that the dumping area has heterogeneous bulk rock material in the site. The same procedure was also conducted to the PAF material. In order to have a better evaluation of cover material effect in improving the leachate water quality, acid producing capacity was increased by adding pyrite mineral to the PAF Mix material in the 2% w/w. Fly ash was collected at Asam-asam coal-steam power plant, which belongs to the State Electricity Corporation, Republic of Indonesia (P.T. PLN – Perusahaan Umum Listrik Negara). The fly ash that is used in this simulation is the same material with the FA AI that's characterized on previous Chapter 3. The static test results of material after mixing and also fly ash can be seen in Table 4.14.

Table 4.14 Static test results of material for column test

Sample	paste pH	TS (%)	MPA (kg H_2SO_4/ton)	ANC (kg H_2SO_4/ton)	NAPP (kg H_2SO_4/ton)	NAG pH	NAG pH 4.5 (kg H2SO4/ton)	NAG pH 7.0 (kg H2SO4/ton)
PAF mix	4.16	1.10	33.78	1.95	31.83	2.33	42.65	9
NAF mix	5.77	0.11	3.32	2.65	0.67	6.04	0	5.87
Fly ash	11.81	0.59	17.97	224.69	-206.72	10	0	0

Organic material was obtained from the palm oil processing company that has a plantation area adjacent to the Asam-asam, also the same organic material used in Chapter 3. This organic material is a waste from the empty fruit bunches of oil palm that can be found easily in surrounding mine site. In Asam-asam mine, this material was used as raw material in organic compost making after cutting down the size using organic waste shredder, into the size of 100 until 200 mm. Organic matter measurement of EFB can be seen in Table 4.15.

Measurement of organic C, H and N is carried out by using digestion and microwave analysis. Two samples of EFB, AI-EFB1 and AI-EFB2, is analyzed to compare the result. Based on the result, mean concentrations of C are 43.12% and 43.97% with C/N results are 11.87 and 14.42. This result shows the organic matter quality of EFB, which is quite high and indicates the available carbohydrate to be decomposed and consume the oxygen.

Table 4.15 Organic matter measurement of EFB

Sample's Name	Weight of Sample (µg)	H (%)	C (%)	N (%)	Ash contents (µg)	Ash (%)	100 - Ash (%)
	824.90	5.39	42.62	1.44	85.90	10.41	89.59
AI-EFB1	689.70	5.41	42.71	1.37	69.30	10.05	89.95
	813.80	5.67	44.03	0.82	58.50	7.19	92.81
	705.60	5.39	42.80	1.27	62.90	8.91	91.09
AI-EFB2	752.60	5.82	44.85	0.68	31.60	4.20	95.80
	818.90	5.64	44.27	1.10	59.60	7.28	92.72

Major element and mineralogical analysis were carried out by using XRF and XRD analysis, respectively. Rigaku 3100 X-ray fluorescence spectrometer was used for XRF analysis while XRD analysis was performed using Rigaku RINT 2000 X-ray diffractometer. The results of the elemental major analysis of PAF Mix, NAF Mix, fly ash and EFB are provided in Table 4.16.

Table 4.16 Result of XRF analysis for elemental composition

Element	PAF Mix	NAF Mix	Fly Ash	EFB	Element	PAF Mix	NAF Mix	Fly Ash	EFB
	Major (%)					Minor (ppm)			
SiO_2	75.38	71.42	42.10	23.28	As	2,848.00	9.00	25.00	74.00
TiO_2	0.67	0.92	0.60	0.32	Mo	5.00	8.00	0.00	37.00
Al_2O_3	13.10	17.03	9.93	3.28	Rb	16.00	41.00	42.00	244.00
FeO	2.39	2.45	24.99	3.39	Sr	40.00	85.00	857.00	113.00
MnO	0.00	0.04	0.44	0.08	Ba	102.00	216.00	4,046.00	55.00
MgO	0.53	0.81	7.66	1.52	Y	16.00	24.00	24.00	44.00
CaO	0.08	0.16	11.52	2.48	Zr	214.00	282.00	139.00	72.00
Na_2O	0.34	0.36	0.53	0.05	V	106.00	167.00	129.00	39.00
K_2O	0.39	0.85	0.53	9.76	Cr	82.00	108.00	83.00	603.00
P_2O_5	0.04	0.09	0.03	0.49	Co	37.00	21.00	16.00	40.00
LoI	5.61	5.64	0.23	54.24	Cu	22.00	62.00	38.00	0.05
S	1.11	0.10	0.59	0.82	Zn	47.00	13.00	17.00	0.03

Based on the XRF analysis in Table 4.16, major elements of PAF Mix and NAF Mix quite similar. The dominant elements are silica, aluminium and iron (measurement value>1%). Sulfur concentration in the PAF Mix is higher than in NAF Mix, due to the sulfide mineral that makes it has higher capacity in producing acid. Another noticeable difference is the calcium oxide content, which fly ash has higher concentration than NAF Mix. Calcium oxide (CaO) contributes to the ability of material in neutralizing the acidity, therefore as the higher CaO concentrations the potential in producing acidity is lower since it has self-neutralizing material within the rock. Interestingly, SiO_2 also dominates the result of EFB result that possibly happened due to the uptake of plant during the growing process.

From the XRD analysis, the PAF Mix consists of quartz (SiO_2), illite ($KAl_2Si_3AlO_{10}(OH)_2$), kaolinite ($Al_2Si_2O_5(OH)_4$), siderite ($FeCO_3$), pyrite (FeS_2), and arsenopyrite ($AsFe_S$). Meanwhile, the NAF Mix consists of quartz (SiO_2), chlorite ($(Mg,Fe)_5(Al,Si)_5O_{10}(OH)_8$), kaolinite ($Al_2Si_2O_5(OH)_4$), siderite ($FeCO_3$), illite ($KAl_2Si_3AlO_{10}(OH)_2$) and jarosite ($KFe_3(SO_4)_2(OH)_6$). The fly ash material has mineralogy as follows: quartz (SiO_2), illite-montmorillonite ($KAl_4(Si,Al)_8O_{10}(OH)_4.4H_2O$), chlorite ($(Mg,Fe)_5(Al,Si)_5O_{10}(OH)_8$), dolomite ($CaMg(CO_3)_2$), gypsum ($CaSO_4.2H_2O$), siderite ($FeCO_3$), aluminum oxide ($Al_2O_3$), andradite ($Ca_3Fe_23(SiO_4)_3$) and magnetite ($Fe_2Fe_3O_4$).

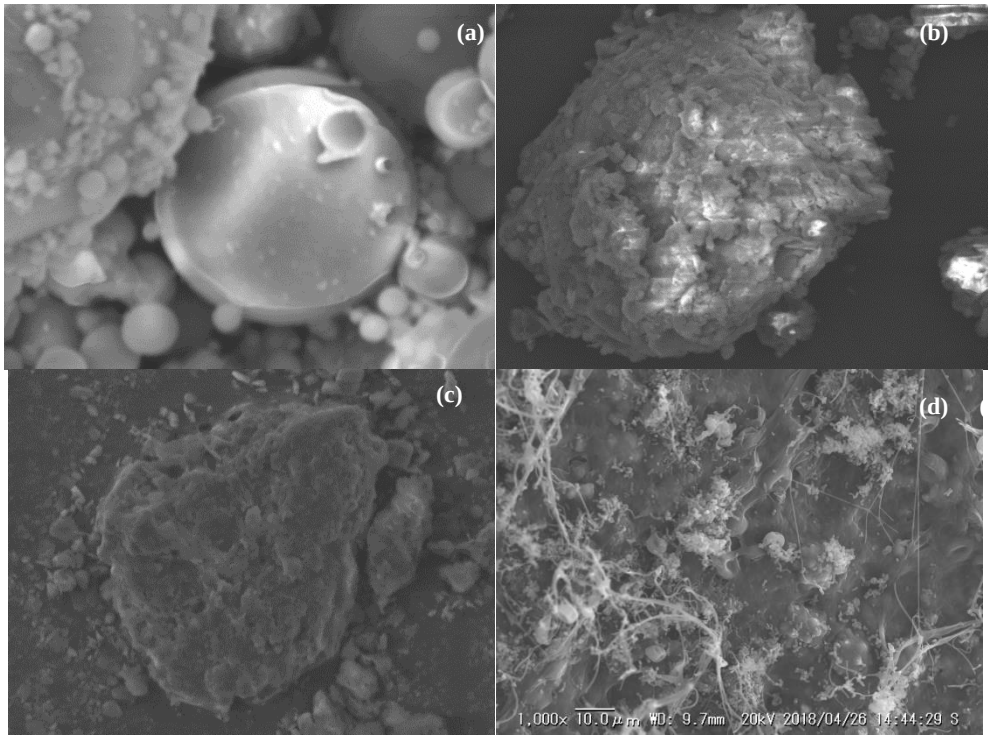

Fig. 4.10 SEM image of Fly Ash 1000x (a), PAF Mix 2000x (b), NAF Mix 2000x (c), and EFB 1000x (d)

The situation of material surface of SEM data is provided in Fig. 4.10. Fly ash material mostly has a spherical shape with various particle sizes, as described in Chapter 3. Meanwhile, PAF Mix and NAF Mix material have heterogeneous shapes and sizes of particle. The common matter during the observation is both PAF Mix and NAF Mix material have a rough surface, as a product of weathering that happened because the minerals in the material have interaction with water and air. Furthermore, EFB shows the fibrous surface that commonly seen in the vegetation. Moreover, several groups of small size shape, less than 3 μm can be seen that might be an indication of microorganisms' existence.

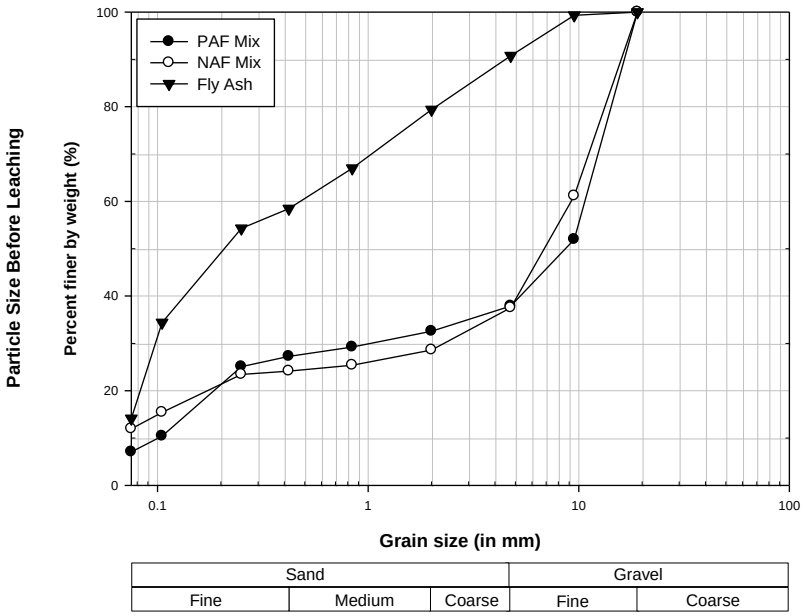

Fig. 4.11 Particle size distribution of material before the leaching test

Fig. 4.11 provides the particle size distribution of PAF Mix, NAF Mix and fly ash prior the simulation. The grain size of PAF and NAF Mix is almost similar which passed the #20 mm sieve (size opening = 19 mm) with the d_{50} equals to 0.80 mm and 0.75 mm, respectively while d_{20} of both materials equal to 0.20 mm. Meanwhile, the fly ash particle size is finer than the PAF Mix and NAF Mix particles. It has d_{50} = 0.21 mm and d_{20} = 0.08 mm.

4.7.1.2 Methods

The leaching simulation followed a method of Free Draining Column Leach test from AMIRA, with modification. A column that was used in this simulation has of diameter 100 mm and total height of 300 cm, while column to the control column per layer has a diameter of 100 mm and total height of 100 mm. Layering scenario was selected due to the consideration of mining method that is used in mine site. Moreover, layering scenario has been proven as an effective method for AMD prevention based on the previous study (Kusuma, 2012; MEND, 2003).

The simulation consists of column with and without fly ash and organic material cover layer. This was carried out to investigate the effect of cover in the AMD generation. In the column with cover, there are two scenarios of PAF and NAF material:

PAF and NAF materials by 80% and 50%, and PAF and NAF materials by 50% and 50%, respectively. The purpose is to compare the effectiveness of cover in the case of a different PAF amount. The NAF Mix material was placed together with fly ash by blending uniformly with ratio 1:2 of NAF Mix and fly ash. In the control column, PAF Mix, NAF Mix and cover layer behavior were investigated. Further information about the column configuration is provided in Fig. 4.12 while the weight distribution of each layer shown in Table 4.17.

Table 4.17 Weight distribution of material in the column

Column	Weight (g)			
	PAF	**NAF**	**FA**	**OM**
PAF80%-COVER	800.44	200.44	400.80	150.01
PAF80%-NO COVER	800.53	200.53	-	-
PAF50%-COVER	400.32	400.24	800.6	150.23
PAF	600.63	-	-	-
NAF	-	600.81	-	-
Cover	-	-	150.68	150.07

Leaching test was conducted for 56 days in the total, with phases of wetting and drying in order to resemble the mining field condition. The drying phase was a daily cycle, with 12 hours heating by the lamp (measured temperature in the column, T = 35 – 40^{o}C) and 12 hours natural drying. Spraying by 250 ml of deionized water was conducted for wetting phase while the leachate water collected in the flask 300ml. After the leachate water came out, it directly measured for pH, ORP (oxidation and reduction potential) and EC (electrical conductivity). Then, leachate water was filtered with 0.45 µm filter and acidified. Major cation-anion measurement then conducted by using Dionex ICS-90 ion chromatography. On the other hand, metal content was measured by using ICP-OES Seiko Instruments VISTA-MPX and the total dissolved organic carbon (TOC) measurement also carried out by using TOC analyzer Shimazu TOC-V CHS.

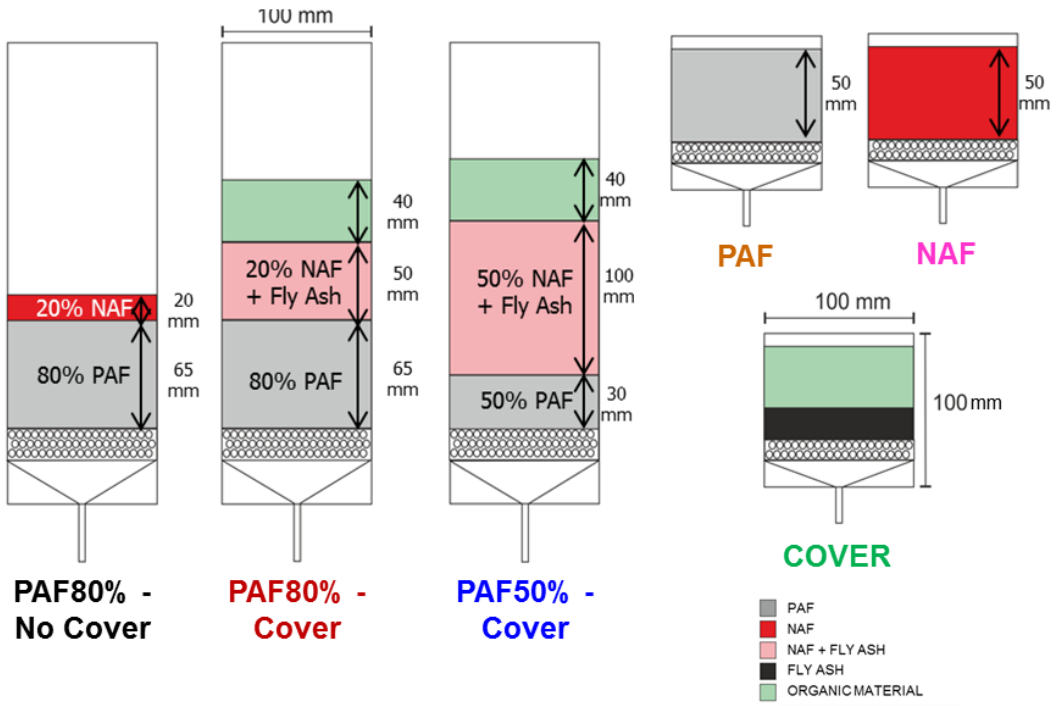

Fig. 4.12 Leaching column configuration

4.7.2 Results and discussions

From the simulation, two main aspects can be observed based on the wetting and drying phase that was carried out. Wetting phase causes the water flowing through the column after having interaction with the material inside the column. These consist of water – organic material interaction and water – mineral interactions that have leachate water as the final result. Therefore, the quality of water and the dissolved matter content in the leachate were observed to obtain formation about the possible reaction within the column. Meanwhile, drying phase will reduce the moisture content by evaporating the water and let the mineral to be oxidized further by the oxygen. It affects the AMD generation, reduced the particle size due to the weathering process that will break down the rock into smaller size. Thus, the rock material change on the layer within the column was also observed to have a better understanding of fly ash and organic material.

The pH and EC measurement result of six columns are presented in Fig. 4.13. During the simulation, measured pH of mostly columns had stable value. Column PAF resulted in the acidic leachate water, with pH value ranged from 2.71 – 3.21 and the average value during the pH measurement was 2.88. This outcome was expected, since from the

mineralogy analysis the PAF material has pyrite and arsenopyrite existence detected from XRD and high total sulfur concentration from XRF analysis. Moreover, static test has analyzed the acid producing capacity of PAF Mix material which showed high potential in generating AMD. Interestingly, PAF80%-NO COVER also produced leachate water that in the similar value in PAF column, even though in PAF80%-NO COVER column contained NAF layer material above PAF layer. PAF80%-NO COVER pH value ranged from 2.34 – 3.31 with the average pH value was 2.75. This suggests that with the case of the huge difference between PAF volumes available at the mine site, method of layering PAF with NAF layer is ineffective to improve the AMD.

On the contrary, the column with the fly ash and organic material cover, PAF50%-COVER and PAF80%-COVER column, produced near neutral to alkaline leachate water. PAF50%-COVER pH ranged from 7.28 – 9.48 with the average pH value was 8.52 while PAF80%-COVER pH ranged from 7.95 – 9.30 with the average pH value was 8.47. This result was in concordance with the result of Cover column that has a high pH value of leachate water, ranged from 8.48 – 10.89 with the average 9.59. The alkaline solution from fly ash and organic material cover layer improves the AMD by consuming the acidity. Therefore, even though PAF Mix could generate acidic water, the flowing water from cover material will buffer the pH and improve the water.

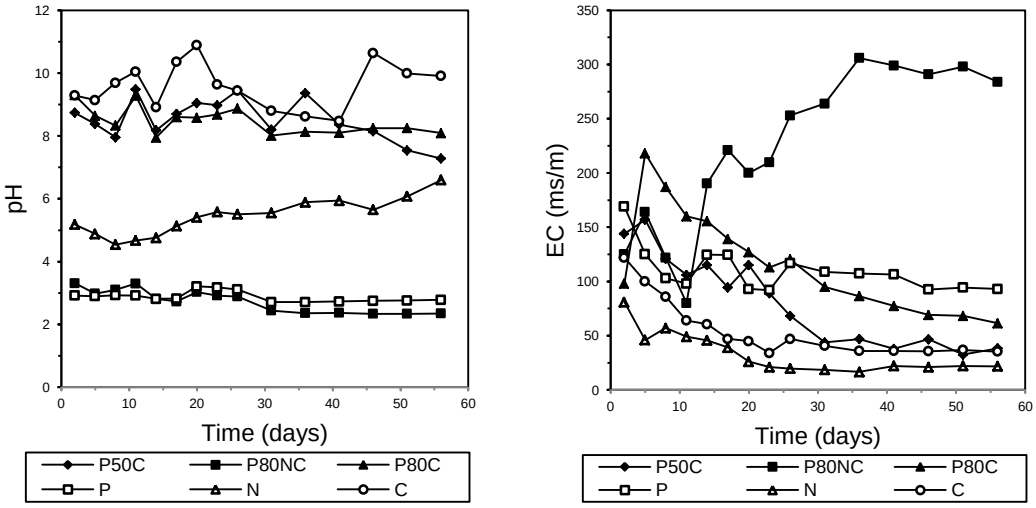

Fig. 4.13 pH and EC leachate water measurement result

P50C=PAF50%-Cover; P80NC=PAF80%-No Cover; P80C=PAF80%-Cover; P=PAF; N=NAF; and C=Cover

EC or conductivity is a measure of the ability to pass current in aqueous solution from the dissolved material, usually from free ion in the solution. The measured value of EC shows the total amount of anions or cations in the solution, where both cations and anions have their own charge. The decrease of the conductivity is due to ion-association and electrostatic shielding effects (Appelo & Postma, 2005). At 25^{o}C, the EC (µS/cm) divided by 100 could estimate the amount of cations/anions in the solution. Generally, EC value has an opposite order with the pH. If pH decreases, the more ions dissolve in the solution as the pH contributes in the changes of ion solubility. As consequences of this condition, EC value will escalate since the electric current from dissolved ion also increase. This basic principle is used in explaining the condition within the materials in the column.

Based on the measurement result, PAF80%-NO COVER had the highest EC on the average (see Table 4.1), as expected from the low pH measurement result. The greatest dissolved metal concentration can be expected from this column. By comparing the EC from the PAF80%-COVER and PAF80%-NO COVER, the significant value difference can be seen. Therefore, it was assumed that the cover had contributed in decreasing the number of dissolved ions of the leachate water. In the case of the lower ratio of PAF material, PAF50%-COVER column also showed lower EC value that indicates even less ions dissolved in the column than PAF80%-COVER. This result supports the fly ash and organic material contribution assumption previously.

Table 4.18 Statistic of leachate water measurement result

Sample	pH			EC (mS/cm)		
	Average	Minimum	Maximum	Average	Minimum	Maximum
PAF50%-COVER	8.52	7.28	9.48	0.85	0.35	1.62
PAF80%-NO COVER	2.75	2.34	3.31	2.15	0.83	3.00
PAF80%-COVER	8.47	7.95	9.30	1.19	0.60	2.30
PAF	2.88	2.71	3.21	1.07	0.88	1.69
NAF	5.42	4.54	6.60	0.34	0.16	0.81
Cover	9.59	8.48	10.89	0.56	0.33	1.22

Among the columns, the lowest EC value was owned by NAF column. Even though the pH of NAF was lower than Cover column, EC of C was constantly higher than NAF. This is due to the several ions that easily dissolve in alkali condition. In addition, the single layer columns with lower mass (PAF, NAF and Cover) had a lower EC value compared to the column with layer combination. This was understandable since the more mineral concentration in the column means more ions likely to be dissolved in the

leachate water. From the investigation, good correlation between the pH and EC trend could be observed.

Major cation and anion

Most groundwaters contain great concentrations of calcium (Ca^{2+}), magnesium (Mg^{2+}), sodium (Na^{+}) and potassium (K^{+}) as major cations and bicarbonate (HCO_3^{-}), sulfate (SO_4^{2-}) and chloride (Cl^{-}) as major anions. The dissolution of minerals happens as the main natural sources of cation-anion presence in the water (Younger, 2007).

Based on the result of major cations-anions measurement, similar trend could be observed from the initial flush of all columns. Both columns showed an anomaly initial data that was extremely high. This was expected as shock loading phenomenon, which happened because of the weathering that already occurred previously. First flushing caused the entire oxidized mineral to dissolve in the water immediately, thus increased the total major cation-anion compared to the rest. After neglecting the initial measurement, steady changes could be seen that formed certain trend of major cation-anion dissolution.

Table 4.19 Statistic data of major cation-anion measurement

Element	Statistic	Measurement Result (in mg/l)					
		PAF50%-	PAF80%-	PAF80%-	P	N	C
Sulfate	Max	1,271.61	2,237.64	1,921.94	1,504.35	922.73	381.57
	Min	106.98	876.97	714.41	590.71	113.33	107.83
	Average	689.25	1,662.23	1,137.37	833.04	359.81	202.88
Sodium	Max	26.40	19.72	34.66	14.46	9.40	37.41
	Min	4.63	0.00	6.45	1.23	0.00	2.79
	Average	13.85	5.03	11.05	4.11	3.24	9.05
Potassium	Max	61.56	18.73	33.26	13.15	28.59	310.31
	Min	15.08	0.00	20.69	4.44	10.03	20.32
	Average	34.92	8.21	24.61	6.94	16.86	95.30
Magnesium	Max	32.45	79.90	53.25	68.05	36.57	1.65
	Min	4.39	33.30	9.95	7.19	5.89	0.00
	Average	15.20	61.43	40.07	21.28	14.58	0.17
Calcium	Max	284.00	71.93	475.70	34.70	41.71	59.53
	Min	10.26	25.87	53.82	4.90	6.29	21.24
	Average	116.18	53.13	172.08	12.80	14.90	43.08

In the simulation, the major anion was sulfate while the major cations were calcium, magnesium, sodium and potassium. From the result, the largest sulfate concentration was found from PAF80%-NO COVER column, around 2,237.64 mg/l on the average (Table 4.18). In this column, sulfate anion was likely dissolved from the weathering of sulfide mineral, pyrite and arsenopyrite. In the groundwater system, two principal

natural sources of sulfate dissolution are the weathering of sulfide mineral, gypsum and/or anhydrite. Correspondingly, both gypsum and anhydrite could also become the main source of calcium concentration in the groundwater, that happen as major cation in the groundwater system. Based on the sulfate measurement (Fig. 4.14), it can be said that PAF80%-NO COVER column has the most acidity generated within the column. This was also supported by the lowest pH value among the columns as mentioned earlier. Interestingly, PAF80%-COVER had quite a high sulfate concentration in the beginning. But as the time passed, the sulfate kept decreasing and finally had the similar sulfate concentration like the other column. This trend was contrastingly with PAF80%-NO COVER column sulfate concentration trend. It implied the role of cover in the behavior change of sulfate dissolution.

Generally from major cation-anion concentration result, it can be observed different trend depend on the major element of anion in the column. A significant amount of calcium can be seen from the measurement result of both PAF50%-COVER and PAF80%-COVER, 116.18 mg/l and 172.08 mg/l, respectively. Column without fly ash and organic material, PAF80%-NO COVER, gave lower value than column to cover, which means a cover layer contributed for the increasing Ca in the leachate water. Ca content of the column without the cover possibly was produced from silicate mineral dissolution while most Ca of column with cover were originated from fly ash that contain high calcium, in the form of lime (CaO), gypsum and dolomite, based on the XRD analysis. Those minerals dissolute easily after reacting with water, that also supported by the pH measurement that significant increased. The dissolution of those minerals produces the hydroxide ion which will consume acidity in the water and increase the water pH.

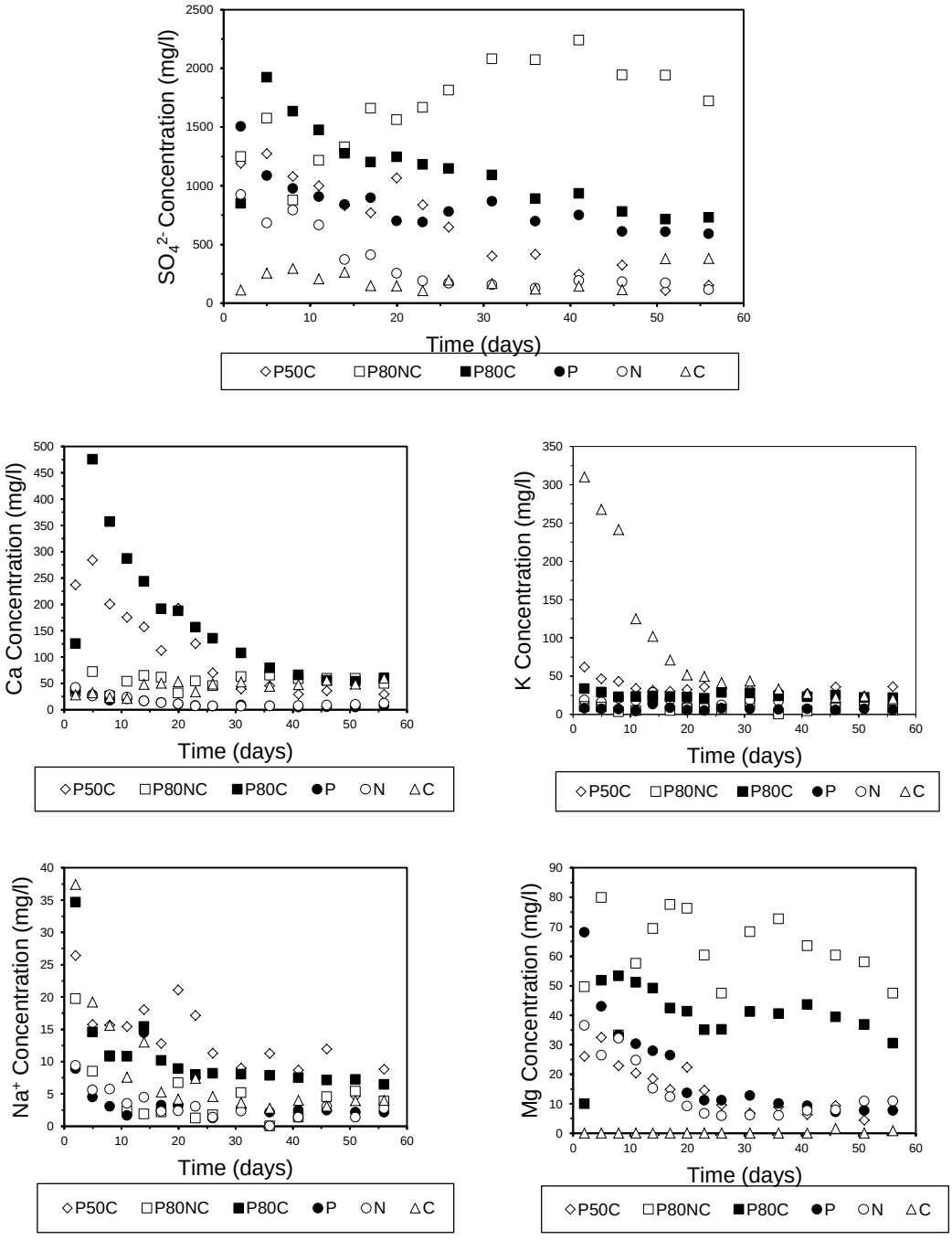

Fig. 4.14 Major cation-anion measurement result of each column
P50C=PAF50%-Cover; P80NC=PAF80%-No Cover; P80C=PAF80%-Cover; P=PAF; N=NAF; and C=Cover

Potassium (K) dissolution showed a similar trend for the rest of the column, except for initial measurement of C. After time passed, the K concentration remained stable similar to the rest of the columns. On the contrary, magnesium (Mg) showed a noticeable difference in measurement for each column. The smaller column, which is P, N and C, gave a higher result of Mg for P compared to other 2 columns. Mg usually

dissolved from carbonate mineral, together with Ca source mineral groups such as silicate minerals. This cation also can generate from weathering products of minerals, especially clay minerals. Since the pH of leachate water in PAF80%-NO COVER was low, the concentration of Mg in this column became higher as the result of dissolution because of the acidic water. For sodium (Na), the source of this cation was expected from mineral in fly ash dissolution, because Na was increased in the column to cover rather than without the cover. Moreover, it also confirmed by the higher concentration of Na in the C rather than in P and N column.

In the water, the total charges of positive and negative should be equal. At around 25^{o}C, the measured electrical conductivity can give an estimation of the sum of anions or cations (Appelo and Postma, 2005). Despite the major cations and anions presence in the water that was mentioned previously, other elements also can contribute significantly to the charge balance. Therefore, by plotting the result of measured major cations and anions, balance of charge concentration and the existence of other elements can be analyzed. Major cations and anions were provided in Fig. 4.15.

Based from the measurement result, the column that produced the most balance between major cations and anions was C. This happened because the leachate water was constantly in the high pH, so that the dissolution of metal concentration barely occurred. Column with cover, PAF50%-COVER and PAF80%-COVER, had an imbalance portion between cations and anions. All of them had greater sulfate concentration, showed by the data plotting above Σcations = Σanions linear line. There was slightly difference between PAF50%-COVER and PAF80%-COVER, however, compared to the rest the PAF80%-NO COVER imbalance was larger. Sulfate concentration dominated the PAF80%-COVER, which means in this column there was a larger cations dissolution that came from sulfide oxidation since the sulfate concentration was anomalous. Therefore, it could be expected from the column with the cover to have a high dissolved metal concentration that possibly obtained from sulfide mineral oxidation or else from the dissolution of mineral as chemical weathering products.

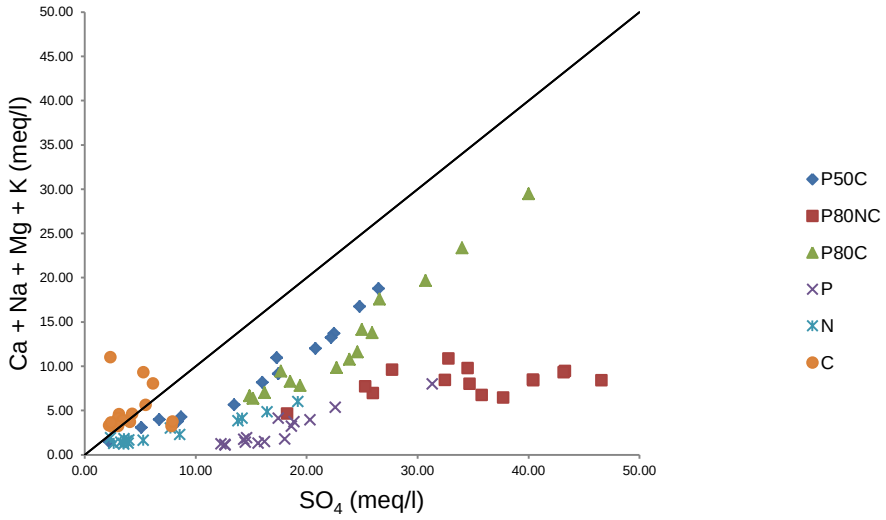

Fig. 4.15 Major cations and anions in the leachate water of column
P50C=PAF50%-Cover; P80NC=PAF80%-No Cover; P80C=PAF80%-Cover; P=PAF; N=NAF; and C=Cover

Fig. 4.14 provides the bar chart of major cation concentration portion on average of each column. Using the chart, dominated cation can be seen statistically. PAF50%-COVER and PAF80%-COVER showed similar portion, where the dominant cation was calcium. P and N column each separately had contributed in the calcium concentration in the column based on their major cation that was produced, however the major calcium concentration was obtained from cover material, which assumed came from fly ash. Magnesium likely originated from PAF Mix and NAF Mix materials, as shown in the portion of P and N column. C showed an insignificant amount of magnesium, therefore the previous assumption becomes rational.

Similar like calcium, potassium in the leachate water of column with cover material has high possibility had been dissolved from material in the cover, as shown in Fig. 4.16. This could be originated from mineral in the fly ash and also EFB, which is empty fruit bunches (EFB) from the palm fruit plant.

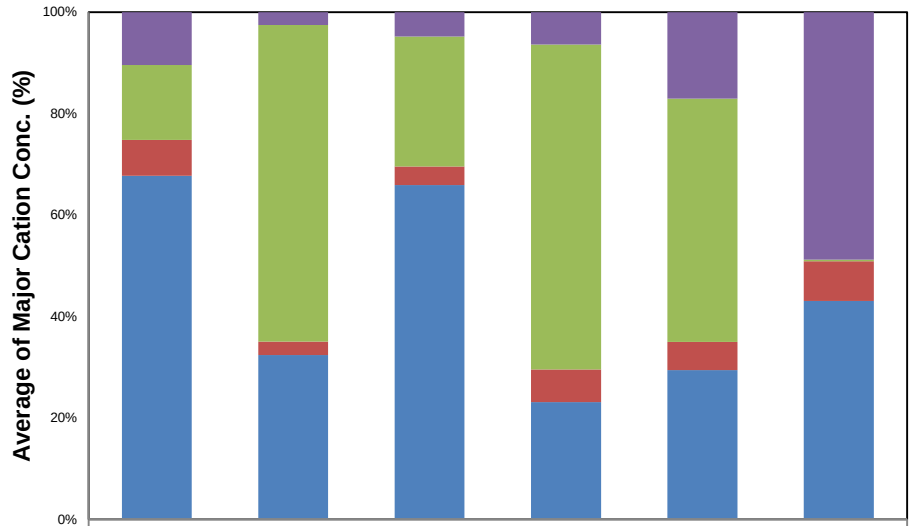

	P50C	P80NC	P80C	P	N	C
K	0.90	0.21	0.63	0.18	0.43	2.44
Mg	1.27	5.12	3.34	1.77	1.21	0.01
Na	0.60	0.22	0.48	0.18	0.14	0.39
Ca	5.81	2.66	8.60	0.64	0.75	2.15

Fig. 4.16 Portion of average concentration of major cations
P50C=PAF50%-Cover; P80NC=PAF80%-No Cover; P80C=PAF80%-Cover; P=PAF; N=NAF; and C=Cover

Metal concentrations

Measurement by ICP-OES showed the dissolved metal concentration on the leachate water because of the wetting, drying and flushing phase. Similar trend could be observed from aluminium (Al) and copper (Cu) metal concentrations while there are slightly different that can be found from the measurement of manganese (Mn), iron (Fe) and zinc (Zn). The measurement result of metal was provided in the Fig. 4.17. Based on the graph, it can be seen that generally on the graph there was a sudden change that increase the metal concentration dramatically. This happened because during the column leaching experiment, the duration of flushing period was extended, from every 2 days to become every 4 days. This was conducted in the consideration of stable pH of leachate water and EC, therefore, longer drying phase in order to increase the reaction rate was applied to the column. Thus, higher dissolved metal concentration could be observed.

Total iron dissolution concentration on the average was very high for PAF80%-NO COVER and PAF columns, 276.54 mg/l and 19.22 mg/l, respectively. The other columns had iron concentration which is lower than 1 mg/l. Even though the trend of

iron dissolution based on the measurement result was similar to Al and Cu trend dissolution, the noticeable dissimilarity can be discovered. PAF80%-NO COVER and PAF column had a greater difference in the value of iron concentration than Al and Cu. This possibly happened because the iron dissolution source had mainly been from sulfide mineral oxidation by the oxygen. This oxidation reaction will produce more product as the contact time between surface of sulfide mineral and oxygen in the air is increased. As consequences, iron also increases significantly. For Mn and Zn, not only PAF80%-NO COVER and PAF column that had a significant number in the concentration, but the NAF column also had a slightly higher concentration compared to the other columns. Therefore, in the system of column with and without cover, NAF material has contributed to increase Mn and Zn concentrations

Table 4.20 Statistic of metal concentration measurement result

Metal	Statistic	Concentration (mg/l)					
		PAF50%-COVER	PAF80%-NO COVER	PAF80%-COVER	PAF	NAF	Cover
Al	Max	0.72	99.92	0.56	19.06	0.46	0.53
	Min	0.04	0.05	0.05	0.15	0.03	0.05
	Avg	0.27	35.23	0.25	6.89	0.15	0.23
Cu	Max	0.07	6.96	0.06	2.11	0.15	0.20
	Min	0.00	0.03	0.00	0.05	0.01	0.00
	Avg	0.01	2.54	0.02	0.76	0.05	0.03
Fe	Max	1.32	276.54	1.56	19.22	0.85	0.67
	Min	0.07	0.66	0.05	0.63	0.06	0.05
	Avg	0.38	84.79	0.36	6.29	0.38	0.23
Mn	Max	0.24	56.95	0.39	7.22	9.82	0.25
	Min	0.08	0.20	0.08	0.24	0.23	0.08
	Avg	0.12	20.34	0.17	2.50	3.00	0.13
Zn	Max	0.27	22.94	0.38	7.71	1.36	0.22
	Min	0.03	0.33	0.01	0.54	0.20	0.02
	Avg	0.07	9.49	0.09	3.39	0.62	0.07

Total dissolved organic carbon

Organic material in the cover layer was obtained from EFB material, originated from palm fruit plantation adjacent to the mine site. EFB contains mostly organic carbon (C) that can be assumed to be represented as CH_2O, stoichiometrically. This layer acts as an active part for reacting with oxygen during its degradation process under aerobic condition, which can be simplified in the reaction as in the equation 4.2.

$$(CH_2O) + O_2 \rightarrow CO_2 + H_2O \qquad \textit{Equation 4.2}$$

From reaction above, if the organic material decomposition occurred, it has a role in consuming the oxygen when it penetrates the column. This process reduces the

possibility in the AMD generation since initial oxidation of sulfide mineral needs oxygen as the oxidizing agent. Furthermore, when the organic material dissolved in the water and flowing to the PAF layer where sulfate anion available, both will react together to produce hydrogen sulfide. Then hydrogen sulfide will bind together with metal to form metal sulfide and precipitate to metal. This reaction could occur in the presence of sulfate-reducing bacteria (SRB) which use the organic material as carbon source and electron donor. Sulfate in this process is used as electron acceptors for its energy generation. This reaction only can be carried out on the condition without the presence of oxygen, because SRB is an anaerobic bacteria. This process follows reaction based on the equation 4.3.

$$2(CH_2O) + SO_4^{2-} \rightarrow H_2S + 2HCO_3^- \qquad \textit{Equation 4.3}$$

From the equation 4.2, it can be concluded that the degradation process of organic material has function to improve AMD negative effect. Aerobic process could reduce the oxygen level that penetrates the layer while anaerobic process, with the presence of SRB, can consume the sulfate anion, bind the dissolved metal in the solid form and contribute in the alkaline matter.

In the column leaching experiment, the weight of EFB was distributed evenly for the column that has cover layer, as mentioned earlier in PAF80%-COVER and PAF50%-COVER. Based on dissolved organic carbon measurement (DOC), column without cover also contain organic carbon because their results always over zero (see Fig. 4.17). NAF, PAF and PAF80%-NO COVER showed an insignificant difference in DOC measurement results, even for the behavior concentration in the leachate water. A column that contains only cover material, Cover column, shows decreasing trend of DOC. Initial stage shows very high value of DOC compared after measurement. This is due to the fast consumption of organic matter decomposition during the initial stage, as already discussed in the previous section.

PAF80%-COVER and PAF50%-COVER had an amount of DOC in the two and three magnitudes higher than without the cover, respectively. It implied that organic material had reacted in the cover by aerobic respiration, hence consume the oxygen.

Interestingly, even though both of the covers had the same weight amount of organic material, PAF50%-COVER had a constant higher amount of DOC rather than PAF80%-COVER. There are two possibilities that might be occurred in the column with cover. Firstly, fly ash has a significant amount of organic material that contributes in the dissolution of organic carbon in the leachate water. Organic carbon possibly originated from the incomplete combusted carbon. Secondly, the dissolved carbon from the cover layer was flowed in similar amounts for both columns. Since PAF80%-COVER had more sulfate anion, it reacted with the dissolved organic matter in the un-oxidized layer of PAF. Hence the DOC amount in the PAF80%-COVER was lower than PAF50%-COVER column.

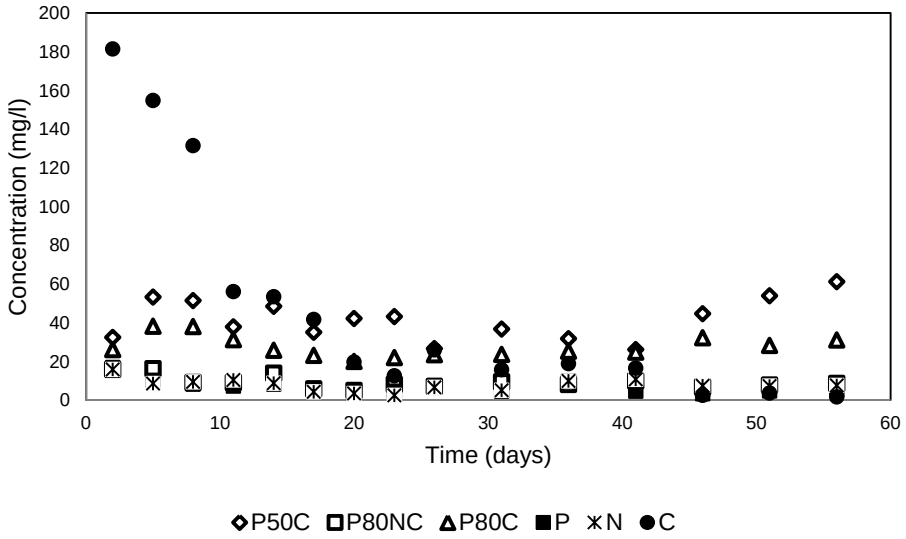

Fig. 4.17 Dissolved organic carbon measurement
P50C=PAF50%-Cover; P80NC=PAF80%-No Cover; P80C=PAF80%-Cover; P=PAF; N=NAF; and C=Cover

SEM-EDX

From the image of SEM result as shown in Fig.4.18, PAF Mix before leaching test were confirmed the weathering products on the surface of the material. After the leaching test, PAFcolumn in the PAF layer showed smoother result, as the effect of flushing process that dissolved the oxidation product from the weathering process. However, from the PAF layer material of PAF80%-Cover and PAF50%-Cover rough surface was investigated. This is possibly the coating result from the precipitation of calcium, which formed gypsum. This was supported by the presence of calcium in the PAF layer, from

the measurement result of surface element concentration, as provided in Table 4.21. Other increasing element on the surface was the iron. With the leachate water that was near neutral to alkali, there was also possible for iron precipitation and had resulted in coating the surface of the material.

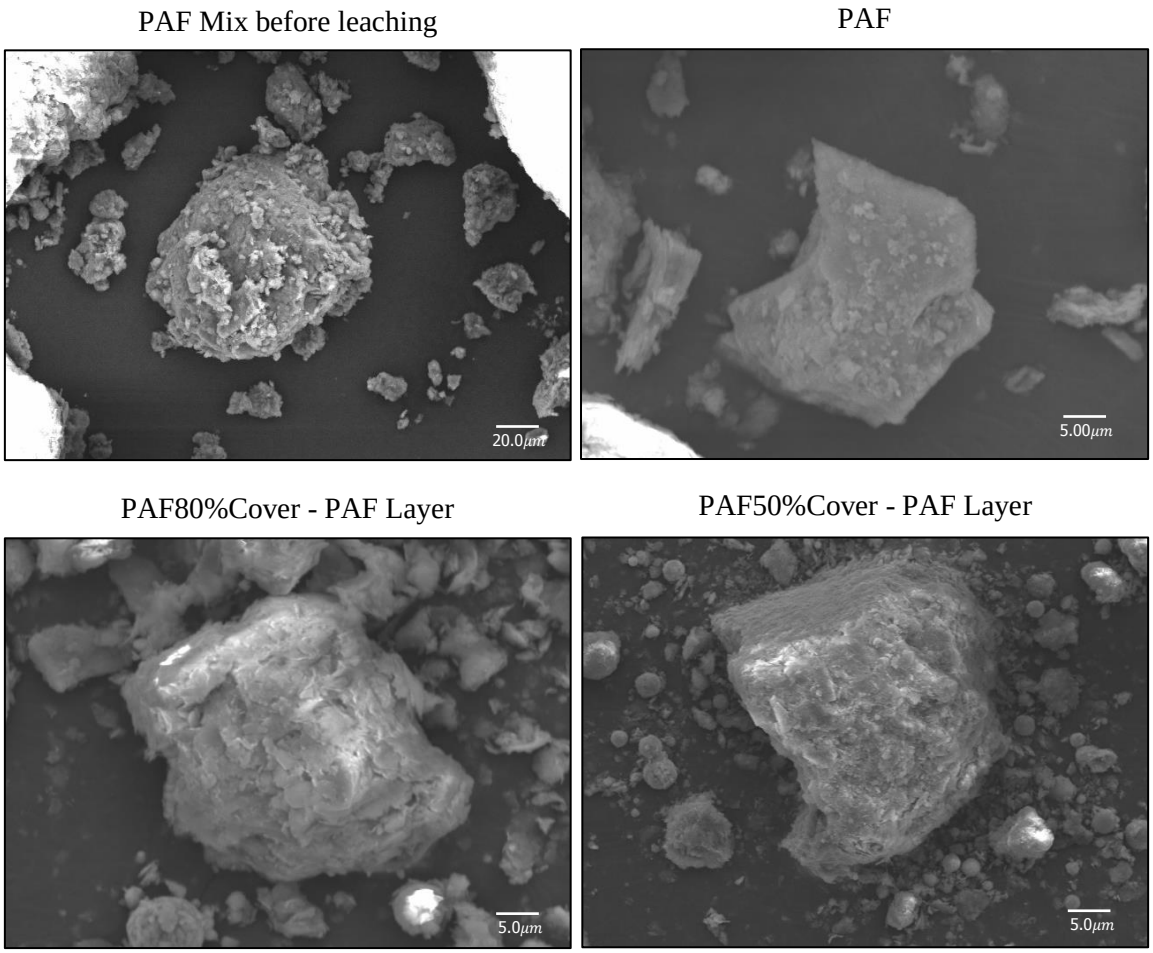

Fig. 4.18 SEM image of PAF layer

Table 4.21 Surface element measurement of PAF and fly ash material

Sample's Name	Elements	At%
PAF Mix - Before leaching	O	56.6
	Al	14.1
	Si	27.6
	K	0.5
	Ti	0.5
	Fe	0.7
PAF	C	10.2
	O	41.0
	Al	17.8
	Si	25.0
	K	4.0
	Fe	2.0
PAF50%Cover - PAF Layer	C	11.5
	O	61.0
	Fe	3.2
	Al	7.0
	Si	7.7
	Ca	0.6
	Ti	9.1
PAF80%Cover - PAF Layer	C	6.9
	O	53.7
	Mg	2.4
	Al	13.9
	Si	19.5
	K	0.8
	Fe	2.9
Fly Ash – Before leaching	C	7.1
	O	51.3
	Mg	2.7
	Al	1.4
	Si	9.8
	Ca	3.5
	Fe	24.1
Cover - Fly ash layer	C	7.1
	O	53.9
	Mg	4.3
	Al	4.7
	Si	23.6
	Ca	2.2
	Fe	4.3

4.8 Conclusions

In this chapter, several experiments regarding optimization of fly ash and EFB are carried out. The utilization of fly ash and EFB together in dry cover simulation is also carried out. The result of those experiments can be summarized as follows:

1. Due to the difference in neutralizing capacity, the usage of fly ash can be distinguished based on the NAG pH test. Type 1 is recommended to neutralize both PAF low and high capacity. Type 2 is recommended to neutralize PAF low capacity.

2. Based on kinetic test, it is clearly shown that fly ash of both types better to be applied in the overburden dumping area than the bottom ash.

3. NAPP ratio can be used as the reference for determining the minimum amount of fly ash volume in the dry cover strategy. However, the maximum number of NAPP should be not more than 10 kg H_2SO_4/ton in order to make sure the acidic water can be completely improved by the addition of coal ash. Due to the lower neutralizing capacity, it is better to avoid using fly ash Type 2 to improve the AMD generation originated from PAF rock high capacity.

4. For fly ash Type 1, blending method is the best method to be carried out for dry cover prevention strategy. This is due to the cementation effect that happens very fast in the fly ash Type 1 that makes the water that flowing in has intermediate reaction, thus decrease the reaction of water with fly ash particles due to the agglomeration.

5. Thickness can be also used as an alternative reference in determining the fly ash amount that needed for dry cover strategy. Based on the type fly ash, it is better to use thickness with minimum 0.5 times of PAF from Type 2 if the PAF has low capacity in producing acidity. Meanwhile, the 0.25 times fly ash Type 1 can be used in dry cover strategy of PAF low capacity. However, if the PAF is high capacity then Type 1 should be used.

6. EFB thickness of the dry cover is an independent factor that mainly depends on its decomposition rate due to microbial activity which consumes the oxygen. Based on research, for the long-term usage of EFB based on its decomposition rate, 75 cm – 160 cm of thickness can be constructed in

7. Based on the result of a simulation of the application of both materials in the cover layer, several points can be concluded

- In the case of PAF abundance, conventional method of dry cover system by placing NAF rock to the PAF rock is not efficient for AMD prevention method. Acidic water with dissolved heavy metals is still generated, in the similar behavior with the PAF rock without the addition of NAF rock. Therefore, this method needs to be improved. This is also supported by the field measurement result in Chapter 2, where no significant reduction of oxygen and water that infiltrates the NAF layer.
- Utilization of fly ash and organic material as cover layer is effective to prevent AMD generation, by increasing the leachate water pH, consuming the oxygen in the upper layer and reducing the dissolved metal concentration. The dissolution of heavy metals from fly ash seems insignificant in this experiment. Based on the measurement of major cations-anions, dissolution of calcium from fly ash can be seen in the leaching column. Calcium can react with sulfate and formed the gypsum therefore decrease the permeability of the layer. Moreover, the TOC measurement also showed the increasing value of DOC in the column with fly ash and organic material cover, thus possibly react with sulfate and precipitate the metals.
- Fly ash and organic material combination as cover layer thus far shows no negative impacts may happen due to its utilization. Therefore, it is important to conduct this experiment in the field scale to know the behavior of leachate water in the field situation.

References

Andrina, J., Wilson, G. W., Miller, S., & Neale, A. (2006). Performance of the Acid Rock Drainage Mitigation Waste Rock Trial Dump At Grasberg Mine. *Journal American Society of Mining and Reclamation*, *2006*(2), 30–44. https://doi.org/10.21000/JASMR06020030

Demers, I., Mbonimpa, M., Benzaazoua, M., Bouda, M., Awoh, S., Lortie, S., & Gagnon, M. (2016). Use of acid mine drainage treatment sludge by combination with a natural soil as an oxygen barrier cover for mine waste reclamation: Laboratory column tests and intermediate scale field tests. *Minerals Engineering*. https://doi.org/10.1016/j.mineng.2016.11.017

Francisca Gomez-Rico, M., Font, R., Vera, J., Fuentes, D., Disante, K., & Cortina, J.

(2008). Degradation of organic pollutants in Mediterranean forest soils amended with sewage sludge. *Chemosphere*, *71*(11), 2129–2138. https://doi.org/10.1016/j.chemosphere.2008.01.023

Kusuma, G. J., Shimada, H., Nugraha, C., Hamanaka, A., Sasaoka, T., Matsui, K., … Sulistianto, B. (2013). Study on Co-placement of Coal Combustion Ash-coal Waste Rock for Minimizing Acid Mine Drainage Generation: A Preliminary Result of Field Column Test Experiment. *Procedia Earth and Planetary Science*, *6*(0), 251–261. https://doi.org/http://dx.doi.org/10.1016/j.proeps.2013.01.034

MEND. (2004). *Design, Construction and Performance Monitoring of Cover Systems for Waste Rock and Tailings Volume 3 Site Characterization and Numerical Analyses of Cover* (Vol. 3).

Neuschütz, C., & Greger, M. (2010). Stabilization of mine tailings using fly ash and sewage sludge planted with phalaris arundinacea L. *Water, Air, and Soil Pollution*, *207*(1–4), 357–367. https://doi.org/10.1007/s11270-009-0142-5

Newman, L. (1999). Preferential Flow in Vertically Oriented, Unsaturated Soil Layers, 1–134. Retrieved from papers3://publication/uuid/229C9547-5A75-45F8-BCC4-24F966834A15

Nugraha, C., Shimada, H., Sasaoka, T., & Ichinose, M. (2009). Acid Mine Drainage Management at PT . Kaltim Prima Coal : A Summary of Improvement Studies. *8th International Conference on Acid Rock Drainage*, 1–10.

Peppas, A., Komnitsas, K., & Halikia, I. (2000). Use of organic covers for acid mine drainage control. *Minerals Engineering*, *13*(5), 563–574. https://doi.org/10.1016/S0892-6875(00)00036-4

Smart, R., Skinner, B., Levay, G., Gerson, A., Thomas, J., Sobobieraj, H., … Stewart, W. (2002). ARD test handbook: Project P387A prediction and kinetic control of acid mine drainage. *Project P387A, Prediction and Kinetic Control of Acid Mine Drainage*, (May), 42.

Song, Q., & Yanful, E. K. (2010). Effect of Water Addition Frequency on Oxygen Consumption in Acid Generating Waste Rock. *Journal of Environmental Engineering*, *136*(7), 691–700. https://doi.org/10.1061/(ASCE)EE.1943-7870.0000213

Steenari, B., Karlsson, L. G., & Lindqvist, O. (1999). Evaluation of the leaching characteristics of wood ash and the influence of ash agglomeration. *Biomass and Bioenergy*, *16*, 119–136.

Stewart, W. A., Miller, S. D., & Smart, R. (2006). Advances in Acid Rock Drainage (Ard) Characterisation of Mine Wastes 1. *7th International Conference on Acid Rock Drainage 2006, ICARD - Also Serves as the 23rd Annual Meetings of the American Society of Mining and Reclamation*, *3*, 2098–2119. https://doi.org/10.21000/JASMR06022098

Teh, C. B. S. (2016). Availability, use, and removal of oil palm biomass in Indonesia. *Report Prepared for the International Council on Clean Transportation*, 1–39. https://doi.org/10.13140/RG.2.1.4697.4485

Wang, J., Zhang, C. B., Ke, S. S., & Qian, B. Y. (2011). Different spontaneous plant communities in Sanmen Pb/Zn mine tailing and their effects on mine tailing physico-chemical properties. *Environmental Earth Sciences*, *62*(4), 779–786. https://doi.org/10.1007/s12665-010-0565-8

Younger, P. L. (2007). *GROUNDWATER in the Environment*. *Environment*. https://doi.org/10.1111/j.1745-6584.2007.00336.

CHAPTER 5

Effect of fly ash and organic material as a cover layer of iron-oxidizing bacteria

5.1 Introduction

In the AMD prevention strategy, microorganism presence is rarely to be considered for its impact on the AMD generation process. However, in nature, the microorganism existence is impossible to be ignored. Even in the extreme environment typical AMD, at least two archaeal and eight bacteria divisions can thrive and sustain its life (Baker & Banfield, 2003). These microorganism communities catalyze sulfur and iron oxidation and use the electron from that reactions in their metabolism as an energy source to grow and to maintain cell functions (Younger, 2002). Oxidation of sulfur and iron is the fundamental reactions in the AMD process. Therefore the microbial activity may act as the limiting factor for AMD reaction rate. Furthermore, iron-oxidizing bacteria presence in the AMD system, as the most well studied in AMD bacteria communities, can catalyze an AMD reaction up to a factor of hundreds (Singer & Stumm, 1970). Thus, it is prominent to take into account the bacteria presence effect in the AMD study, especially for AMD management strategy.

The effectiveness of dry cover systems is also highly possible to be affected by iron-oxidizing bacteria activity. Oxygen is the major oxidizing agent in the AMD reaction because it mainly reacts with sulfide mineral and transforms it into soluble forms. The reaction takes place in the wide range of pH, with decreasing reaction rate as the pH gets lower. However, as it is already known that further iron oxidation results in the transformation of ferrous iron to ferric iron. In the water with pH 3 or lower, ferric iron is in the soluble form that happens to be stronger oxidizer than oxygen (Skousen, Sexstone, & Ziemkiewicz, 2000). With the decreasing rate of oxygen oxidation, ferric iron may swap oxygen's role in oxidizing sulfide mineral. Iron-oxidizing bacteria exists in these kinds of circumstances and accelerates the AMD generation.

This chapter aims to know the presence of iron-oxidizing bacteria from the coal mine site. Moreover, further column leaching test in the smaller dimension scale was

carried out to know the effect fly ash and organic material to the iron-oxidizing bacteria activity.

5.2 Iron-oxidizing bacteria growth from coal-bearing rock in mining

5.2.1 Materials and Methods

5.2.1.1 Materials

The materials in this experiment were the coal-bearing rocks from PT. Arutmin Indonesia coal mining. Isolation iron-oxidizing bacteria growth then was conducted both in the laboratory and the field. Six rock samples were collected from site for isolation bacteria growing in the laboratory and five rock samples were collected for isolation growth of iron-oxidizing bacteria in the field. For laboratory experiment, each rock sample was oven dried in 55^{o}C for 48 hours prior to the test.

From the static test result in Table 5.1, rock samples were categorized into PAF that has low to intermediate potential in acid producing, following the result of the static test (Sobek, 1976). Those six samples of PAF then crushed into a powder sample that will be used for further experiment in the laboratory.

Table 5.1 PAF rock geochemical characterization

Sample Name	Lithology	TEST			Geochemical Classification***
		pH paste	NAPP* (kg H_2SO_4/ton)	NAG** pH	
PAF–A	Sandstone	4.80	3.27	4.40	PAF
PAF–B	Sandstone	3.20	5.14	4.00	PAF
PAF–C	Sandstone	3.90	3.29	3.80	PAF
PAF–D	Claystone	3.90	5.25	3.40	PAF
PAF–E	Claystone	3.90	4.13	4.10	PAF
PAF–F	Sandstone	4.20	3.33	4.40	PAF

*Net acid producing potential
** Net acid generating
***after Sobek, 1976 & PT Arutmin Indonesia classification

XRF measurement results of rock samples are provided in Table 5.2. Based on the result, it is shown that sandstone rock has higher quartz mineral concentration. This can be seen from the SiO_2 percentage that higher than claystone, ranging from 73.9% to 90.2% and 63.4% to 64.8% for sandstone and claystone, respectively. Significant difference can also be seen from Al_2O_3 where rock with sandstone lithology has lower weight percentage than claystone. This is due to the claystone mainly composed of clay minerals, result in higher Al_2O_3 while sandstone generally composed of quartz minerals.

Table 5.2 XRF result of rock sample

Sample	SiO_2 (%)	TiO_2 (%)	Al_2O_3 (%)	FeO (%)	MnO (%)	MgO (%)	CaO (%)	Na_2O (%)	K_2O (%)	P_2O_5 (%)	LoI (%)	S (%)
PAF–A	73.9	0.9	15.8	1.0	0.0	0.7	0.1	0.4	0.8	0.0	6.3	0.1
PAF–B	84.2	0.5	8.4	0.9	0.0	0.5	0.1	0.3	0.2	0.0	4.7	0.2
PAF–C	90.2	0.5	5.5	0.6	0.0	0.3	0.1	0.3	0.2	0.0	2.2	0.1
PAF–D	63.4	1.1	20.8	1.4	0.0	0.9	0.1	0.4	1.3	0.0	10.4	0.2
PAF–E	64.8	1.2	22.0	1.4	0.0	0.7	0.1	0.3	0.4	0.1	8.7	0.1
PAF–F	77.9	0.9	14.6	1.0	0.0	0.5	0.1	0.3	0.3	0.1	4.0	0.1

Meanwhile, isolation growth of iron-oxidizing bacteria were also conducted in the field. Several types of coal-bearing rock was collected, e.g. claystone, sandstone and siltstone. In order to know acid producing capacity of rock samples, static test was carried out. Result of static test is provided in Table 5.3. Based from the static test result, it is shown that all of rock samples are classified into PAF rock that have an extensive range of net acid producing potential, i.e. NAPP, from 35 kg H_2SO_4/ton to104 35 kg H_2SO_4/ton.

Table 5.3 Static test result of rock sample in the field

Sample Name	Lithology	Test				Geochemical Classification***
		pH paste	TS (%)	NAPP* (kg H_2SO_4/ton)	NAG** pH	
PAF–1	Claystone	3.3	1.1	35	2.2	PAF
PAF–2	Claystone	5.7	0.5	17	2.5	PAF
PAF–3	Sandstone	4.3	3.4	104	1.9	PAF
PAF–4	Silstone	5.3	0.8	25	2.2	PAF
PAF–5	Sandstone	4.0	1.0	30	2.2	PAF

5.2.1.2 Methods

In order to know the presence of iron-oxidizing bacteria in the mine, isolation-growth of microbes was carried out from rock samples. Rock sample is added to either Erlenmeyer flask, in the laboratory, or plastic bottle, in the field. The HBS solution medium at pH 2.0 is also put in, together with trace element and ferrous iron stock solution. This is done for ensuring the iron-oxidizing bacteria within the rock could thrive, by providing the known optimum condition.

In the laboratory, powdered rock was added in a separate flask for each rock. After the cells was detected, 5 ml of the solution was inoculated to the new medium in order to maintain the growing process. Inoculation was conducted after the ferrous iron in the solution medium, as the electron donor, almost oxidized to ferric iron. The amount of ferric iron in the solution measured by using total iron measurement, with o-phenanthroline method for Fe[II] and total Fe. The activity level of the cells was

observed by the light microscope with 40x magnification and cell counting by the cell chamber or called as a hemocytometer. Further method will be explained as follows.

1. Microorganisms isolation-growth and inoculation

Isolation-growth of the microbes was conducted in 6 sterilized flasks for each 6 rock samples separately. Samples were pulverized before added to the solution media. Two conditions of solution media were carried out: with and without yeast extract. Solution media were composed of material as described below.

- Heterotrophic basal salts (HBS – 450 mg/l $(NH_4)_2SO_4$, 50 mg/l KCl, 50 mg/l KH_2PO_4, 500 mg/l $MgSO_4 \cdot 7H_2O$, 14 mg/l $Ca(NO_3)_2 \cdot 4H_2O$ and 142 mg/l Na_2SO_4; pH 2.0 with concentrated H_2SO_4)
- Trace element 1000x concentrated (pH 2.0 with H_2SO_4): 10 g/l $ZnSO_4 \cdot 7H2O$, 1.0 g/l $CuSO_4 \cdot 5H2O$, 1.09 g/l $MnSO_4 \cdot 5H_2O$, 1.0 g/l $CoSO_4 \cdot 7H2O$, 0.39 g/l $Cr_2(SO_4)_3 \cdot 7H2O$, 0.6 g/l H_3BO_3, 0.5 g/l $Na_2NoO_4 \cdot 2H_2O$, 0.1 g/l $NaVO_3$, 1.0 $NiSO_4 \cdot 6H_2O$, 0.51 g/l Na_2SeO_4, 0.1 g/l $Na_2WO_4 \cdot 2H_2O$
- $FeSO_4 \cdot H_2O$ as iron stock solution

For isolation-growth, 150 ml HBS solution was added to the 300 ml flask, along with 150 µl of trace element, 1500 µl of $FeSO_4 \cdot H_2O$ 1 M and 0.75 g pulverized sample (0.5%w/w). Then flasks were placed in the bio-shaker with a temperature of 30^oC, as the optimum temperature of bacteria to grow, and speed of shaking around 100 rpm, to increase the oxygen supply in the flask. Iron-oxidizing bacteria is aerobic bacteria, therefore oxygen is needed.

After cell growth was observed, then inoculation was conducted in order to maintain the growing of the cell. During the cell growth, it consumes ferrous iron from iron stock by oxidizing the ferrous iron to ferric iron. As a result, the ferrous iron concentration will be depleted, and finally, there will be no more ferrous iron in the solution. This will decrease the cell growth activity. Therefore, it is important to carry inoculation for maintaining bacteria growing. Every process of isolation-growth and inoculation should be done on a clean bench for avoiding contamination of other microorganisms. A clean bench is a sterile

cabinet that is provided with filtered air supply to protect the work from contamination. Clean bench is also usually has a germicidal UV light source to keep a biosafety inside the cabinet. During the work, it is necessary to heat the cap and the top of the flask with fire before and after, especially for different flask with different samples and condition. The fire will sterilize the cap and the top of the flask thus minimizes contamination. Furthermore, aseptic method could also be conducted to prevent contamination. Quantified volume of the solution or microorganisms is added to a sterilized flask by bringing the flask mouth near a fire. The work should also be done near the fire area to ensure no contamination from other microorganisms.

In the field, five rocks were freshly sampled and air-dried for 24 hours, in total 500 g for each rock. After that, the rocks were roughly crushed into powder size and divided several times by coning-quartering method. 2.5 g of powdered rock was then inserted into a sterilized plastic bottle that has 200 ml capacity. 100 ml of HBS medium solution, 100 µl of trace element and 1000 µl of $FeSO_4 \bullet H_2O$ 1 M was also added into the bottle. After adding the solution and rock, the plastic bottle was closed tightly with the cap, thus make the oxygen available is only the one left in the bottle. The experiment was done in duplicate.

The condition of the experiment follows the actual condition in the mine, where the temperature ranges from 23^{o}C to 35^{o}C. All of the bottles were placed in direct sun during the daylight. Color change from colorless to yellowish orange is observed from the plastic bottle.

2. Direct microscopic counting

The number of cells in a population can be measured by counting a sample number under the microscope called a direct microscopic method (Madigan, Martinko, Stahl, & Clark, 2010). Cell counting was conducted by using the cell counting chamber, a hemocytometer. It is a tool invented by the anatomist Louis-Charles Alassez, from France, to perform blood cell counts. This tool consists of thick glass microscope slide with a tiny square grid of perpendicular lines in the middle. The grid consists of 5x5 large grids and 4x4 small grids in

one large grid (see Fig. 5.1). This square in total has a specified dimension so that the area covered by the lines is known, which makes it possible to count the number of cells in a specific volume of solution.

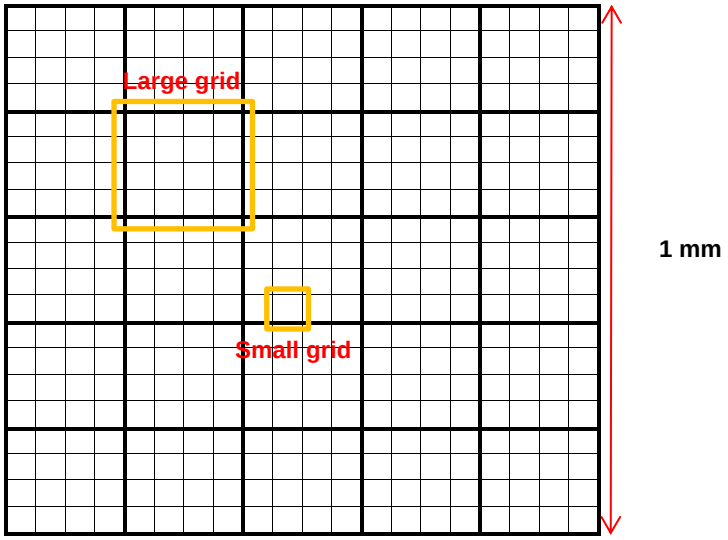

Fig. 5.1. Illustration of the grid in the hemocytometer

The result of total cells is divided by total volume of the grid to get total cell per ml in the final measurement. Before starting the direct cell counting, the liquid sample is loaded in the hemocytometer. Then a thin glass cover is placed above the hemocytometer surface and hold by a metal cover. The depth of cell counting chamber is 0.020 mm, and the total surface area of the grid is one mm^2. Therefore, after counting the cell divided by the total counted small grids, as *n*, then total cells per volume will be obtained by following the formula below.

$$\text{number of cell per volume } \left(\frac{\text{cells}}{\text{ml}}\right) = n \text{ x } 25 \text{ x } 16 \text{ x } \frac{1}{0.020 \text{ mm}^3} \text{ x} 10^3$$

For simplification, an average number of counting cell, cell/grid, could be multiplied by $2x10^7$ to obtain the number of cells per ml. The data will be reliable statistically after the counting found 50 cells for counting in the small grid or 100 cells for counting in the large grid.

5.2.2 Result and discussions

In microbiology, growth is defined as an increase in the number of cells (Madigan et al., 2010). Bacteria can grow by dividing their structural component into double cells. The number of cells will keep doubling if they are suitable in the condition, thus this

called as generation, and the cells grow during that process. This process is in the exponential growth because of the doubling. Before reaching the exponential growth phase, bacteria have a lag phase when a microorganism is incubated or inoculated into a fresh medium. This lag phase happens because the bacteria need time to adjust to the new environment, by recovering their cells if the previous one lacks nutrient. If the new medium is similar to the previous one, theoretically lag phase will not occur.

In this experiment, the first trial in the laboratory is set to grow only iron-oxidizing bacteria. The pH medium is 2.0, which acidophilic bacteria can thrive in this extereme condition. Moreover, 10 mM of ferrous iron is added to the solution. Iron-oxidizing bacteria can obtain the energy from oxidation of ferrous iron while it also can produce their own carbon resources from inorganic carbon source. This oxidizing process changes ferrous iron to ferric iron, that later may precipitate into iron hydroxide. Fig. 5.2 shows the initial condition, flask before the cell was grown.

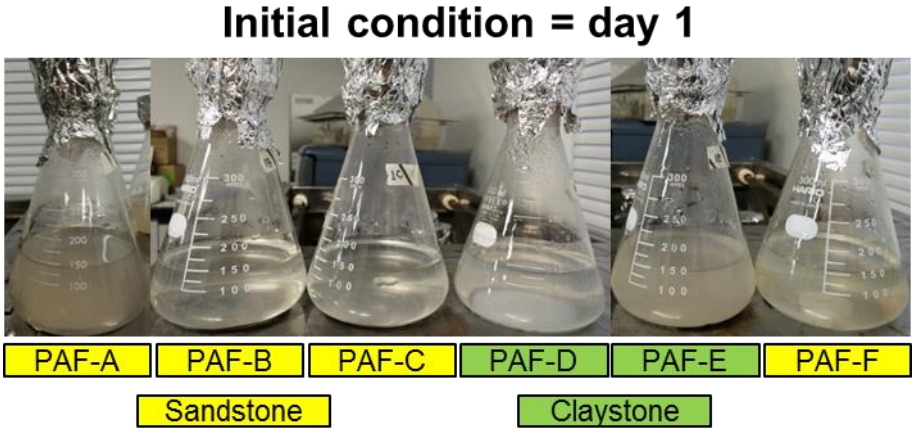

Fig 5.2 The flask condition before shaking was started

The iron-oxidizing bacteria growth in the flask was examined with the unaided eye by observing the change of color in solution media. It will change from the clear-color water to thick-dense yellowish-orange color water, with precipitation in the bottom of flask if the bacteria were active and strong enough to oxidize the ferrous iron. In this experiment, the color change was not clearly visible as seen in Fig 5.3. For this reason, microscopic observation to see the presence of iron-oxidizing bacteria were performed. The result is provided in Table 5.3.

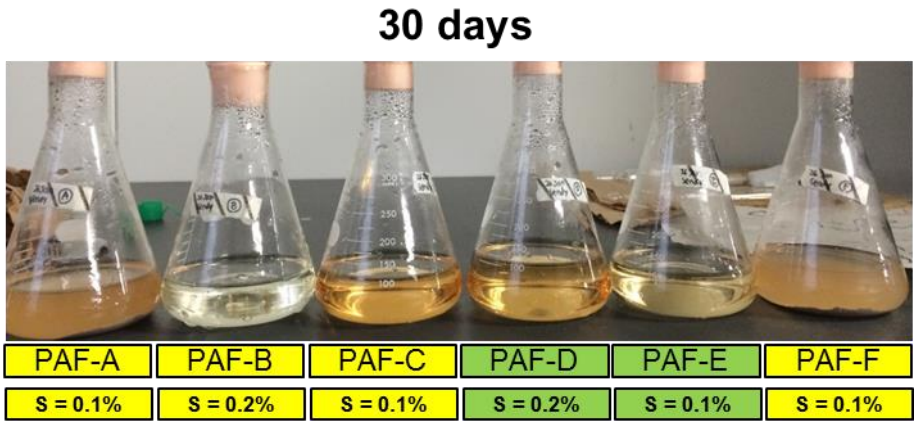

Fig. 5.3 Sample solution condition after 30 days shaking

The result showed the presence of bacteria could be observed during the isolation-growth, by the appearance that was changed before and after measurement. Change in sample B cannot be observed, even though the examination by microscope also already carried out. It is probably due to the presence of inactive and low number of bacteria, hence it cannot be observed even though changes was seen in the solution The possibility is that the iron-oxidizing bacteria still in the lag phase, because the microbe were introduced to new media of soil from liquid media. In addition, the changing from clear to dense solution showed that there was reaction occurred in the solution. Therefore, inoculation was conducted to maintain the growing phase, with the same solution media condition as before.

Table 5.4 Physical changes and the bacteria presence observation

Observation	**Sample Name***					
	PAF–A	**PAF–B**	**PAF–C**	**PAF–D**	**PAF–E**	**PAF–F**
Color change	V	V	V	V	V	V
Turbidity change	V	V	V	V	V	V
Bacteria presence (microscope)	V	V	V	V	V	V

After several inoculations, significant changes can be observed. With the removal of an amount of rock sample in solution (only 5 ml solution of each flask was added to the sterilized flask with new medium), the color change can be clearly seen to all of the flasks. Various colors of the solution indicated the different level activity of iron-oxidizing bacteria. It means the iron-oxidizing bacteria can be successfully grown from the original rock sample on the mining.

Total iron and ferrous iron concentration measurement were also conducted to know the amount of ferrous iron consumed by the bacteria. Ferrous iron concentration in

sample A, D, E, and F were low, almost 0, which means that in this sample iron-oxidizing is strong enough to oxidize all of the iron in the shorter time compared to sample B and C. Ferrous iron concentration in sample B and C were slightly higher. However, the value of total iron in each flask was different. This indicates that there was ferric iron precipitation happened in the bottom of the sample. Therefore the total iron resulted in various value depend on the sampling. The activity and total amount of bacteria observation results indicated the strongest iron-oxidizing bacteria were bacteria from sample A and F. Thus, the bacteria from this sample were continuing to grow by keeping inoculation to the new sterilized flask and medium. Both of the samples were grown together in one solution media, by mixing the culture into one flask when the inoculation was conducted. After that, with six separate flasks that contained the same amount of solution media and culture volume, iron-oxidizing bacteria were grown until near the cell density expected. From the direct cell-counting measurement result, the final cell density that was obtained from this experiment is 5.73 x 10^{10} cells.

With the same solution, powder sample is added to the sterilized plastic bottle with an aseptic method 0n the mining site. Due to the limitation in the field, counting measurement cannot be carried out. The initial condition of medium in the bottle is provided in the Fig. 5.4.

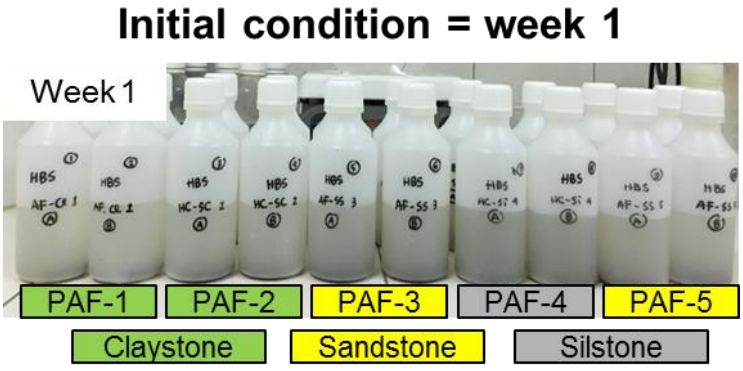

Fig, 5.4 Initial condition of plastic bottle in the mine

During the initial week, changes cannot be observed. Medium solution in all of bottle samples is colorless. The difference of water is observed as the result of powder rocks that inserted into the bottle. After 2 weeks, color changes could be observed. In Fig. 5.5, the changes only can be seen from the bottle of PAF-3. The rock in this bottle is sandstone, with the highest value of total sulfur among all of rock, 3.4%. Therefore,

the fastest color change may be resulted from sulfur content that indicates the higher pyrite mineral amount in the PAF rock. This condition has a positive relationship with the amount of iron-oxidizing bacteria that likely to be higher when more pyrite exits in the PAF rocks. Moreover, the color changes can be further observed in the bottle PAF-5 and PAF-4 after three weeks. These three bottles (in duplicate) are classified as sandstone and siltstone. Slight change of color can be observed from bottle PAF-1 and PAF-2, that classified as claystone, even though insignificant. Hence, this result confirms the iron-oxidation bacteria growth in the laboratory, which shows the sandstone PAF able to grow iron-oxidizing bacteria faster than claystone. This might be happened due to the effective porosity in the sandstone is higher than claystone, as the consequence of the larger particles in sandstone. The larger particles provide higher open void which is filled with air while finer particle of claystone has a lower open void. Therefore, as the open void is larger, the available surface of iron-oxidizing bacteria to grow is higher.

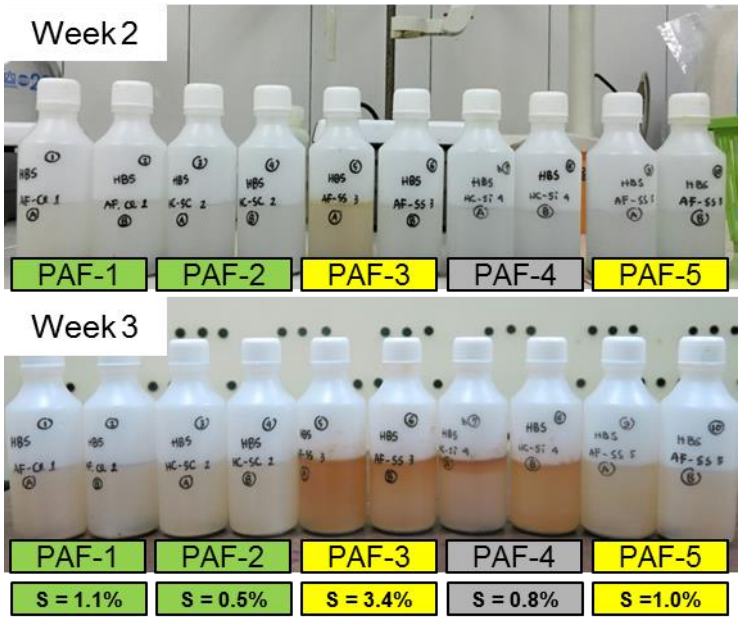

Fig. 5.5 Isolation growth of iron-oxidizing bacteria in the mine site

In the conclusion, iron-oxidizing bacteria could thrive from the PAF rock samples in the coal mining site, even though with different grow rate. Moreover, the type of rock in sedimentary seems to affect the grow rate of iron-oxidizing bacteria. Further experiments is needed to validate this hypothesis.

5.3 Small and large column leaching test

5.3.1 Materials and methods

Similar as previous column leaching test, PAF rocks were mixed homogeneously with ratio 1:1 in the weight percentage. In order to increase the acid-producing capacity, pyrite mineral was added with 2% w_t/w_t. Furthermore, NAF rocks were also mixed with ratio 1:1, while fly ash was obtained as the byproduct from coal combustion of Asam-asam coal-fired power plant. Lastly, organic material was the sampled empty fruit shell bunches of palm fruit plantation adjacent to Asam-asam mine. The column leaching test is carried out in two scales, small with diameter column 50 mm and the large one with diameter column 100 mm. The large column is similar to the column in the Chapter 4.

The scenario of layering and the weight of material of small columns are provided in the Fig. 5.6 and Table 5.5, respectively. *A.t. ferooxidants* were inoculated to the PAF material layer directly with cell density 1.0 x 10^9 cells/g.

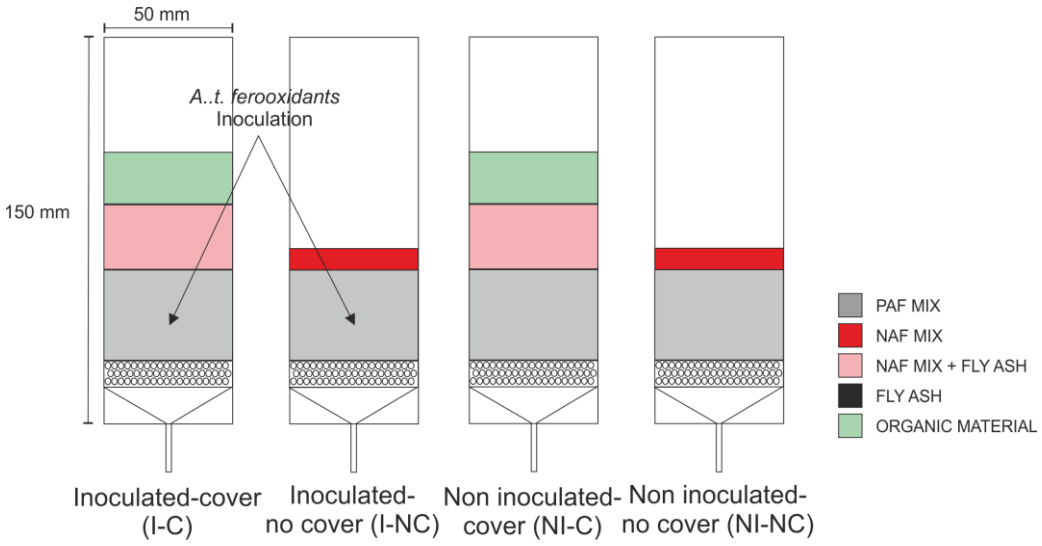

Fig. 5.6 Scenario of column leaching test with bacteria inoculation

This experiment consists of two phases, drying and wetting phase. Drying phase was carried out by heating by lamp for 24 hours and T 30 – 35^o C while the wetting phase was conducted by flushing 150 ml of deionized water on the following day after the drying phase, and natural drying for another 24 hours after that to ensure the all of the water reacted and coming out from the column. Leachate water then directly measured for its pH, electric conductivity (EC) and Eh. Eh was also measured in the experiment in order to know the activity reaction in the leachate water. Eh value shows

the tendency of reaction in the water, whether it is more oxidative or reductive condition. The potential with negative value indicates reducing reactions occurring in the water. It means the element loss its electrons resulting in more positive ions. On the contrary, the positive potential value indicates the oxidizing reactions taking place and the element gain its electrons, as a result more negative ions presence. The more positive the measured oxidizing-reducing potential implies stronger oxidizing agent presence in the water. After that, leachate water sample was filtered with 0.20 µm pore size filter and acidified. Metal concentration was also measured by ICP-OES.

Table 5.5 Weight distribution for each layer in the column

Column	Weight (g)			
	PAF	NAF	FA	OM
I-C	150.41	37.09	74.18	28.30
I-NC	150.13	37.53	-	-
NI-C	150.14	37.53	75.06	28.30
NI-NC	150.52	37.63	-	-

Similarly, detail of the large column leaching test is provided in the Fig. 5.7. The weight distribution in each column is also identical to previous column leaching test in the previous chapter. Moreover, the method of experiment is same as the small column leaching test. The initial cells density is 1.46 x 10^7 cells/g soil.

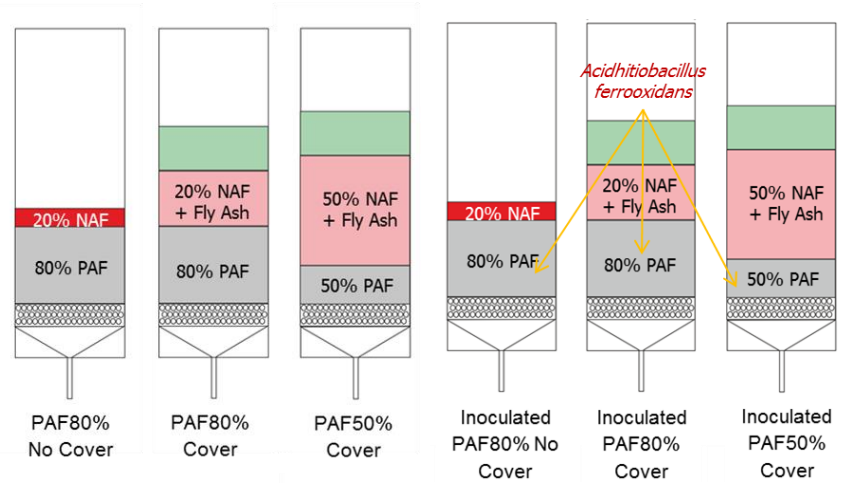

Fig. 5.7 Scenario of large column leaching test

5.3.2 Results and Discussions

Measurement of pH and electrical conductivity were provided in Fig. 5.8. In the initial measurement, the anomaly value of very low pH and high EC compared to the rest value can be observed. Shock loading phenomenon seems to occur in the columns

(Younger, 2002). Shock loading happened because of the rock material already heavily contacted with air and oxidized. It caused the first flushing measurement have higher acidity and dissolved metal contents than the rest of cycle measurements. Therefore, to obtain better data interpretation the initial value of measurement was neglected.

Both columns of inoculated bacteria, I-C and I-NC column, had lower pH and higher EC at the beginning of the cycle. However, as the wet-dry phase cycle was continuously conducted, pH value of the I-C column increased constantly until it had the similar pH value with I-NC column. The similar behavior of pH was started from day 12 until day 18, until the end of the measurement, which was surprisingly stable. On the other hand, pH and EC value of a column with and without inoculated cells always had a gap between them. This implies that the inoculated bacteria have a role in decreasing the pH, by oxidizing ferrous iron to ferric iron. Ferric iron is an oxidizing agent that can oxidize sulfide mineral faster than oxygen in the acidic pH. The lower pH of a column in this experiment means more sulfide mineral oxidation process occurred within the column. Therefore, the result informed that the gap between I-NC and NI-NC column occurred because the active cells keep growing in the column with inoculated bacteria while non-inoculated bacteria column have no biochemical contribution, depend only on the chemical reaction process.

As explained in the previous chapter, the fly ash and organic material as the cover layer have the effect to increase the pH by neutralizing the leachate water and oxygen consumption. Since oxygen is needed for iron-oxidizing growth, decreasing activity of iron-oxidizing bacteria also confirms the impact of decreasing oxygen. Moreover, because pH in the column increased, it also affects the bacteria growth. The condition of pH 2 is the optimum for iron-oxidizing bacteria growth even though these bacteria have been found could thrive in the pH six solutions. Therefore, near-neutral to alkaline solution condition is not suitable for iron-oxidizing bacteria growth.

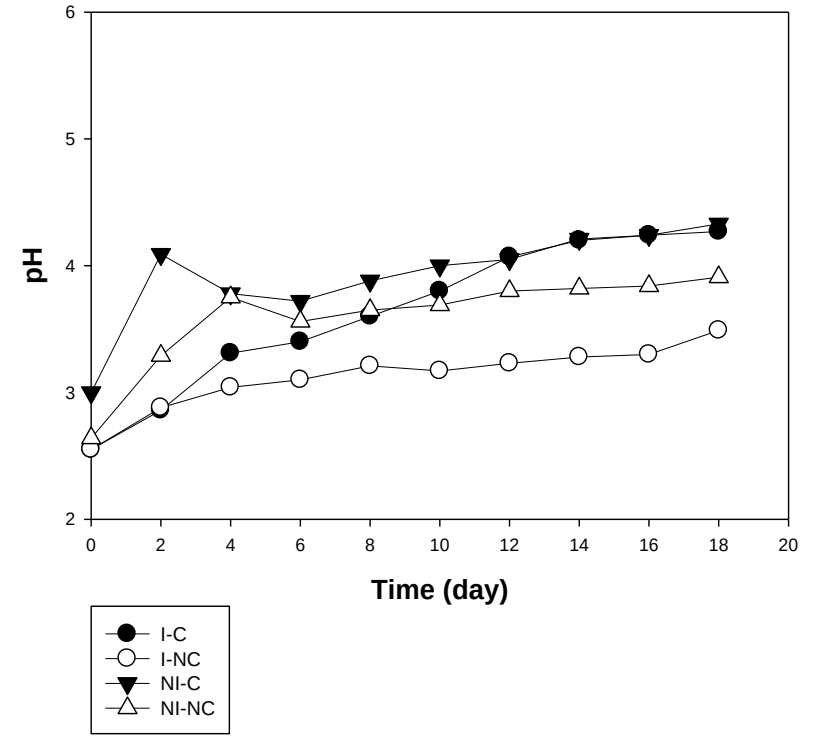

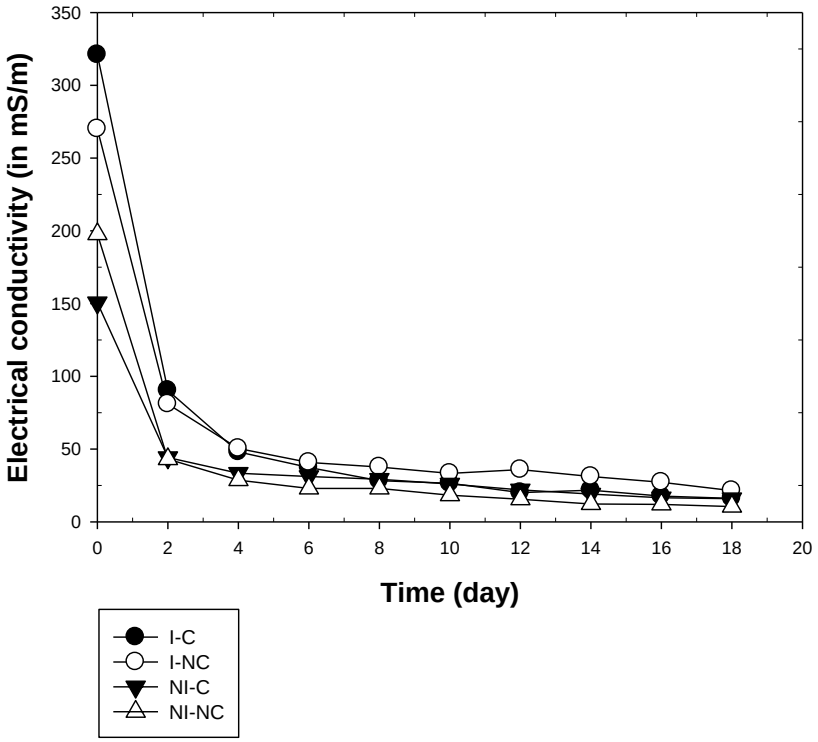

Fig. 5.8 Graphic of pH and EC result measurement

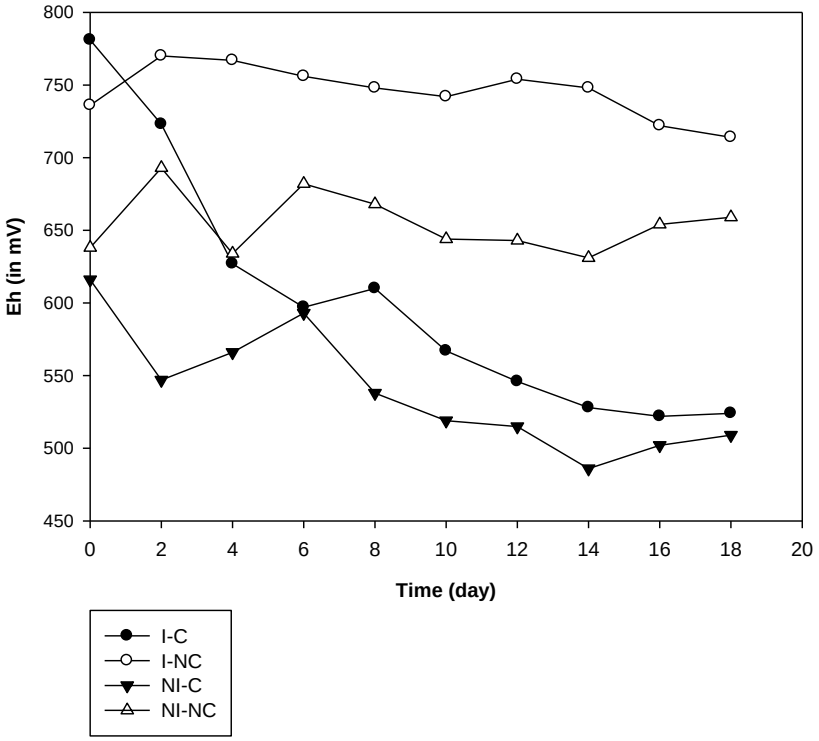

Fig. 5.9 Eh (oxidation-reduction potential) measurement

The result of Eh measurement was provided in Fig.5.9. At 25^{o} C, the ferric-ferrous iron ratio (Hem & Cropper, 1959; Merkel & Planner-Friedrich, 2005) could be examined by using the Nernst equation as the following:

$$Eh = 0.\ 771 + 0.0592 \log \frac{[Fe^{3+}]}{[Fe^{2+}]}$$

The relationship between ferric iron concentration and Eh is linear, thus higher the Eh means higher ferric iron in the solution. The initial measurement showed in the beginning, the column with the inoculated bacteria gave a high value of Eh. This indicated the oxidizing reaction occurred in both I-C and I-NC columns. Iron-oxidizing bacteria activity that uses ferrous iron as an electron donor and transformed it into ferric iron is likely accounted for this high potential value (Bose, Gardel, Vidoudez, Parra, & Girguis, 2014). Higher ferric iron concentration in the water system implies a higher possibility of iron-oxidizing bacteria activity.

Interestingly, the second measurement of I-C showed the drastic decreasing curve line. The trend stayed decreasing until the I-C is in the similar stable value with NI-C

near the end of the measurement. In this column, iron-oxidizing bacteria growth was reduced because of the existence of fly ash and organic material. This was also supported by the gap existing between I-NC and NI-NC column since both columns have no fly ash and organic material that resulted in the could increase the activity of iron-oxidizing bacteria. Therefore, the behavior of potential reduction in the column remained the same.

The metal concentration measurement of the leachate water showed the result that is in concordance with the direct measurement result of pH, EC, and Eh, as provided in the Fig. 5.10 and Fig. 5.11. For the columns without fly ash and organic material cover, the result of metal concentration showed higher results in the column with inoculated bacteria compared to without bacteria. Meanwhile, the column with fly ash and the organic material cover showed no significant difference in the metal dissolution, even with inoculated bacteria. This result supports the pH and Eh measurement, which indicate the role of bacteria in the metal dissolution. The increasing acidity will also affect the mobility of metals.

However, the different behavior was shown by the iron measurement. Column with fly ash and organic material cover dissolved more iron compared the column without cover even though the pH of the column with cover is higher. The higher the measurement of EC indicated a higher ratio of ferric iron concentration than ferrous iron, even though less total iron was available. This iron probably dissolved from the fly ash, as observed from past studies where the iron was leached from fly ash (Dutta, Khanra, & Mallick, 2009). Moreover, the slightly lower pH of leachate water (pH>5) was supported this assumption.

Generally, based on this research iron-oxidizing bacteria presence could increase the oxidation of sulfide mineral thus decrease the pH and increase the metal solubility. This could be a severe problem in the dry cover method. However, the application of fly ash and organic material could decrease the activity of these bacteria by increasing pH of the solution and also consume the oxygen in the surface. Iron-oxidizing bacteria are acidophilic and aerobic bacteria that the optimum condition of its growth will be in the

acidic environment with enough oxygen. Therefore, the utilization of both fly ash and organic material could inhibit the growth of iron-oxidizing bacteria.

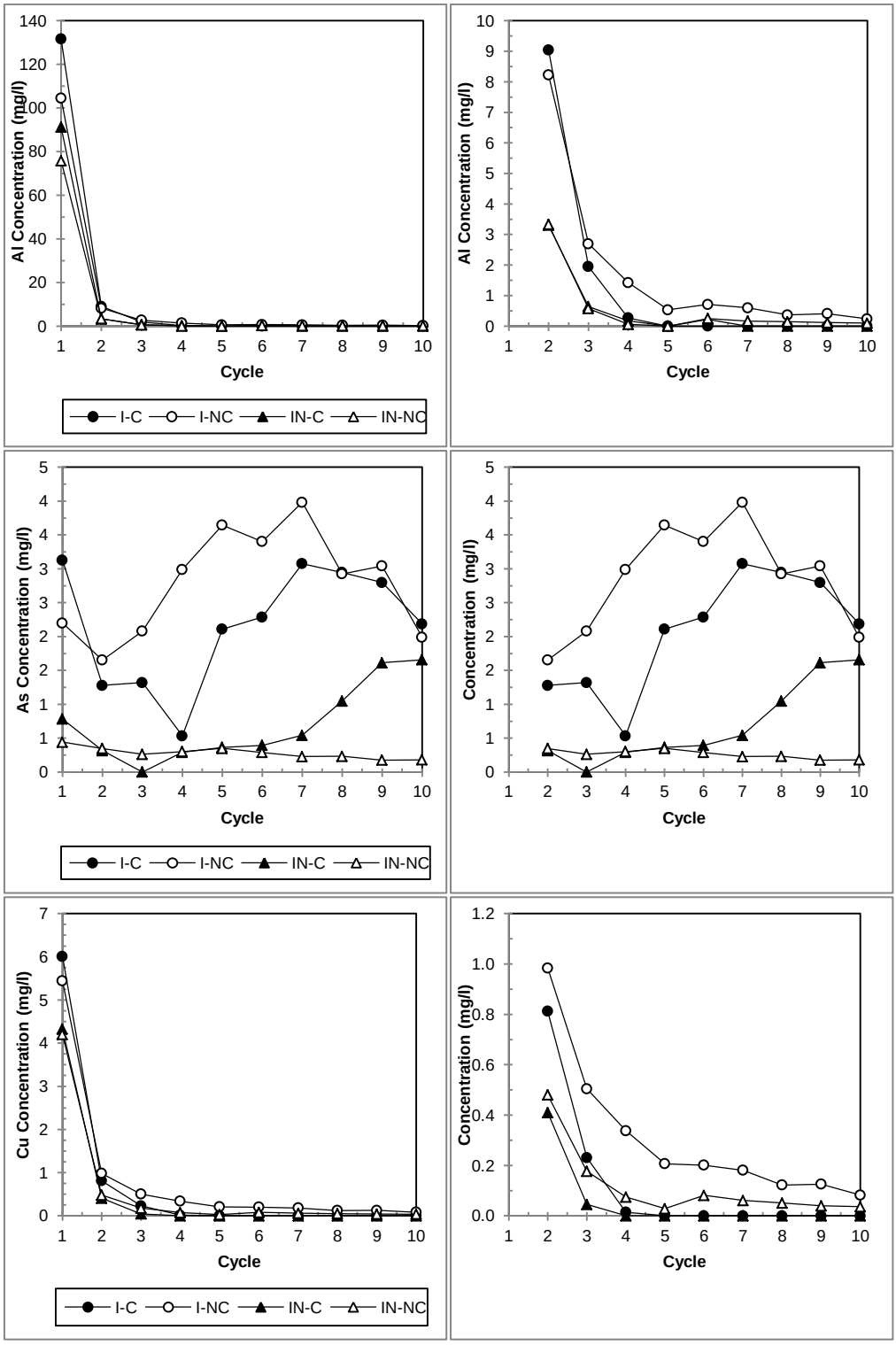

Fig. 5.10 Metal concentration with (a) and without (b) initial measurement

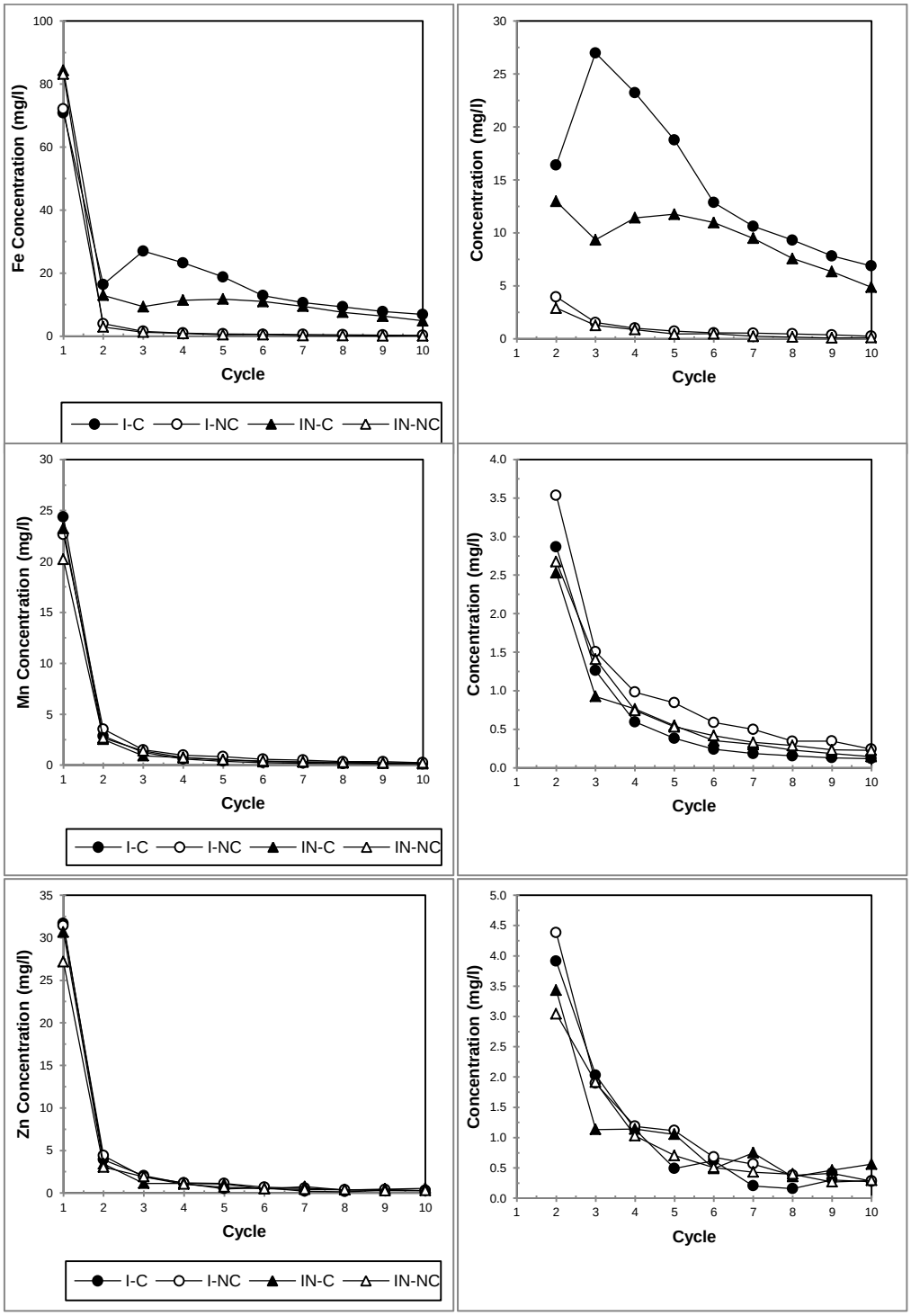

Fig. 5.11 Metal concentration with (a) and without (b) initial measurement (*cont.*)

The large column leaching test experimental result is provided in Fig. 5.12. Based on the result, the increasing pH can be seen from all of the columns with cover material, continuously from an initial time until the final measurement day. This similar trend happens due to the cover material effect that can immediately buffer the pH of AMD.

Moreover, the difference between column with addition bacteria and without addition bacteria is insignificant. This result indicates the capability of cover material to neutralize the water pH and eliminate the effect of iron-oxidizing bacteria to AMD generation in PAF rock.

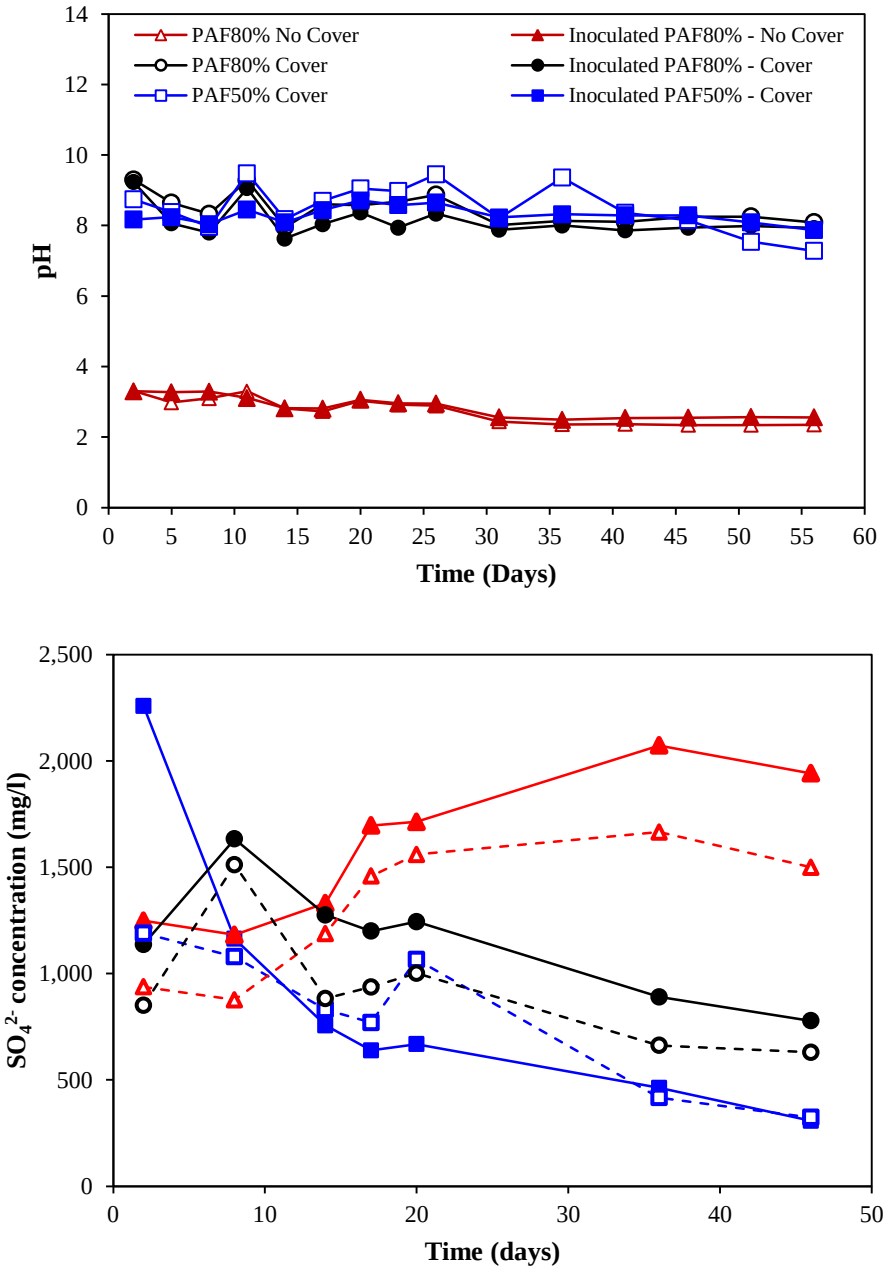

Fig. 5.12 Result of the large column leaching test

However, when the dissolved sulfate concentration result is observed, it can be seen that the column which has bacteria addition shows a higher value compared to the

column that has no bacteria addition. It is also observed that sulfate can be less dissolved when the thickness of cover material increase. This can be seen from the result of inoculated PAF50% Cover that reduce its dissolution in the matter of time until it has similar value with PAF50% Cover column without bacteria addition. The rest of the columns have a continuous gap between the same column scenario until the final day of measurement. Hence, thickness of cover material can be increased in the application of dry cover strategies in order to reduce the role of iron-oxidizing bacteria to the AMD generation.

5.4 Conclusions

This chapter discusses the role of iron-oxidizing bacteria to the AMD generation and its inhibition growth by using fly ash and organic material. Several important findings can be summarized as follows.

1. Isolation-growth of iron-oxidizing bacteria were successfully conducted from the original rock sample on the mining site. By observing the capability of oxidizing the ferrous iron, it can be concluded that in the similar condition, acidic pH water ($pH \leq 2$, temperature around $30^{o}C$ and aerobic), the presence of iron-oxidizing bacteria have a vital role in oxidizing ferrous iron to ferric iron. It happens in the very fast reaction. Thus the catalyzation process in AMD generation can take place. Moreover, sandstone provides more active iron-oxidizing bacteria than siltstone and clay stone as observed during the experiment.

2. Iron-oxidizing bacteria still could enhance the AMD generation, even though the common practice of dry cover prevention method was already applied. As a result, more acidic condition and increasing metal content occurred. However, dry cover using fly ash and organic material as one of the cover layers could improve the quality of leachate water and reduce the growth of iron-oxidizing bacteria. By increasing pH of the solution and also consume the oxygen in the surface. Iron-oxidizing bacteria are acidophilic and aerobic bacteria that the optimum condition of its growth will be in the acidic environment with enough oxygen. Therefore, the utilization of both fly ash and organic material could inhibit the growth of iron-oxidizing bacteria.

3. In small-scale column leaching, the effect of iron-oxidizing bacteria to AMD generation can be observed. However, in the large scale column, the difference is insignificant. The cover could increase the pH of both columns that are inoculated and non-inoculated.

4. The higher thickness of cover layer could decrease more sulfate production in the AMD system, thus preventing more AMD production because of iron-oxidizing bacteria.

References

Baker, B. J., & Banfield, J. F. (2003). Microbial communities in acid mine drainage. *FEMS Microbiology Ecology*, *44*(2), 139–152. https://doi.org/10.1016/S0168-6496(03)00028-X

Bose, A., Gardel, E. J., Vidoudez, C., Parra, E. A., & Girguis, P. R. (2014). Electron uptake by iron-oxidizing phototrophic bacteria. *Nature Communications*, *5*, 3391. https://doi.org/10.1038/ncomms4391

Dutta, B. K., Khanra, S., & Mallick, D. (2009). Leaching of elements from coal fly ash: Assessment of its potential for use in filling abandoned coal mines. *Fuel*, *88*(7), 1314–1323. https://doi.org/10.1016/j.fuel.2009.01.005

Hem, J. D., & Cropper, W. H. (1959). Chemistry of iron in natural water - A survey of ferous-ferric chemical equilibria and redox potential. U.S. geol. Survey Water-Supply Paper, 1459.

Madigan, M. T., Martinko, J. M., Stahl, D. A., & Clark, D. P. (2010). Brock Biology of Microorganisms. New York: Benjamin Cummings.

Merkel, B. J., & Planner-Friedrich, B. (2005). *Groundwater Geochemistry: A Practical Guide to Modeling of Natural and Contaminated Aquatic Systems*. (D. K. Nordstorm, Ed.) (Second). Freiberg.

Singer, P. C., & Stumm, W. (1970). Acidic Mine Drainage: The Rate-Determining Step. *Science*, *167*(3921), 1121–1124.

Skousen, J. G., Sexstone, A., & Ziemkiewicz, P. F. (2000). Acid Mine Drainage Control and Treatment, (41), 1–42.

Younger, P. L. (2002). Mine water pollution from Kernow to Kwazulu-Natal: Geochemical remedial options and their selection in practice. *Geoscience in South-West England*, *10*(3), 255–266.

CHAPTER 6

Conclusions

6.1 Conclusions

Based on site investigation, observed coal mine which located in Indoensia encounters a serious issue of acid mine drainage problem due to the high capacity in acid producing as well as large volume of rocks. Moreover, non-acid forming rocks have been found insufficient in volume and also lack in neutralizing capacity. Awareness of severe situations that has to be faced in the future currently escalating, especially because numerous coal mines already in the final stage of mining. Attempts for treating and preventing the long-term acid mine drainage generation has been carried out, showed its failure, based on the site observation that was conducted.

In order to solve the issues, dry cover strategy is proposed based on the common material that easy to be found in the coal mine. This research proposes the utilization of coal ash and organic material to be used as an additional cover layer to minimize AMD. Coal ash posing great neutralization process due to its carbonate materials and also silicate minerals that able to produce alkalinity after reacting with water. Moreover, organic materials can consume oxygen during its degradation, which in turn can act as an oxygen barrier.

Individual characterization has been conducted to the each possible layer material. Based on the characterization of coal ash, two types of coal ash are distinguished. Due to the burning temperature process of coal, Type 1 coal ash has high neutralizing capacity (>100 kg H_2SO_4/ton) while Type 2 coal ash has intermediate neutralizing capacity (<50 kg H_2SO_4/ton). Therefore, these fly ashes can be used to neutralize AMD generation in the overburden dumping area. Moreover, by comparing organic materials, it can be observed that organic material usage in dry cover is independent to the PAF, mostly depend on the decomposition rate that affected by organic matter quality, water moisture and also temperature. Organic material can be used as material to consume oxygen in dry cover method. Based on the experiment, an empty fruit bunch (EFB) shows the higher reduction rate of oxygen on the time basis compared to dehydrated

sewage sludge. The rate differs into 3.6 times higher. Therefore, EFB can be used in dry cover system.Classification of fly ash and also the organic material decomposition rate then can be used to have the optimization of field usage.

Due to the difference in neutralizing capacity, the usage of fly ash can be distinguished based on the NAG pH test. Type 1 is recommended to neutralize both PAF low and high capacity. Type 2 is recommended to neutralize PAF low capacity. NAPP ratio can be used to determine the amount of fly ash in dry cover method. Based on the result of column simulation, NAPP ratio less than 10 kg H_2SO_4/ton is recommended to be used. Moreover, thickness ratio of fly ash and PAF is also important to be considered. In order to have hydraulic conductivity reduction, it is recommended to have thickness ratio more than 0.25 times for coal ash Type 1 and thickness ratio more than 0.50 times for coal ash Type 2.

Simulation of column leaching test shows the effect of combination between fly ash Type 1 and also EFB to prevent AMD generation. NAF material only to be used as dry cover shows insignificant impact n reducing water and oxygen to infiltrate. Moreover, based on the kinetic test, at some point the behavior of NAF is similar to the PAF that increase the acid producing capacity. Therefore, additional layer becomes a prominent factor to avoid AMD generation. During the simulation, pH of leachate water increases significantly and also metal dissolution can be lowered as the result of precipitation of metals, consequences of fly ash and EFB reaction within the systems.

Not only leachate water, cover material can also decrease the growth of iron-oxidizing bacteria. These bacteria have a role in increasing AMD reaction by oxidizing ferrous iron to ferric iron because of its metabolic process. Ferric iron in the acidic condition is able to oxidize sulfide mineral faster than oxygen in the 10^7 fold faster, thus accelerate AMD generation. However, because iron-oxidizing bacteria are an acidophilic and aerobic bacteria, the process of pH neutralization by fly ash and oxygen consumption of organic material can decrease the growth activity of iron-oxidizing bacteria, as the condition becomes not suitable for iron-oxidizing bacteria continue to grow. Furthermore, thickness of cover material is also a vital role to decrease iron-oxidizing bacteria.

ACKNOWLEDGEMENT

First and foremost, I wish to express sincere gratitude to Prof. Hideki Shimada, as my supervisor, for all the support and guidance during the study at Laboratory of Rock Engineering and Mining Machinery, Department of Earth Resources Engineering, Kyushu University. His patience and support during the discussion, encourage me towards the completion of my research. I also would like to express the deepest appreciation to my committee for their advice and support, Assoc. Prof. Takashi Sasaoka, Prof. Yoshinari Hiroshiro, and Assoc. Prof. Naoko Okibe. My gratitude is especially delivered to Assoc. Prof. Naoko Okibe who kindly teaches and supports me through discussion during my research as well as her valuable comments and constructive suggestions as my chief committee to improve the results of this dissertation.

My deep appreciation also goes to Prof. Rudy Sayoga Gautama at Institut Teknologi Bandung, for his help and advice for my research, along with the endless support while I was studying in Kyushu University. This appreciation is also extended to Dr. Ginting Jalu Kusuma, for his sincere advice of my life and study in Japan.

The same gratitude is also delivered to Assistant Prof. Akihiro Hamanaka and Dr. Sugeng Wahyudi at Laboratory of Rock Engineering and Mining Machinery, for all of their support, discussion and help that were given to me during the study. I would like also to appreciate Fujita-sensei for helping me a lot during my research.

I would like also to express my gratitude and appreciation for Green Asia, which provide me with various programs during the master course study such as, environmental and economic classes, practice school and laboratory rotation that broaden my knowledge not only for my own study but also the general knowledge about society. I also extend my gratitude and appreciation for Green Asia Professor and staff to help me a lot during this master program.

I would like also to thank all of Rock Engineering members, for helping me in my experiment research along with the discussions that have been done so far which improved my research. Thanks are also extended to all of the support that I received, from friends in Indonesia and PPI Fukuoka, especially Salma, Kak Intan, Mas Pandhe, Niko, Febby, Evan, Aby, Harnas, Teh Cici, Mas Angga, Intan and the others that cannot be mentioned one by one but not decreasing theirs significant value.

This research will never be completed without the continuous support from the Mining Environment Laboratory in ITB, especially from Abie Badurrahman, and also the Department of Mining Engineering staff, Firly Rachmaditya B. and Tri Karian. Moreover, the invaluable support from PT Arutmin Indonesia and PT Bukit Asam has been made the fieldwork can be successfully carried out. Hence, special appreciations extend to the management and staff of Asam-asam mine, Ahmad Juaeni, Achmad Rizky Nevianto, Wawan, M. Zaenal Kahfi, and the rest of the staff, particularly from Engineering and Environment division. In addition, the sincerest gratitude is also extended to PT Bukit Asam staff, especially from Geological department.

Finally, I dedicate this dissertation to my parents, Ennys Husni and Suryati, and my loving family, Fitri Anggraini, Rini Yolanda, Aaliyah Azkiyatunisa and Kiki. Without them, it will be impossible to even start and finish this study.

Fukuoka, July 2018

Author